PROFESSIONAL JOURNAL ON PRECISION ENGINEERING

μ MIKRONIEK

ISSUE 2
2014
(VOL. 54)

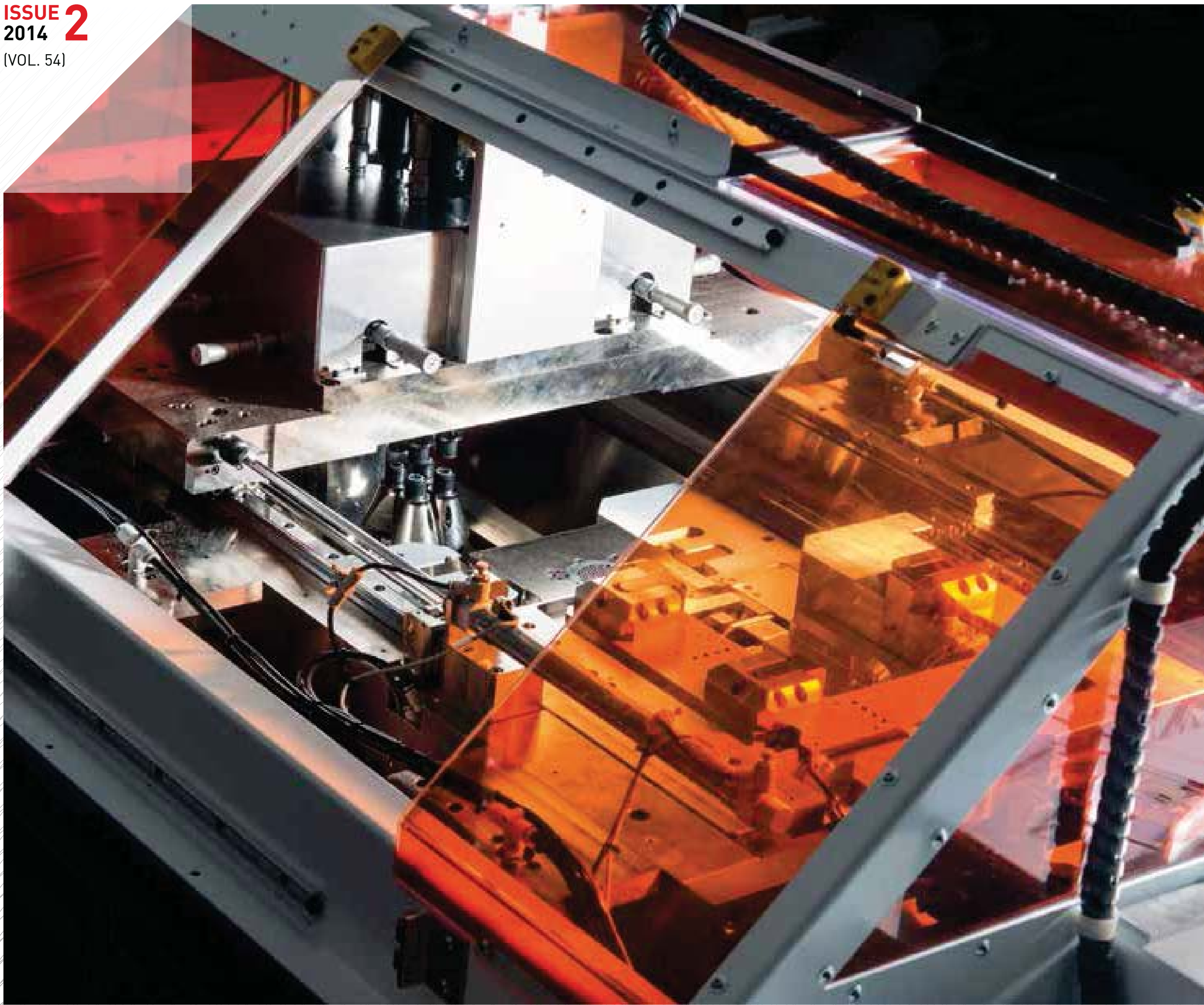

- FROM MICRO- TO **NANOPOSITIONING**
- **ROBUST AUTONOMY** OF ROBOTS
- WAVELENGTH SCANNING INTERFEROMETRY
- **QUALITY CONTROL 4.0**

PLUS
OFFICIAL CATALOGUE
HIGH-TECH SYSTEMS 2014
7-8 MAY, 'S-HERTOGENBOSCH

Mikroniek is a publication of the DUTCH SOCIETY FOR PRECISION ENGINEERING www.dspe.nl
DSPE

PUBLICATION INFORMATION

Objective
Professional journal on precision engineering and the official organ of DSPE, the Dutch Society for Precision Engineering. Mikroniek provides current information about scientific, technical and business developments in the fields of precision engineering, mechatronics and optics.
The journal is read by researchers and professionals in charge of the development and realisation of advanced precision machinery.

DSPE
YOUR PRECISION PORTAL

Publisher
DSPE
High Tech Campus 1, 5656 AE Eindhoven
PO Box 80036, 5600 JW Eindhoven
info@dspe.nl, www.dspe.nl

Editor
Hans van Eerden, hans.vaneerden@dspe.nl

Advertising canvasser
Gerrit Kulsdom, Sales & Services
+31 (0)229 – 211 211, gerrit@salesandservices.nl

Design and realisation
Twin Media, Culemborg
+31 (0)345 – 470 500, info@twinmediabv.nl

Subscription costs

The Netherlands	€ 70.00 (excl. VAT) per year
Europe	€ 80.00 (excl. VAT) per year
Outside Europe	€ 70.00 + postage (excl. VAT) per year

Mikroniek appears six times a year.

ISSN 0026-3699

The main cover photo (equipment for optical wafer stacking) is courtesy of IMS.

IN THIS ISSUE

ISSUE 2
2014

08

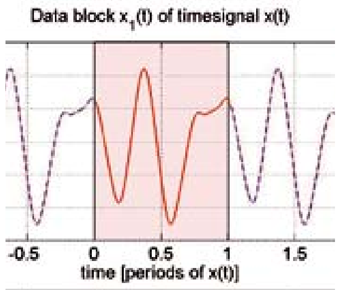

18

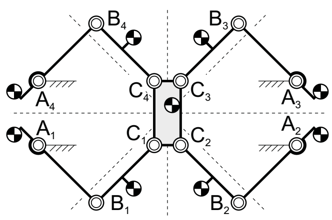

SUPPLEMENT
OFFICIAL CATALOGUE
HIGH-TECH SYSTEMS 2014

FEATURES

EDITORIAL

GENERATING **INTERNATIONAL BUSINESS** IN THE HIGH-TECH PRECISION INDUSTRY

Following the Hannover Messe earlier this month (at which the Netherlands acted as partner country), this May will see the High-Tech Systems international conference and exhibition on high-end system engineering. This event will give us another opportunity to showcase our country on the international stage, underlining, once more, the importance of 'country branding', even in the global high-tech market. The Netherlands has one of the world's strongest economies and is particularly renowned for its high-tech systems and materials, as well as its high-tech solutions for global issues.

This is exactly what NBI International focuses on. The first impression a country or region makes can play a key role in terms of attracting investors and boosting trade relations. NBI is an international centre for purchasing issues; it realises demand-driven sales processes based on international procurement needs. It also supports expansion into international markets, provides international trade-oriented acquisition and organises a platform for international investment opportunities. NBI has developed a strong international network featuring economic departments of ministries, trade departments of embassies, investment, trade and export promotion agencies, and the private sector.

To contribute to a sustainable environment and prosperous life, improving and strengthening industry should be at the top of every government's to-do list. The global demand for high-tech products is growing, but companies are having to invest more and more in marketing and sales because of ever-increasing global competition.

To realise effective sales processes, companies have to make choices regarding their approach to marketing. As such, NBI International has developed a work method to analyse the exact demands of various sectors and countries. NBI has set up a network of 60 countries to facilitate this analysis and to access procurement information. One country NBI is working with is Vietnam. Countries like Vietnam can only climb up the industrial value chain if their supply base is strong, so that's where the country's priorities should lie. Japan and Korea, for instance, have a strong presence in Vietnam and draw on its supply base.

International marketing is expensive and it takes a lot of patience to generate new business abroad. NBI International knows, however, that there are companies and government bodies in Vietnam that are very interested in working with the Netherlands.

High-tech expertise and international marketing should go hand in hand.

Chris Aelberts
General Director of NBI International

PS: We will be holding a seminar on business opportunities in Vietnam at the NBI Expo 2014 in Eindhoven on 7 May.

QUALITY CONTROL 4.0

Industrial production of the future ('Industrie 4.0', in the German government's industrial policy) will be characterised by the demand for mass customisation, micrometer-critical dimensions, higher throughput, increased cost of resources, and ultimately 100% automated factories and 100% quality control. This quality control involves every product in real time with respect to the properties being critical to its quality (CTQs). Therefore, it has to be in immediate proximity to the machine, instantaneous and without interfering with the production process.

THOMAS LIEBIG, JASPER WINTERS, SAM HELMER, WOUTER JONKER AND ROB SNEL

AUTHORS' NOTE

Thomas Liebig (optics designer), Jasper Winters (mechatronics designer), Sam Helmer (business developer Smart Industries), Wouter Jonker (project manager) and Rob Snel (system engineer) all work at TNO in the Industrial Applications group.
The work leading to the results presented here has received funding from the European Community's Seventh Framework Programme under grant agreement n° FP7-285030. It was presented in the TNO stand at the Hannover Messe, 7-11 April 2014.

ROB.SNEL@TNO.NL
WWW.TNO.NL/INDUSTRIALAUTOMATION

For products made by die forming, as shown in Figure 1 for example, optical coherence tomography (OCT) represents a well-established method to determine the complete 3D surface shape from which the CTQs can be derived. It is an optical measurement technique based on the coherence of light. It therefore offers many of the known advantages of optical measuring methods such as a high accuracy and being contactless. The use of a laser source is not required. Also, the current method can cope with a high variation in product and material properties, such as reflectivity, roughness and bending angle of the surface to be characterised. Depending on the roughness of the surface, a resolution of a few micrometers down to a few nanometers can be achieved in the axial direction.

Up to now, the OCT measurement is performed on a sample basis in off-line laboratory facilities because of the time required to execute and process the measurements, as well as the sensitivity of the apparatus. Accordingly, high costs are associated with the loss of invested resources, ranging from raw materials to energy and labour. Post-processing and coping with false-positive products also have to be taken into account.

Novel system architecture

New light sources and sensors together with a system architecture that does not only focus on the optical instrument itself, but also incorporates the production process and environment, enable the acceleration of the measurement procedure by a factor of 100. TNO transferred this technology to the work floor in cooperation with industrial partners and supported by the EU. A prototype has already been tested very successfully in a production environment; see Figure 2.

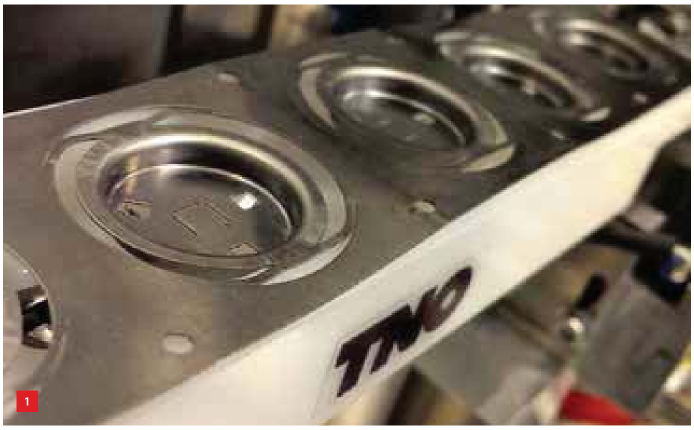

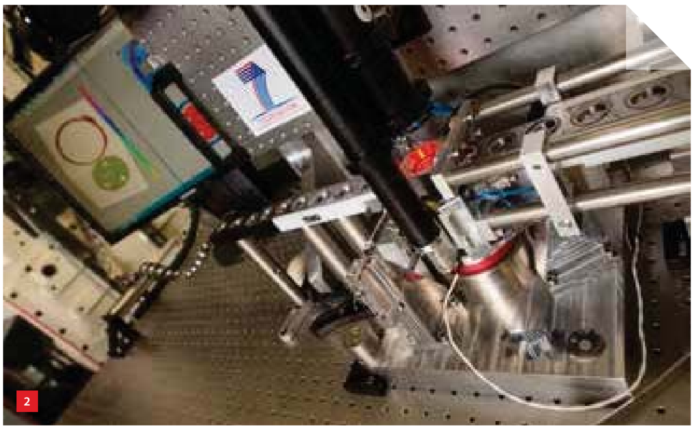

1 *Cold-formed product (diameter approx. 24 mm).*

2 *Set-up of a fast OCT measurement system for 100% quality control in industrial series production.*

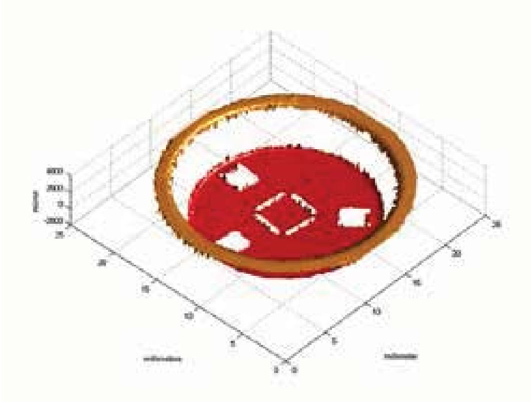

3a

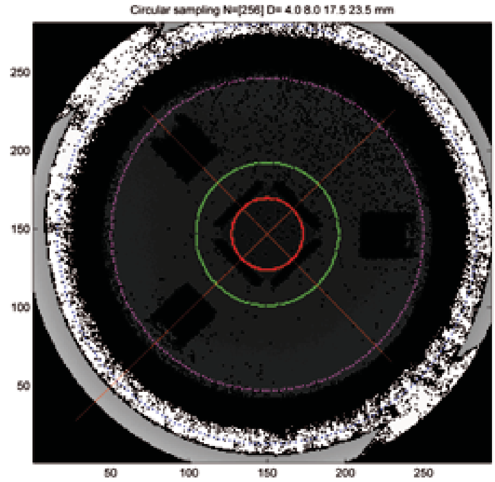

3b

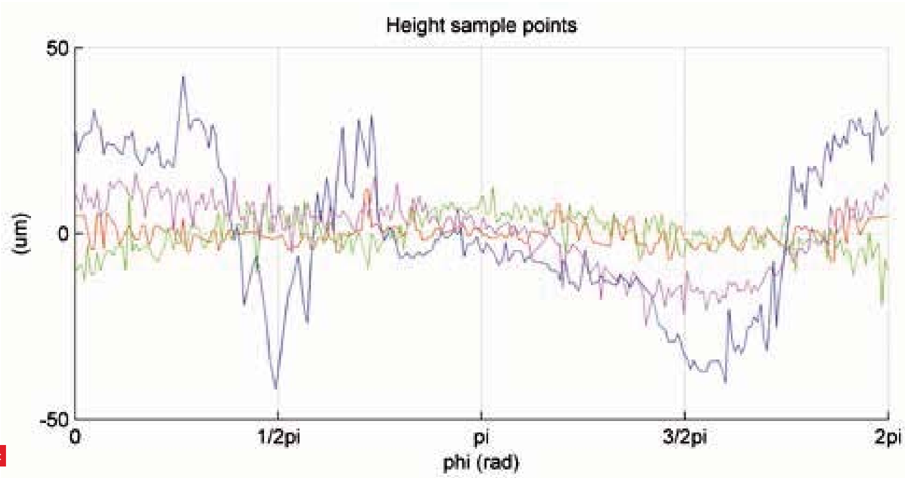

3c

3 *Extraction of CTQs.*
(a) The 3D point cloud of the measured product.
(b) 2D projection of the point cloud in grey scales; the coloured circles indicate measurement paths.
(c) Sampling of the various circles with different diameters; the correspondingly coloured lines show clear differences in height profile.

The 3D surface shape of die-formed products, made at a rate of > 1 products per second, can be measured in-line right next to the machine with micrometer precision; see Figure 3. The exemplary products are cups with a diameter of about 24 mm and a depth of about 8 mm. They are characterised by features with tolerances and dimensions only a few microns large. This way, they already exceed the stability of the production process even today. A further reduction of the CTQs is highly desired. Therefore, the delay in feedback between measurements and control system has to be eliminated. This enables so-called zero-defect production.

The know-how acquired with the development and integration of this smart OCT system proves to be very advantageous to other projects. In these, TNO is adapting OCT and related technologies to other products and production processes in cooperation with partners from industry. ■

TNO

TNO is the Netherlands organisation for applied scientific research. It is an independent research organisation employing about 3,800 professionals. TNO connects people and knowledge to create innovations that boost the sustainable competitive strength of industry and well-being of society. In addition, TNO provides one of the largest independent centres for the development and production of optical components and systems in Europe. It is focused on industrial applications with a long-standing experience in the semiconductor and space industry. WWW.TNO.NL/EN

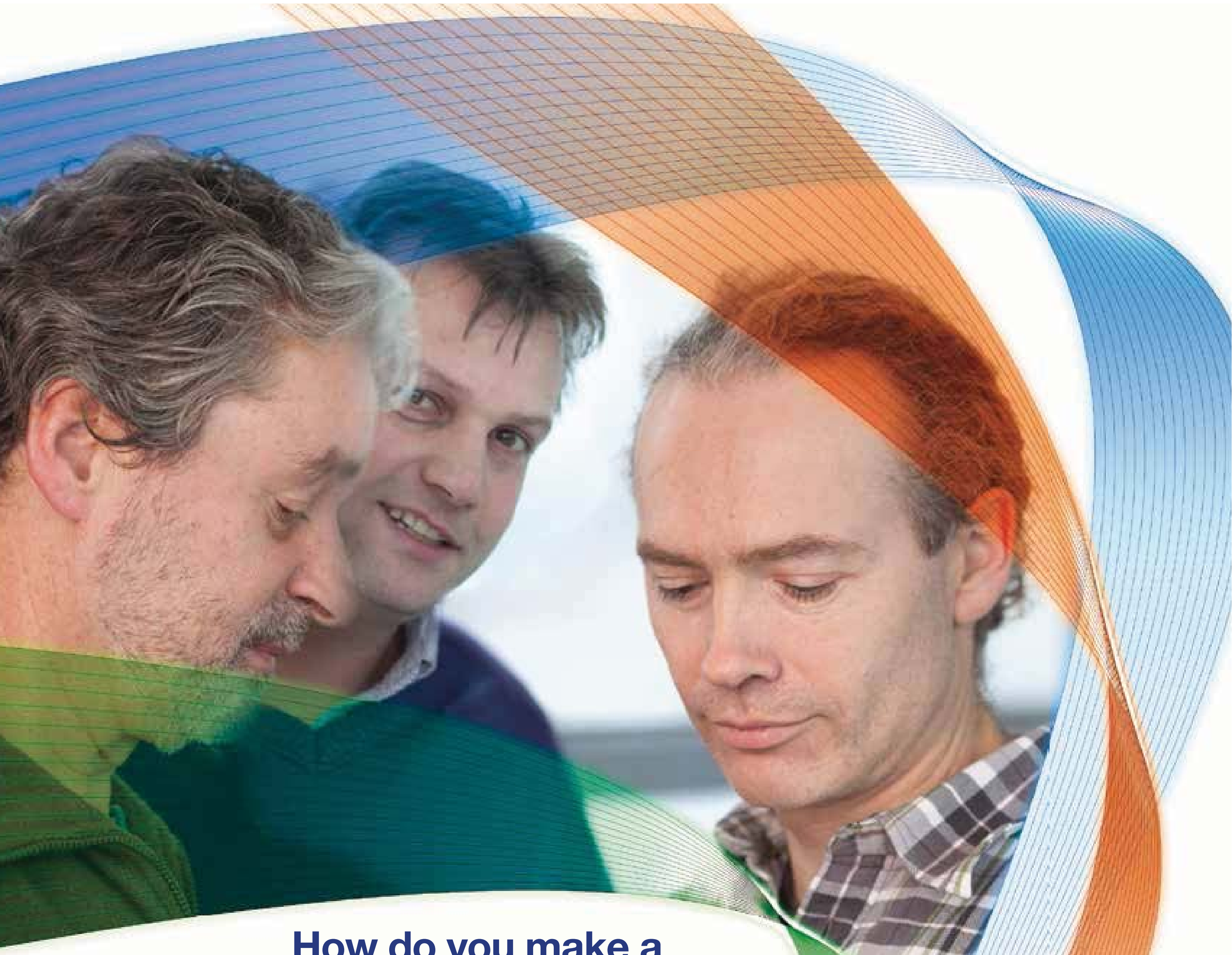

PARTICIPANT HIGH-TECH SYSTEMS 2014

THE TRANSFORMATION FROM **TIME TO FREQUENCY** DOMAIN

A series of three articles will feature Frequency Response Function (FRF) measurements. The FRF, describing the frequency-dependent behaviour of linear systems, is an indispensable tool in the engineering of dynamic systems. This series is not meant to be mathematically rigorous but aims at an understanding of the main steps to determine the FRF based on real measurements from an application point of view. Part 1 deals with the transformation of time-domain signals to the frequency domain and may serve as a stand-alone guide for basic signal analysis.

AUTHORS' NOTE

Pieter Nuij, senior system architect, and David Rijlaarsdam, group leader, both work at NTS Systems Development in Eindhoven, the Netherlands.

pieter.nuij@nts-group.nl
www.nts-group.nl

PIETER NUIJ AND DAVID RIJLAARSDAM

Why transform?

Although we 'live' in the time domain and naturally ask ourselves *when* things happen, asking the question *how often* things happen often leads to revealing answers. Figure 1 shows a time signal of the torque measured through the outgoing shaft of a gearbox. The spectrum of the same signal is displayed in Figure 2 and clearly shows discrete frequency components that can be related to the gear ratios of the gearbox. Although the time signal also contains this information, it is not visible in the time trace in Figure 1.

Three articles

This article covers the steps that are necessary to convert a time-continuous signal into a discrete spectrum. Potential errors due to aliasing and leakage will be explained and solutions will be presented. An overview of several types of test signals will be presented. The second article will introduce the FRF, explaining the choice of test signals in their relation to the coherence function and the measurement of the FRF in open-loop and in closed-loop systems. The third article will focus on the extension of frequency-domain methods towards nonlinear systems and the application of such methods to define and optimise the performance of such systems. Each article will be illustrated with examples.

Discrete spectrum

To determine the spectrum of a continuous time signal the signal must be converted into a sequence of numbers that form the input for a numerical algorithm running in a computer. Figure 3 shows the necessary steps for this conversion.

The continuous time signal is conditioned and amplified/attenuated in an analogue electronics stage before it is low-pass-filtered to limit its frequency content. After filtering, the signal is sampled and becomes a discrete time signal. The individual samples are converted from an analogue signal into a quantised signal with discrete values.

Limiting the frequency content of the continuous time signal before sampling is important, but it is sometimes neglected, causing erroneous results. Figure 4a shows a continuous time signal with frequency f_{signal} that is sampled with sampling frequency f_{sample}. The resulting discrete time signal is a true representation of the continuous time signal. In Figure 4b a different signal with frequency $f_{signal} + f_{sample}$ is sampled with the same sampling frequency f_{sample}. The reconstructed discrete time signal seems to be the representation of a continuous time signal with frequency f_{signal}.
This example clearly shows that sampling can introduce errors called aliasing components. To prevent this from

1 *Time trace of torque measurement.*
2 *Spectrum of torque measurement.*
3 *Necessary steps to convert a continuous time signal into numerical data points.*

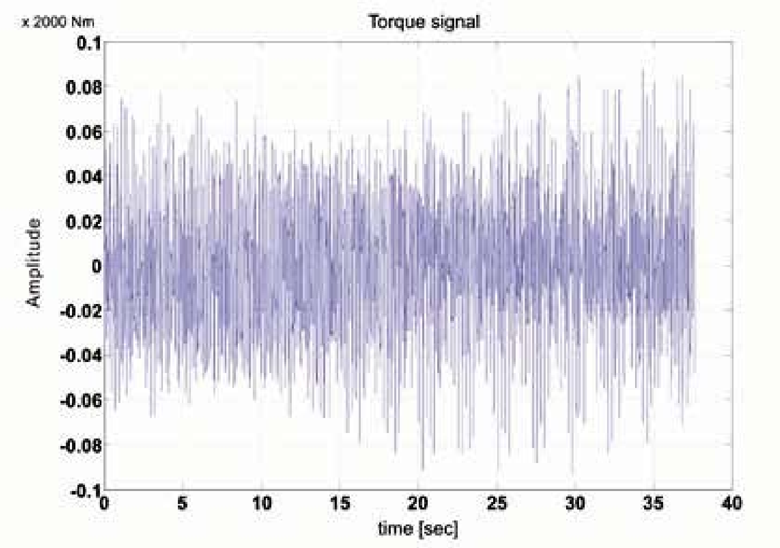

1

happening, the sampling frequency must be at least twice the frequency of the highest frequency component present in the continuous time signal. Since the frequency content of the signal to be analysed is often unknown, low-pass filtering to limit the frequency content is required. The filter used for this purpose is called an anti-aliasing filter.

Like any filter the anti-aliasing filter will introduce frequency-dependent phase shifts in the filtered signal. This is not a problem when measuring FRFs as long as all measurement channels used for the FRF calculations experience equal phase shift. In the last block in Figure 3 the discrete time analogue signal is quantised, rounded to the nearest discrete amplitude value of the 2^n possible values that can be represented by an n-bits digital word. Optimal use of the amount of bits requires matching of the amplitude of the signal to the voltage range that can be accommodated by the AD converter (ADC). This is done by choosing the correct amplification or attenuation factors in the signal-conditioning front-end. Poor ranging will cause harmonic distortion and a high noise floor but due to the advent of high-quality 24-bits ADCs the ranging requirements become less stringent.

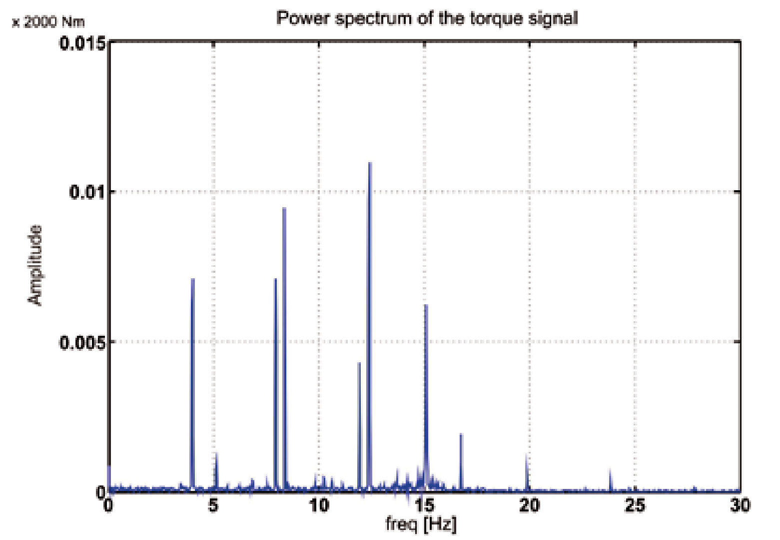

2

Certified Precision Engineer competencies

The content of this series of three articles is in part covered in the "Experimental Techniques in Mechatronics" course, provided by The High Tech Institute (HTI). This course has been selected for the DSPE Certification Program (see page 58).

WWW.DSPEREGISTRATION.NL WWW.HIGHTECHINSTITUTE.NL

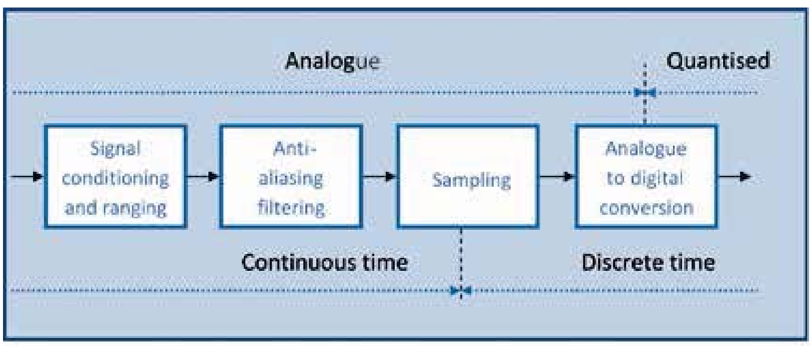

3

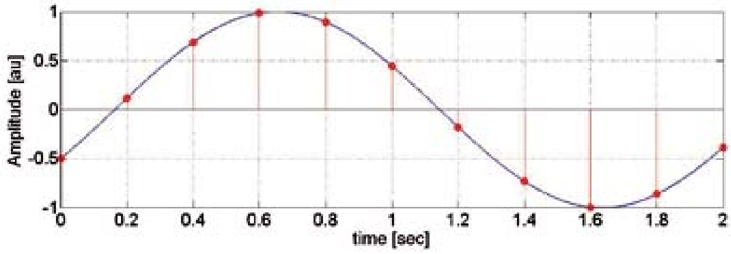

4a

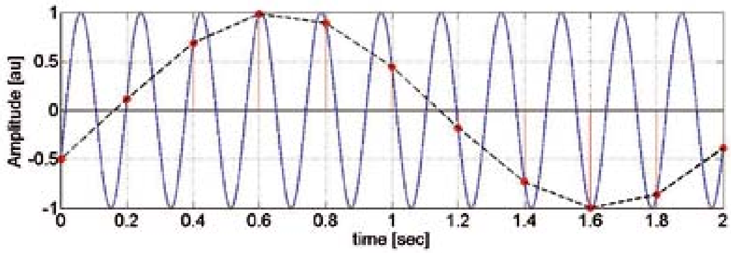

4b

4 *Introduction of errors by sampling.*
(a) Signal (blue) with frequency f_{signal} sampled with frequency f_{sample} (red).
(b) Signal (blue) with frequency $f_{signal} + f_{sample}$ sampled with frequency f_{sample} (red). The reconstructed signal is the aliasing component (black).

5 *Analysis of time signal x(t) in blue.*
(a) Periodically reconstructed time signal based on measurement signal $x_1(t)$ in red.
(b) Some of the signal components present in $x_1(t)$.

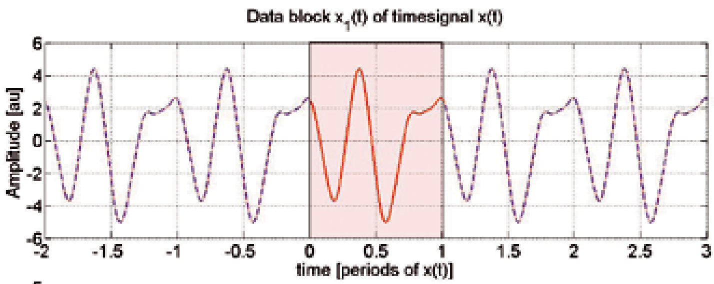

5a

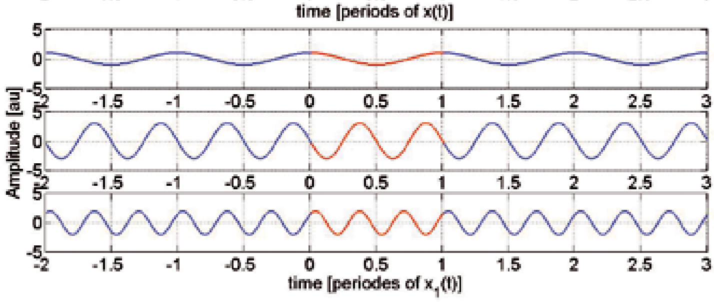

5b

Frequency analysis

The common way to describe the frequency content of a time signal is to use a series of cosines with specific frequencies, amplitudes and phases. The Fast Fourier Transform (FFT) is a very efficient algorithm for calculating these cosine-based signal components. However, as will be demonstrated, the results must be interpreted carefully.

Figure 5a shows a time signal $x(t)$ of which frequency components are to be identified (= transformed from time to frequency domain). Since the signal is periodic with a period of T, it consists of a series of cosine components with frequencies being a multiple of $1/T$ Hz. So if T is 1 s, $x(t)$ will consist of a series of harmonics of 1 Hz.
A segment $x_1(t)$ of $x(t)$ is captured and this measurement record will be processed. If the length T_1 of the segment $x_1(t)$ is equal to T, then the result of the FFT will correctly describe the frequency content of the time signal $x(t)$. This can be seen in Figure 5a, where the repetition of the measurement record $x_1(t)$ results in a signal equal to the original signal $x(t)$. Figure 5b shows some of the cosine components present in the signal. The amplitude and phase values of these cosine components are plotted in the amplitude and phase spectra as displayed in Figure 6. The units on the x axis in Figure 6 are cycles/T_1, with T_1 the period time of the measurement record $x_1(t)$.

T_1 can be calculated from the sampling frequency (f_s) and the size of the measurement record:

$$T_1 = \#\ samples\ /\ f_s$$

Knowing T_1, the frequency axis can be scaled to cycles per second [Hz]. The resulting frequency resolution Δf of the spectrum is equal to $1/T_1$. The highest frequency component that can be present in the spectrum has a value of $f_s/2$ Hz. If a different segment of $x(t)$ is captured, but the length of the segment remains T_1, the amplitude spectrum will remain the same but the phase spectrum will be different. If the length of the segment is changed, the amplitude spectrum will also change.

Figure 7 shows the situation that T_2, the length of the measurement record $x_2(t)$, is not an integer amount of periods T of $x(t)$ any longer. The FFT algorithm will again determine the best fit of a series of cosines, but this time

6 *Spectra of measurement signal $x_1(t)$ in case the measurement record length T_1 is equal to period T.*
(a) Amplitude.
(b) Phase.

7 *Results in case the measurement record length T_2 is not an integer amount of periods T.*
(a) Time signal $x(t)$ in blue and periodically reconstructed time signal based on measurement signal $x_2(t)$ in red.
(b) Amplitude and phase spectra of measurement signal $x_1(t)$ in blue and $x_2(t)$ in red, both with starting time $t = 0$ s.

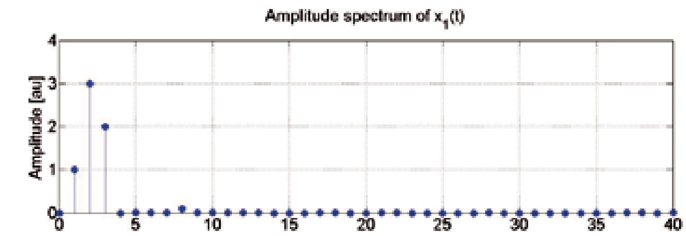

6a

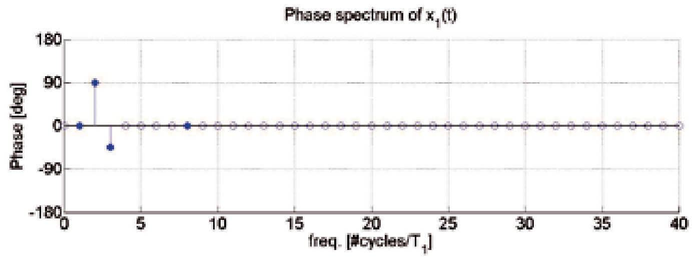

6b

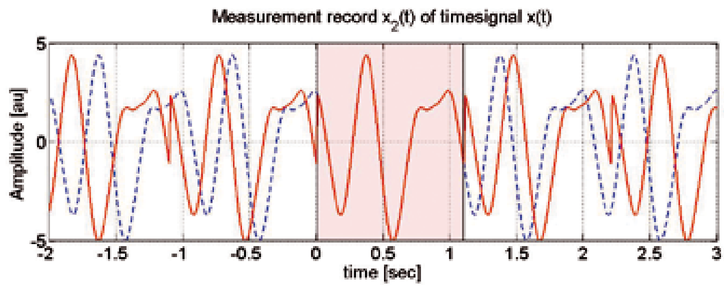

7a

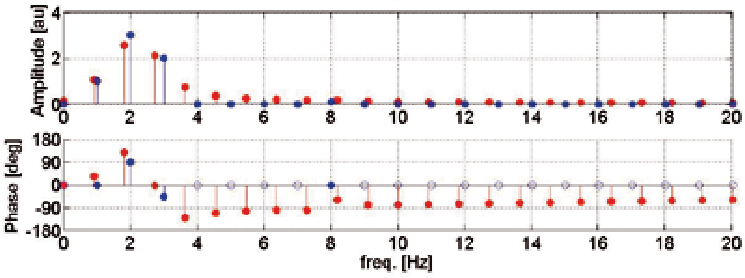

7b

their frequencies will be multiples of $1/T_2$. This series, however, describes a time signal with period T_2, shown as the red curve in Figure 7a. This signal clearly differs from the original signal $x(t)$, which has a period time T of 1 s. The calculated amplitude and phase spectra in Figure 7b in red will differ from the true spectra in blue. This measurement error is called 'leakage' and will always be present unless the length of the measurement record is an exact multiple of the period T of the signal to be analysed. In the frequency analysis of stochastic signals (noise) this error will always occur, since these signals are non-periodic. The leakage error, however, can be reduced by the application of weighting functions.

The Hanning weighting function is a commonly used general purpose weighting function and is defined as:

$$w(t) = \sqrt{(8/3)} \cdot \sin^2(2\pi t/T)$$

Here, T is the record length.

In Figure 8a the weighting function is depicted in black. Applying this weighting function to $x_2(t)$ results in a new time trace $x_{2hanning}(t) = w(t) \cdot x_2(t)$, which represents a signal with reduced discontinuities, see Figure 8a in red. Figure 8b shows the spectra of $x_1(t)$ in blue, $x_2(t)$ in red and $x_{2hanning}(t)$ in black in a logarithmic amplitude format. The leakage error in $x_2(t)$ is clearly visible. This error even obscures the presence of a weak signal component at 8 Hz.

Applying a Hanning weighting function significantly reduces the leakage error, but it cannot be applied to all signals. Since $w(t)$ is not a constant but a function of time, this type of weighting is only allowed for signals with time-independent characteristics. This does not require the signal to be periodic. A noise signal with time-independent mean and variance also fulfils this criterion.

In modal analysis a transient signal (hammer impact) is often used for system excitation. A transient weighting function is applied to improve the signal-to-noise ratio for the analysis of these short transient signals. The transient weighting function is defined as:

$$w(t) = 1 \qquad \text{for } t_0 \le t < t_0 + t_w \text{ and } 0 \le t_0 < T - t_w$$

$$w(t) = 0 \qquad \text{elsewhere}$$

Here, t_0 is the moment the window opens and t_w the length of the window. The system response signal is also a transient and prone to leakage if the system has low damping and must be weighted with an exponential decay window. This window is defined as:

$$w(t) = e^{-(t-t_0)/\tau} \quad \text{for } t_0 \le t < T \text{ and } 0 \le \tau < T$$

$$w(t) = 0 \qquad \text{elsewhere}$$

Here, t_0 is the starting time of the weighting function, τ the time constant and T the record length. Figure 9a shows the transient window and Figure 9b the exponential decay window, both dashed in black.

Signal units

So far the focus was on periodic signals that consist of a series of discrete frequency components with constant amplitudes. Their power distribution over frequency is discrete, so the power is concentrated in infinitesimally narrow frequency lines. The 'strength' of these components is independent of the frequency resolution of the spectrum and can be calculated from the FFT lines like:

$$Ampl(k \cdot \Delta f) = |f(k)| \qquad \text{with amplitude in [units]}$$

or

$$Ampl(k \cdot \Delta f) = |f(k)| / \sqrt{2} \qquad \text{with amplitude in [units RMS]}$$

Here, $f(k)$ is the k^{th} frequency line at $(k-1) \cdot \Delta f$ [Hz].

Signals with a continuous power distribution cannot be quantified with amplitude values. These signals are to be quantified by their Power Spectral Density as function of frequency, $PSD(f)$.
$PSD(f)$ can be calculated from the individual FFT lines by averaging the power per line and scaling it with the equivalent noise bandwidth ENB of the FFT calculation:

$$PSD(k \cdot \Delta f) = \overline{|f(k)|^2} / ENB \qquad [\text{units}^2/\text{Hz}]$$

The ENB depends on the record length and the weighting function used:

$$ENB = \Delta f \cdot window\_factor$$

For a rectangular weighting function (= no weighting function) $window\_factor = 1$, for Hanning $window\_factor = 1.5$.

For signals with a finite total energy, like transients, the Energy Spectral Density as function of frequency $ESD(f)$ can be calculated from the individual FFT lines by averaging the power per line and scaling it with the equivalent noise bandwidth of the FFT calculation and the record length:

$$ESD(k \cdot \Delta f) = \overline{|f(k)|^2} \cdot T / ENB \qquad [\text{units}^2\ \text{s/Hz}]$$

Test signals

Test signals play a decisive role in measuring the FRF of a dynamic system. Important parameters are frequency content, power and amplitude distribution as function of time and the relation between peak value and RMS value (= crest factor).

8a

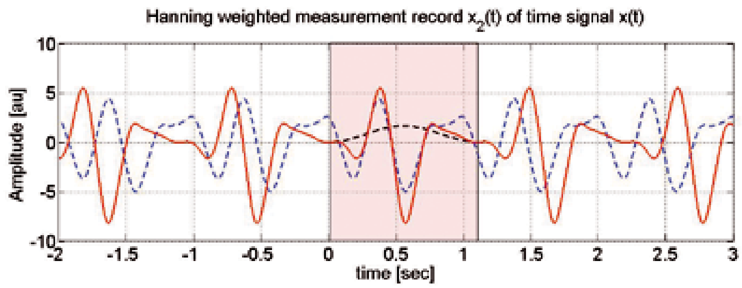

8b

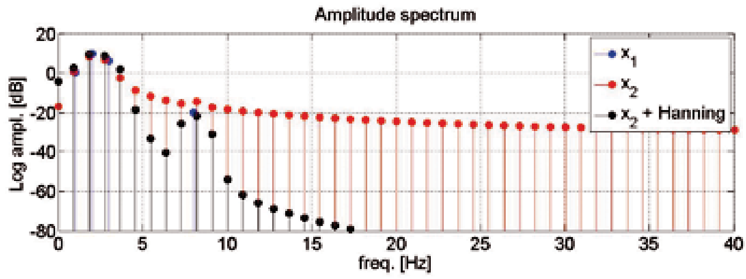

9a

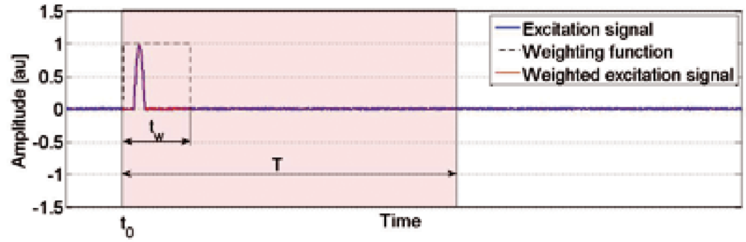

9b

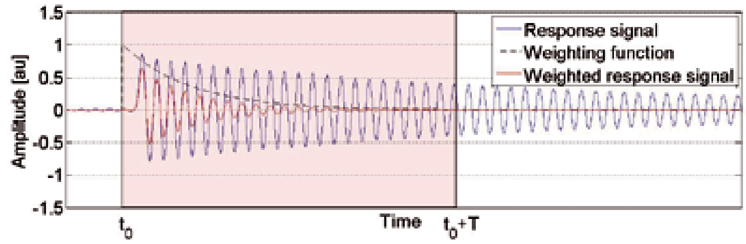

8 *The aim of the Hanning weighting function.*
(a) The function (in black) smoothens out the discontinuities at the beginning and end of the measurement record and thus reduces leakage.
(b) Leakage can obscure signal components.

9 *To be used for transient signals:*
(a) transient weighting function;
(b) exponential decay function.

The most basic test signal is the sinusoid. If the frequency is a multiple of the frequency resolution $\Delta f = 1/T$, then no weighting function is required. The crest factor is only $\sqrt{2}$, which makes it a well-suited signal for testing extremely delicate systems. The sinusoid is ideal for measuring the Higher Order Sinusoidal Input Describing Functions (HOSIDF) to determine nonlinear behaviour, as will be discussed in Part 3 of this series. Since all power is contained in only one frequency line, many measurements are required to cover a frequency range.

Measurement time can be reduced by constructing a test signal that contains power at many frequency lines at the same time. These multi-sine signals can be processed without weighting function if all the frequency components coincide with frequency lines of the FFT. The crest factor can be minimised by manipulating the phase of all frequency components and can even become less than $\sqrt{2}$.

In a special class of multi-sine signals distinct frequency lines do not contain energy. If a nonlinear system is excited by these special odd multi-sines, its response will contain power in the non-excited frequency lines, which serve as detection lines for nonlinear behaviour. It is important to realise that these signals are periodic and thus consist of frequency components with a fixed amplitude and phase. In Part 2 it will become clear that for this reason multi-sines cannot be used for coherence measurements when only one phase realisation is used.

Unlike multi-sine signals, random noise has a continuous spectrum and is not periodic. This results in leakage and so the use of a Hanning weighting function is required. The frequency range can be optimised by filtering. Within this range the PSD can be flat (white noise) or inversely proportional with frequency (pink noise). Noise is uncorrelated with all other signals. The cross-spectrum of noise and any other signal will converge to 0 after averaging, as will be explained in Part 2. This property is used to determine the frequency response function of a system under non-ideal measurement conditions.

The pulse signal differs from the test signals mentioned earlier in the sense that its power distribution over frequency is time-dependent. For modal analysis measurements the pulse is generated by a hammer impact. By changing the hardness of the hammer tip, the frequency range of the pulse spectrum can be influenced. A soft tip will result in a wider pulse, which contains less high-frequency energy. As mentioned in the paragraph on weighting functions, an impact window can be used to increase the signal-to-noise ratio of the measurement. Triggering is important to align the window with the pulse. To capture the total pulse, a pre-trigger delay is required. ■

Summary

Signal	Units	Weighting function	Trigger condition
Sine $f = n \cdot \Delta f$ Sine $f \neq n \cdot \Delta f$	Ampl. [units]	None Hanning	Free run
Multi-sine, linked to Δf	Ampl. [units]	None	Free run
Random	PSD [units^2/Hz]	Hanning	Free run
Pulse	ESD [units^2 s/Hz]	Transient window	Pre-triggered on pulse

Coming up in Part 2

In Part 2 the Frequency Response Function will be introduced as the frequency-domain description of dynamic behaviour of linear dynamic systems. The article will focus on the practical aspects of FRF measurements: choice of test signals, picket-fence effect, measurement noise, and interpretation of the coherence function for detection of nonlinearities. Both open-loop and closed-loop systems will be considered.

LITERATURE

- J.S. Bendat, A.G. Piersol, "Random data: analysis and measurement procedures", Chichester: Wiley-Interscience, 2000, ISBN 0-471-31733-0.
- J.W. Cooley, J.W. Tukey, "An algorithm for the Machine Calculation of Complex Fourier Series", *Math. Comp.* Vol. 19 (90), pp. 297-301,1965.
- R.B. Randall, "Frequency analysis", Naerum: Bruel & Kjaer, 1987, ISBN 87-87355-07-8.

ULTIMATE PRECISION FOR SMARTPHONE LENS ASSEMBLY

As smartphones continue to grow in power and complexity, their manufacturers are demanding ever-greater accuracy and quality from their high-volume production lines. With worldwide sales reaching 1.8 billion units in 2013, this means not only a huge market, but new challenges and opportunities as well for manufacturing solution providers such as IMS.

ILSE BÜTER

AUTHOR'S NOTE

Ilse Büter, M.Sc., is marketing manager at the WWINN Group, to which IMS belongs, in Almelo, the Netherlands.

Each smartphone contains dozens of tiny, complex components. Take its camera lens, for example – not just a lens, but a complex assembly of several lenses, spacers, barrels and other components; see Figure 1. And with each new phone, consumers expect ever improving quality in the photographs they take, placing greater demands on the quality and precision of the lens, and hence on the accuracy of the manufacturing process. At the same time, very large numbers need to come off the production line. To achieve their targets, manufacturers are turning more and more towards automated production.

1 *A smartphone lens. (Photo: MediaXpert)*

At IMS, we design and create systems for such automated manufacture. We use our extensive knowledge and experience of manufacturing and manufacturing processes to create solutions for assembling small, complex products with ultimate precision.

For lens assemblies, we have created a number of production solutions in the form of manufacturing technology and equipment. These have allowed us to reduce the cost price of the lenses while maintaining and even enhancing their quality. We integrate the technologies we develop into manufacturing equipment suitable for use in ISO Class 7 cleanroom environments. The equipment itself operates under ISO Class 5 conditions.

In this article we present two case studies, from the micron to the nanometer range, that describe in more detail what is required to meet the high demands on the automated manufacture of optical components.

Case study 1: Positioning in the micron range

Through the innovative use of state-of-the-art technologies, we developed and produced a manufacturing solution with a robust design in which we use optical systems to allow us to see accurately where a component is located, and linear motors to move and position it with high precision. A complete lens assembly is produced by this equipment every two seconds.

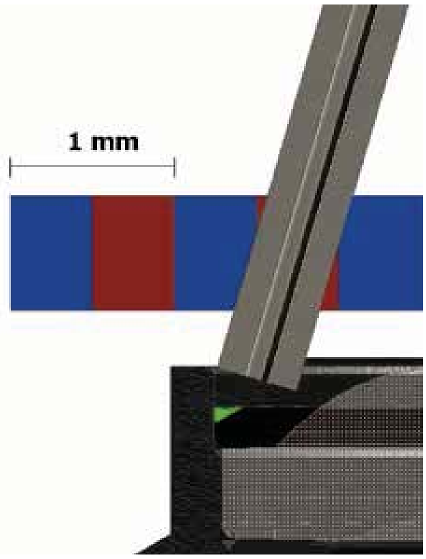

2

3

2 *Adhesive track in a lens assembly.*

3 *The IMS ProMu platform. (Photo: MediaXpert)*

The components are supplied from bulk or tray, or they are produced on the line itself. The extremely precise inline manufactured parts are cut from reel in a die set with a cutting play of 0.5 microns. The combination of optical systems and linear motors is used to orientate, centre and position the components with an X-Y accuracy of 1 micron within a 3-sigma range.

Optics and linear movement

For the project, we developed a special optical system that is the core of the overall positioning system. This system uses negative perspective that allows us seeing two components lying on top of each other in one shot, even if the components have exactly the same dimensions. With the image generated using the optical system, the relative offset between the two components is calculated and used to align them with great precision. If the components have moved, the appropriate correction is applied to both equally.

In a subsequent step, the components are then placed extremely accurately on or in each other. A custom-made linear motor positions the parts relative to each other with 0.5 micron accuracy.

This approach has major advantages: cycle time is reduced because only a single image is needed to calculate an offset, and neither vibration nor temperature drift affects the process. This results in minimal interference and an increase in process reliability.

Adhesive dispensing

Another process handled by this equipment is the dispensing of the adhesive that attaches the components to each other. A trace of adhesive with a thickness of 0.1 mm is dispensed onto the side of the top component of the lens assembly. This must all be achieved within the fixed cycle time of 2 seconds per complete lens assembly. Due to the extremely accurate alignment, the dispensing process can be performed so precisely that the adhesive track is placed at exactly the right location. This allows ensuring a very large usable lens surface and also the use of less adhesive than would be the case without such precise alignment. This is a major improvement compared to the process currently being used by the manufacturer. See Figure 2 for the size of the adhesive track (in green) relative to the lens components.

Modular platform

The IMS ProMu modular platform is the basis for the complete lens manufacturing process. This platform (Figure 3) has a pre-positioning accuracy of 0.02 mm, with fine-positioning to sub-micron accuracy. We can achieve such high accuracy since positioning is unaffected by temperature and vibration variations or differences, which remain under tight control within the platform. The platform design is modular, so multiple platforms can be connected to each other. Another aspect of this modularity is that process units are interchangeable. Platforms can also be easily extended to produce larger numbers or convert them to produce a different product type, for example.

The solution in this case study uses precise positioning by means of an extremely accurate die set, optical systems and linear motors. Combining these with the convenience of a modular platform allows us to simultaneously perform the processes ten times in the manufacturing solution. By using a modular platform and proven technology, the manufacturing solution is also future-proof.

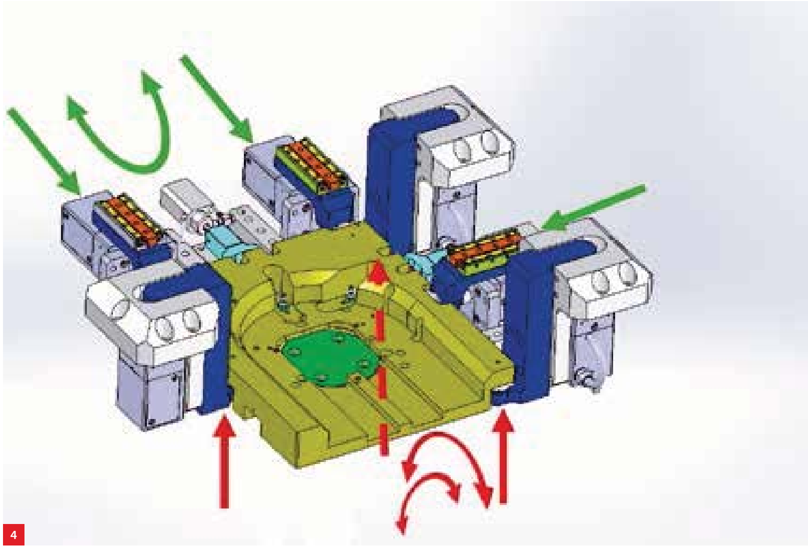

4

Case study 2: Positioning in the nanometer range

In another project, we developed a solution for the precise alignment of optical wafers. We designed and produced the manufacturing equipment with a combination of specialised measurements and process technologies that would go beyond micron accuracy and into the nanometer range.

Interferometry and 6-DoF

The optical wafers are supplied in bulk and pre-oriented at 20 microns. To align them, an interferometer is used in combination with a 6-DoF (Degrees of Freedom) platform. The interferometer is a highly accurate measurement instrument that uses the superposition of electromagnetic waves to measure distances with wavelength precision. The nanosteppers that drive the platform are custom-developed; see Figure 4.

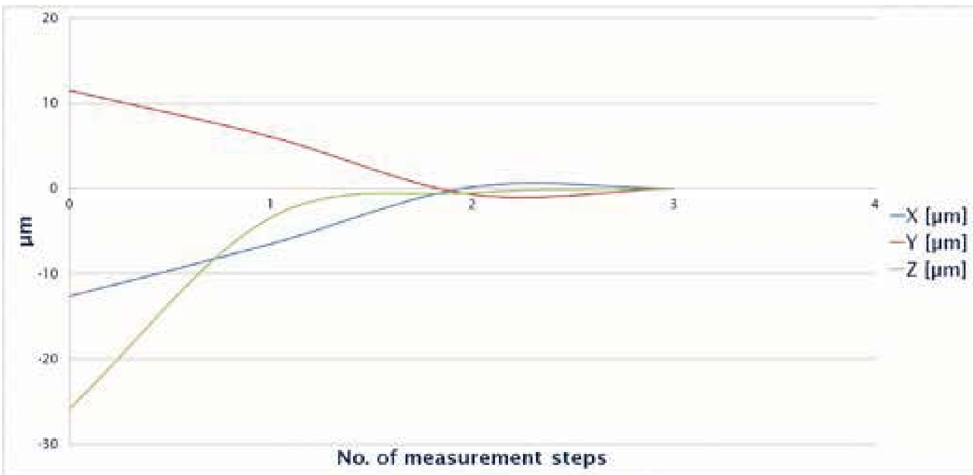

5a

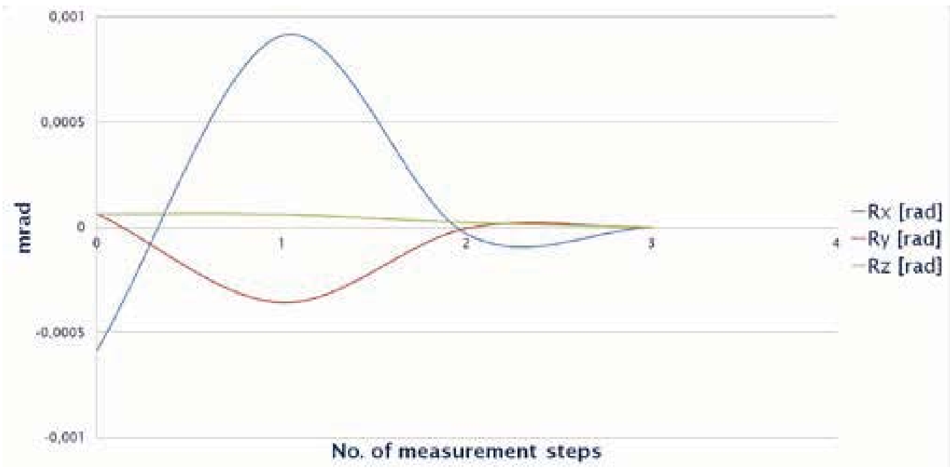

5b

4 *6-DoF platform with nanosteppers.*
5 *Results of interferometric measurement of the deviation of a wafer.*
(a) Accurate alignment x-y-z movement.
(b) Accurate alignment rotation.

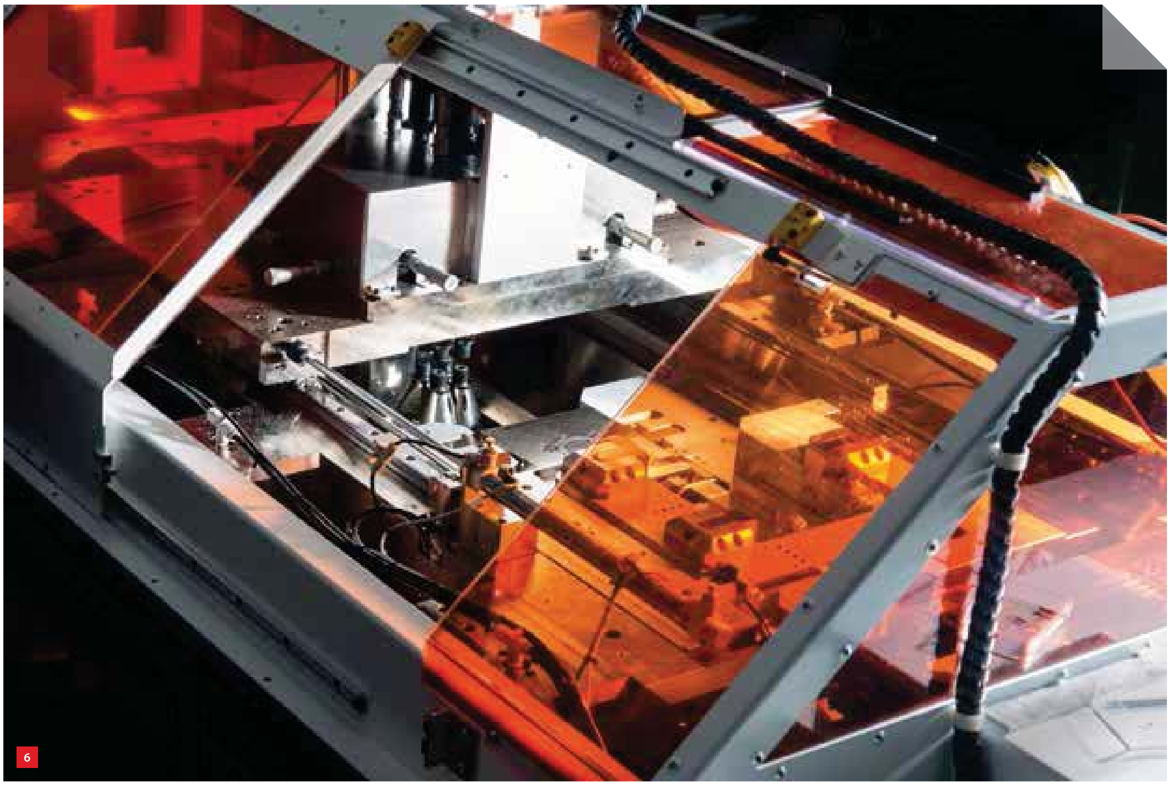

6 *Equipment for optical wafer stacking. (Photo: MediaXpert)*

The optical wafers are then placed on two 6-DoF platforms, and the interferometer is used to measure the deviation of the wafers; see Figure 5. Four points on the wafer are measured and converted to centre coordinates, in terms of X, Y, Z, RX, RY and RZ. Based on these measurements and the centre coordinate, the corrections are calculated. And these corrections are applied by the nanosteppers. These nanosteppers have a closed-loop resolution of 5 nm, which all results in a 100 nm positioning accuracy of the wafers on the platform in the horizontal and vertical plane.

Drift

The reliability of the manufacturing equipment is dependent mainly on the values of drift. Drift is caused by variations in thermal expansion of the parts in the equipment. To reduce this drift and increase manufacturing accuracy, vibrations and fluctuations in temperature must be carefully controlled. The part of the equipment where measurements are made is suspended in a subsystem to prevent disturbance from environmental vibrations, while the temperature in the equipment is kept constant to within 0.1 °C. The resulting drift spec in the equipment is extremely low; just 0.05 nm per hour.
Figure 6 shows the final realisation of the equipment for optical wafer stacking. As input for the measurement system, we also developed equipment for the automatic molding of the optical wafers.

Conclusion

With a specific request for a manufacturing solution, IMS utilises existing technology and further develops it. Adding in our own technology then allows us to achieve an overall solution that is much more specific to the particular requirements than existing solutions and that achieves better results than could be achieved with standard components. ■

IMS

IMS designs and realises innovative, turnkey solutions for manufacturing small, complex components. These solutions are applied at manufacturing companies in the automotive, consumer electronics and medical industries. Examples of small, complex components are camera lenses in mobile phones and lenses in endoscopic instruments.
IMS has two specialist units: IMS Leading Value for realising turnkey manufacturing equipment, and IMS Research for innovative product and process development that makes products suitable for production. IMS works with specialised co-developers to develop high-end technologies for its manufacturing solutions.
IMS is part of the WWINN Group, based in Almelo, the Netherlands.

WWW.IMS-NL.COM

ELIMINATING SHAKING FORCES AND MOMENTS

Shaking forces and shaking moments in high-speed machines and manipulators are a significant cause of base vibrations. These vibrations can be eliminated by designing the manipulator to be shaking-force balanced and shaking-moment balanced, or in short: dynamically balanced. The design and experimental results of a high-speed dynamically balanced parallel manipulator are presented, showing the potential of dynamic balance for machine design.

VOLKERT VAN DER WIJK

AUTHOR'S NOTE

Volkert van der Wijk is a researcher in the Laboratory of Mechanical Automation and Mechatronics at the Faculty of Engineering Technology, University of Twente, in Enschede, the Netherlands. Here, he recently obtained his Ph.D. [1]. This text is an abridged version of [2].

v.vanderwijk@utwente.nl
www.utwente.nl/ctw/wa

Introduction

When machines and manipulators move at high speeds, for instance for pick & place tasks, they exert large dynamic reaction forces – shaking forces – and dynamic reaction moments – shaking moments – to their base. This leads to significant vibrations of the base (frame), of equipment attached to the base (e.g. metrology tools), of the floor, and of other devices on or near the vibrating floor. The machines' precision and accuracy then are reduced, sensors are disturbed, and cycle times are increased since more waiting time is required for vibrations to die out.

To reduce the influence of base vibrations, damping and vibration isolation can be applied. A solution that eliminates the vibrations at its roots is to design the manipulator dynamically balanced, so that the base vibrations do not exist at all. In a dynamically balanced manipulator all elements move such that the sums of dynamic reaction forces and moments on the base are zero. A dynamically balanced manipulator therefore does not need a stiff and heavy frame. Ideally, it solely requires the support of a single cable to compensate for gravity, while it runs at high speeds with high precision.

This article shows how a dynamically balanced parallel manipulator can be designed and tested. For the first time experimental results of a dynamically balanced high-speed manipulator are presented, with which the potential of dynamic balance for machine design is shown.

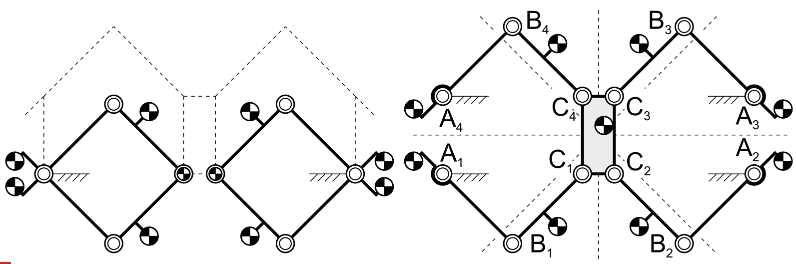

1 *Inherently dynamically balanced 4-RRR parallel manipulator (right) obtained by combining two balanced pantographs that are placed oppositely of one another (left), where each pantograph is divided in two with the platform connecting the parts together.*

Design

A common mistake in the design of manipulators is that first solely the kinematics are considered. A mechanism geometry is selected and optimised for an intended task. When subsequently the dynamics, in particular the dynamic balance, are considered, the possible solutions become limited and are likely to not be advantageous. Therefore, it is of significant importance to consider dynamic balance already at the very beginning of the design process.

To do this, it is proposed to synthesise a balanced manipulator from inherently balanced mechanism architectures, which are basic force-balanced linkages of which the kinematics can be adapted in various ways while maintaining force balance and obtaining moment balance [1] [3]. A force-balanced pantograph is an example of such an inherently balanced linkage. Figure 1a shows two force-balanced pantographs that are placed oppositely of one another and are combined to obtain the balanced 4-RRR

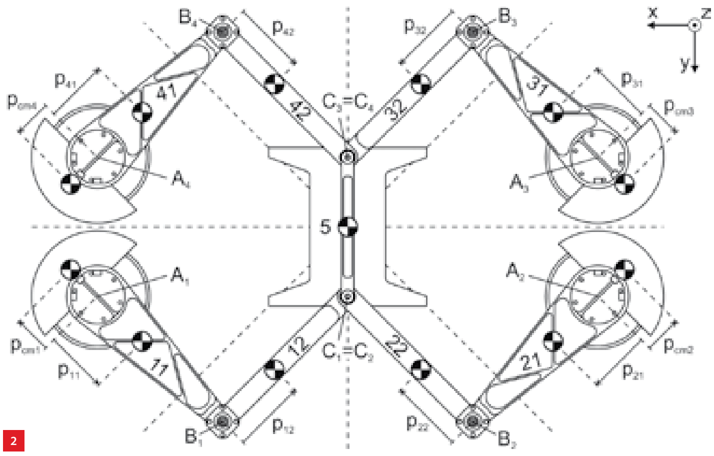

2

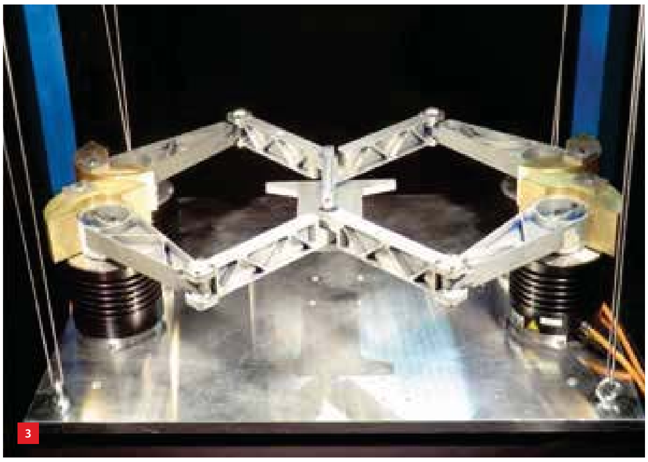

3

parallel manipulator in Figure 1b. Then each pantograph includes part of the mass of the platform and is divided in two with the platform connecting the parts together. As long as the relative motions of the elements are not changed, which is the case for all translational motion of the platform, force balance is maintained too.

Figure 2 shows the CAD of the balanced planar 4-RRR manipulator that was developed and built. For optimal force transmission to the platform and for compactness, the platform was reduced kinematically to a link with two double revolute pairs on each side (C_1 and C_2 coincide with C_3 and C_4, respectively). This configuration will be named the DUAL-V manipulator. The conditions for force balance of the DUAL-V are:

$$\begin{aligned} m_{11}p_{11} + m_{12}l_{11} + m_{42}p_{42} + m_5 l_{11}/2 &= m_{cm,1}p_{cm,1} \\ m_{21}p_{21} + m_{22}l_{21} + m_{32}p_{32} + m_5 l_{21}/2 &= m_{cm,2}p_{cm,2} \\ m_{31}p_{31} + m_{32}l_{31} + m_{22}p_{22} + m_5 l_{31}/2 &= m_{cm,3}p_{cm,3} \\ m_{41}p_{41} + m_{42}l_{41} + m_{12}p_{12} + m_5 l_{41}/2 &= m_{cm,4}p_{cm,4} \end{aligned} \qquad (1)$$

2 *CAD of the balanced DUAL-V manipulator (patented [4]).*

3 *Prototype of redundantly actuated balanced DUAL-V manipulator with counter-masses about the fixed pivots.*

4 *Definition of the DUAL-V manipulator.*
(a) Kinematic variables and parameters of the base.
(b) Workspace.

Figure 3 shows the prototype of the DUAL-V manipulator which was fabricated with the parameters in Table 1. These parameters and the kinematic variables of the manipulator are illustrated in Figures 2 and 4. All arm links $i1$ and $i2$ have equal lengths l_{i1} and l_{i2}, respectively, the fixed pivots are located at distances $a = l_{i1}\sqrt{2}$ and b with respect to the centre, and the platform link 5 has a length $l_5 = 2b$. The theoretical workspace of the manipulator for the given dimensions is shown in Figure 4b and consists of the intersection of two circles with radii $l_{i1} + l_{i2} = 0.56$ m, of which the maximal width along x is $2(l_{i1} + l_{i2} - a) = 0.328$ m, and the maximal width along y is $2\sqrt{[(l_{i1} + l_{i2})^2 - a^2]} = 2a = 0.792$ m.

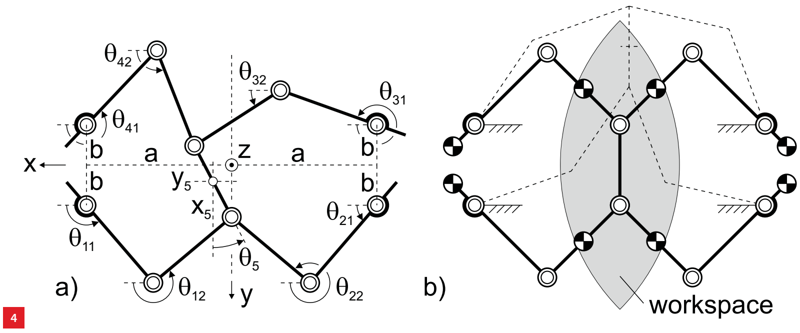

4

Table 1. DUAL-V parameters.

[m]	[kg]	[kgm²]	[m]
l_{i1} = 0.2800	m_{i1} = 1.169	I_{i1} = 0.012967	p_{i1} = 0.0737
l_{i2} = 0.2800	m_{i2} = 0.606	I_{i2} = 0.006417	p_{i2} = 0.1279
l_5 = 0.2200	m_5 = 0.899	I_5 = 0.008168	
a = 0.3960	$m_{cm,i}$ = 7.983	$I_{cm,i}$ = 0.026845	$p_{cm,i}$ = 0.0575
b = 0.1100	$m_{tun,i}$ = 0.188	$I_{tun,i}$ = 0.004100	$p_{tun,i}$ = 0.080

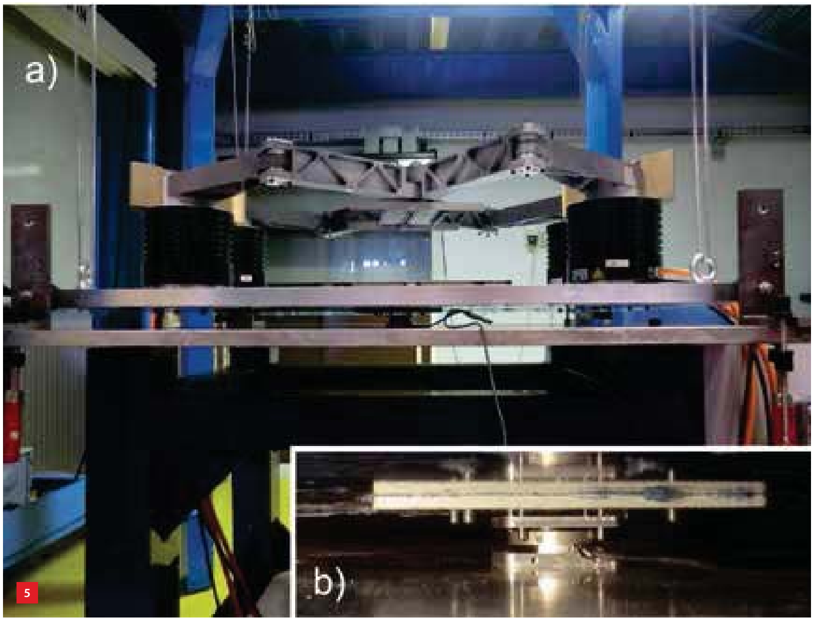

5 *The balanced DUAL-V manipulator prototype suspended by cables and mounted on a six-axis force/torque sensor for measurement of the in-plane shaking forces and shaking moment.*
(a) Experimental set-up.
(b) Close-up of sensor mount.

The links of the manipulator were made of aluminum and the counter-masses were designed with circular brass segments. The main aim of the design of the counter-masses was to have the reduced inertia $I_{cm,i} + m_{cm,i}\, p^2_{cm,i}$ of each counter-mass relative to A_i be as low as possible, since this is advantageous for low actuator torques [5]. Therefore, a high mass of each counter-mass with its centre of mass as close to A_i as possible is needed. A counter-mass material with high density such as brass and a design which can be large in the out-of-plane direction (thick counter-masses) therefore are advantageous.

Each counter-mass was designed such that part of its mass $m_{tun,i}$ = 0.188 kg is a separate element made of lead, placed at a distance $p_{tun,i}$ = 0.080 m from A_i on top of the brass segments. This was done to fine-tune the counter-masses, compensating for production inaccuracies and to be able to remove a small mass for experiments investigating the balance performance with non-perfect counter-masses. The mass and inertia of these tuning masses are included in the parameters $m_{cm,i}$ and $I_{cm,i}$ in Table 1.

With an actuator in each of the four pivots with the base, the manipulator has one degree of actuation redundancy. This is advantageous, since manipulators with actuation redundancy have an increased acceleration capability and have more homogeneous dynamic characteristics (e.g. force transmission to the platform) throughout the workspace [6].

Since all links have equal lengths, links A_iB_i have equal inertia, and links B_iC_i have equal inertia, the DUAL-V is shaking-moment balanced for motion along the orthogonal axes in Figure 2 with non-rotated platform. Since for small rotation motion of the platform and for motion around the orthogonal axes the links remain close to parallel, it can be expected that the obtained force and moment balance still is significant. In fact, motion with a non-rotated platform along the diagonal axes in Figure 2 is near to exact dynamic balance since the links counter-rotate almost linearly with one another.

Experimental set-up

The experimental set-up is shown in Figure 5a. The manipulator was mounted on four ETEL RTMB0140-100 direct-drive actuators, which could deliver maximum torques of 127 Nm. The actuators were mounted on an aluminum base plate of 1.0 m x 0.8 m with a thickness of 25 mm. The unbalanced manipulator for comparison was the same manipulator but without the counter-masses, and for evaluation of the sensitivity of the counter-masses to the shaking forces and the shaking moment, the tuning masses of lead were removed from the brass elements.

To measure the shaking forces and the shaking moment of the manipulator in the horizontal plane, an ATI mini 45 six-axis force/torque sensor was positioned and centred between the base plate and the fixed frame, as shown in Figure 5b. This sensor could measure a maximum of 500 N shaking force in both x and y direction and 20 Nm shaking moment with a measurement noise that was estimated to be about 3 N and 0.02 Nm. To unload the sensor from the gravity force, to align it horizontally, and to prevent damage during assembly, the base plate was suspended by four cables to float just above the sensor. Four pins fixed the sensor with respect to the base plate for in-plane motion while translation in vertical direction was not restricted.

Experiments and experimental results

For motion of the centre of the platform along the orthogonal axes and without platform rotation, the unbalanced manipulator is expected to exhibit shaking forces and a zero shaking moment – the latter because of the symmetric design. The balanced manipulator is expected to have zero shaking forces and a zero shaking moment.

Columns three and five in Figure 6 show the measured shaking forces and shaking moment of the unbalanced and the balanced manipulator, respectively, for the motion shown in column 1 (note: see video at www.ijrr.org/ijrr_2013/484183.htm). This motion has a maximum acceleration of 51 m/s^2 in both directions and 43 rad/s^2

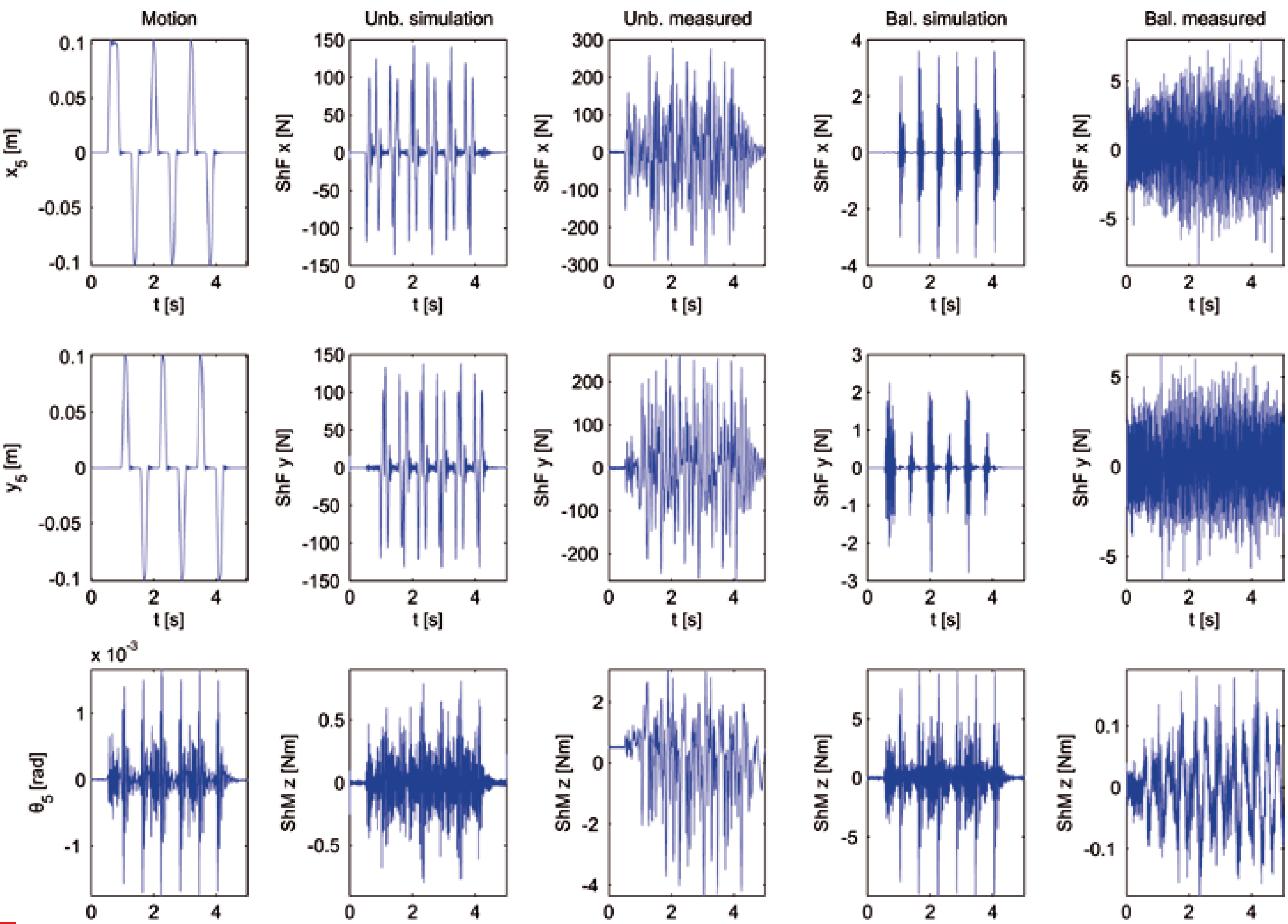

6

rotationally, which therefore is not perfectly balanced motion along the orthogonal axes. For validation, the shaking forces and the shaking moment of the unbalanced and the balanced manipulator from simulation of the measured motion are shown in columns two and four, respectively. From the design of the manipulator the shaking forces of the unbalanced manipulator are expected to be 167 N in both directions.

To evaluate the sensitivity of the balance masses, the tuning masses were removed from each counter-mass for which each product $m_{cm,i}\, p_{cm,i}$ is 96.72% of the value for perfect balance, in other words, there is a 3.28% balance inaccuracy.

The results in Figure 7 also represent the influence of payload on the platform. An equal 3.28% balance inaccuracy is also obtained by placing 0.107 kg in the centre of the platform, instead of leaving the tuning masses out. By moving this mass with 186 m/s^2 along x, a shaking force of $186 \cdot 0.107 = 20$ N is expected.

Since the balance masses add inertia to the manipulator, the balanced manipulator is expected to require higher actuator torques. For the motion with maximum accelerations of 66 m/s^2 along x, 63 m/s^2 along y, and 129 rad/s^2 rotationally along a triangular trajectory with equal sides of 0.173 m, the measured actuator torques of the unbalanced manipulator and the balanced manipulator are shown in columns one and two of Figure 8, respectively. Column three shows the theoretical actuator torques of both manipulators calculated from the inverse dynamic model for equal input motion. The smaller curves represent the unbalanced manipulator.

The improved mass distribution due to the counter-masses is expected to have an advantageous influence on the bearing forces of the balanced manipulator. For simulations of the motion with maximum accelerations of 66 m/s^2

6 Results from simulation and experiments of the unbalanced and the balanced manipulator for the measured motion in column one.

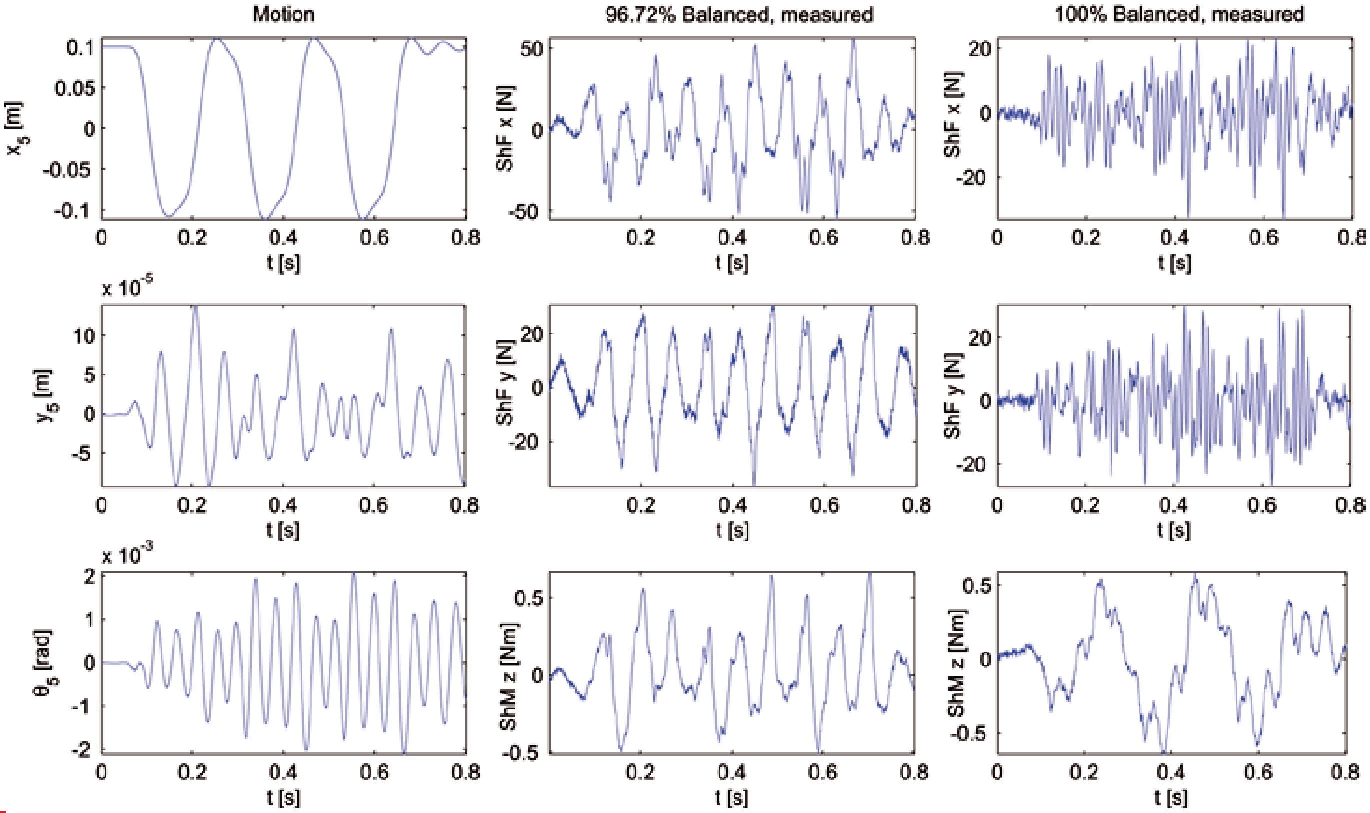

7

along x, 63 m/s² along y, and 129 rad/s² rotationally along a triangular trajectory with equal sides of 0.173 m, columns one and two in Figure 9 show the bearing forces from simulation of the measured motion of the unbalanced and the balanced manipulator, respectively. For validation, columns three and four show the results from simulation of smooth motion along the triangular trajectory with equal maximum accelerations.

7 *Experimental results of the 96.72% balanced manipulator and of the fully balanced manipulator for the motion in column one.*

Discussion

Shaking forces and shaking moments

The measurements in Figure 6 show a significant reduction of the shaking forces of the balanced manipulator. While for the unbalanced manipulator the maximum measured shaking forces are 302 N along x and 263 N along y, the balanced manipulator has maximum shaking forces of 8.4 N along x and 6.4 N along y, being close to the noise level of the sensor. This means a reduction of 97% and 98% of shaking forces along x and y, respectively. The shaking forces of the balanced manipulator are non-zero mainly due to the rotational motion of the platform, since at high speeds the PID-controller allowed significant trajectory deviations.

From simulation of the measured motion, the maximum shaking forces of the unbalanced manipulator are about 142 N along x and 138 N along y (column three), while for the balanced manipulator they are about 3.7 N along x and 2.8 N along y (column four). Also, for these values the reduction of shaking forces is 97% and 98% along x and y, respectively; however the values differ significantly from the measured maximum values.

Also, both values of the unbalanced manipulator differ from the expected 167 N shaking forces. Most likely this is caused by the calculations of the derivative (velocity) and the second derivative (acceleration) of the measured motion, which are needed for the inverse dynamic model. Since the derivatives of the measured position information result in unrealistically high values, the values were filtered with a first-order low-pass filter. However, the simulation results show that this is not sufficient. In addition, the mentioned maximum accelerations were obtained from these derivatives, which explains why the expected shaking forces are closer to the results of the simulation of the measured motion.

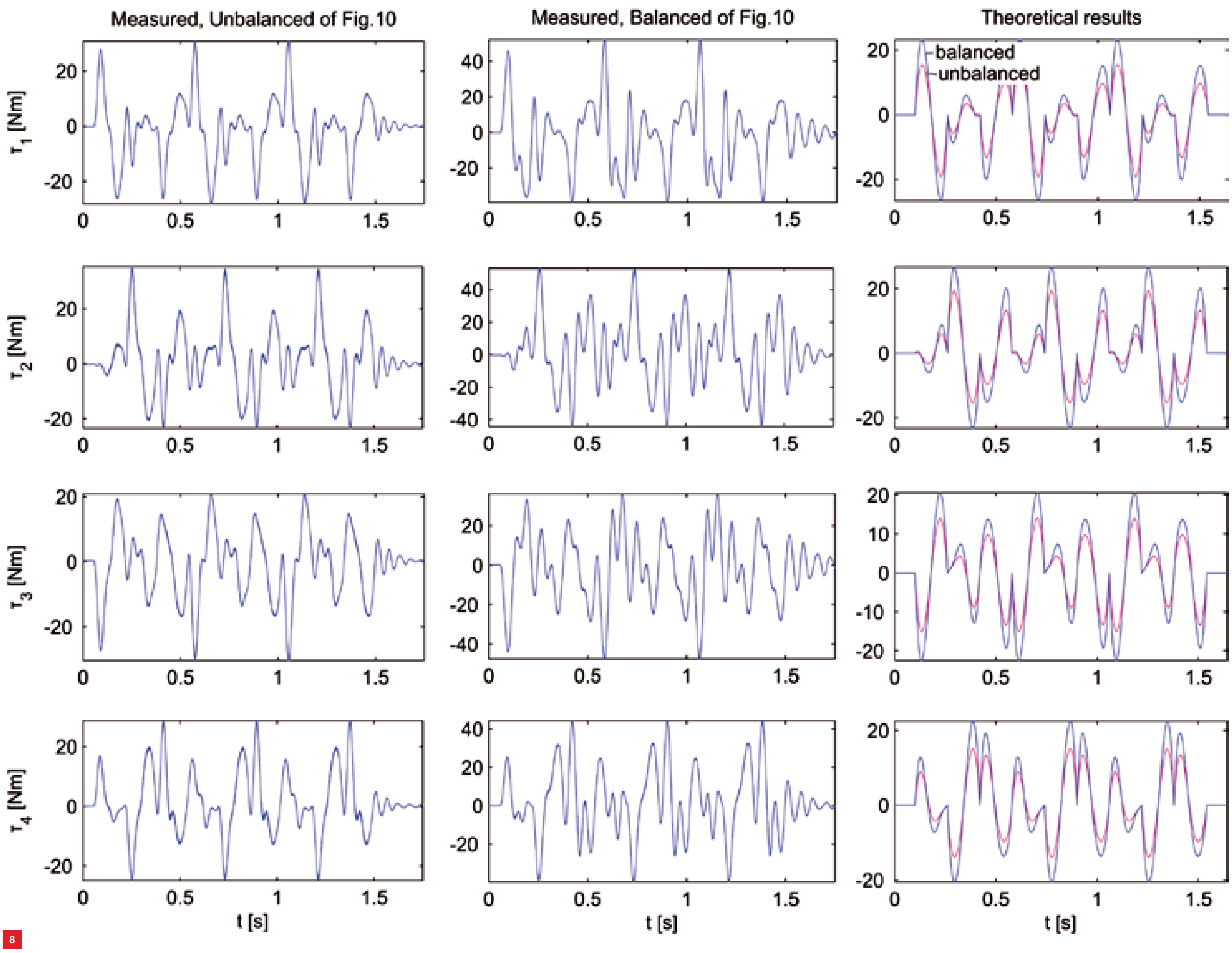

8

8 *Torque results for the motion with maximum accelerations of 66 m/s^2 along x, 63 m/s^2 along y, and 129 rad/s^2 rotationally along a triangular trajectory with equal sides of 0.173 m.*

The measured shaking moment of the unbalanced manipulator has a maximum value of 4.3 Nm, while for the balanced manipulator it is at most 0.19 Nm, which is 96% lower. It is likely that the measurements of the unbalanced manipulator are affected significantly by frame vibrations. In the experimental set-up the relatively large inertia of the manipulator with the base plate in combination with the stiffness of the force/torque sensor caused the base plate to rotate in the lowest eigenmode with measured eigenfrequency of about 3.4 Hz. This may have caused interference of the relatively high shaking forces with the measured shaking moment.

The simulation results of the shaking moment (columns two and four) are dramatically affected by the mentioned differentiation problem. Although the values of the unbalanced manipulator could be realistic, the values of the balanced manipulator are, with a maximum value of 10 Nm, significantly higher as compared to the measured values. The shaking moment is obtained from the simulation as the sum of the actuator torques together with the moments created by the individual reaction forces in A_i with respect to the centre. Due to the differentiation problem, all individual reaction forces are affected, for which the resulting shaking moments become useless.

Measurements for the motion along the triangular trajectory showed 93% and 94% reduced shaking forces and 16% reduced shaking moment for the balanced manipulator.

Sensitivity to balance inaccuracy and payload

The sensitivity of the dynamic balance was investigated for a balance inaccuracy of 3.28%, representing the effect of

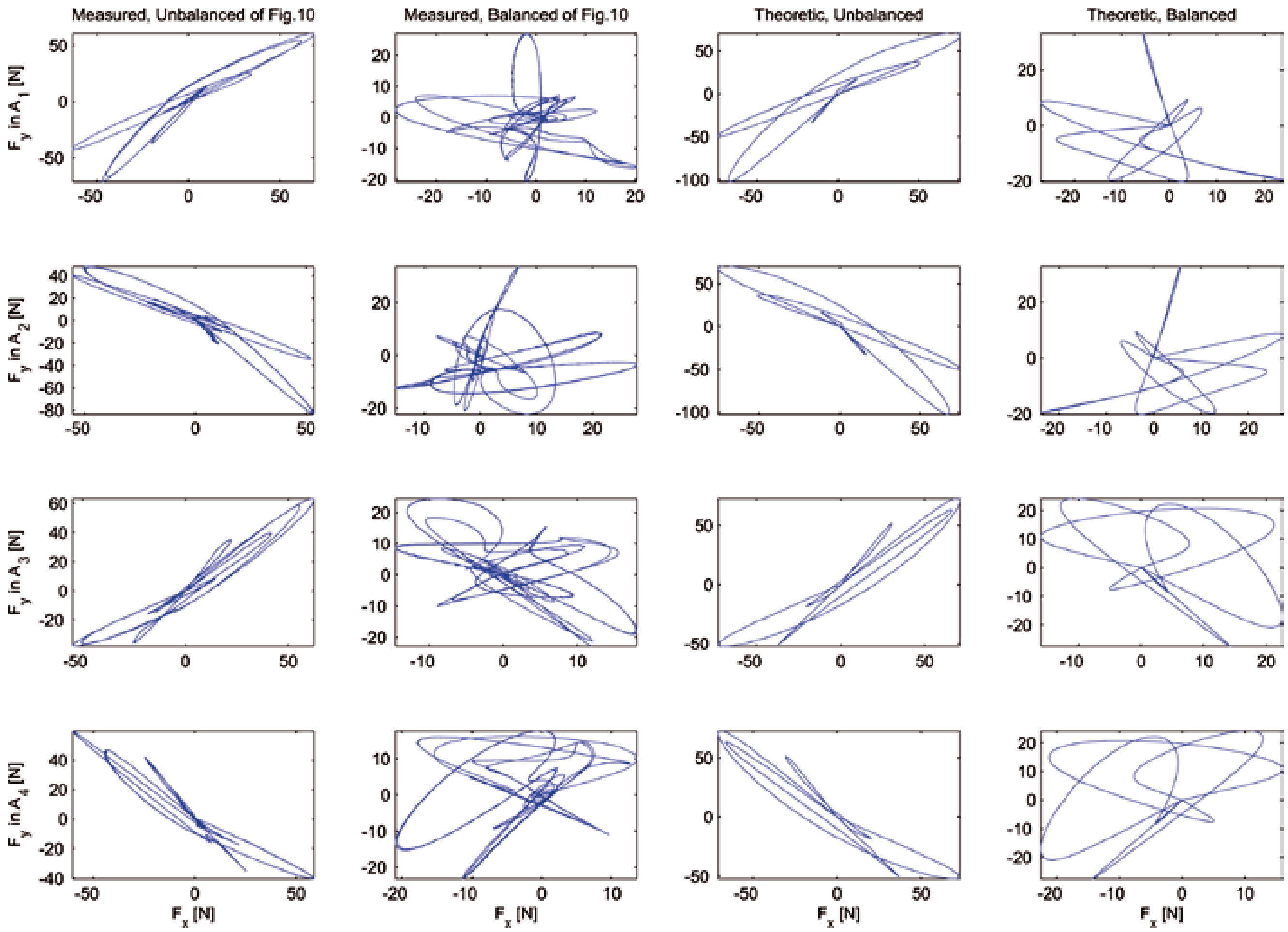

9

9 *Bearing force results for the motion with maximum accelerations of 66 m/s² along x, 63 m/s² along y, and 129 rad/s² rotationally along a triangular trajectory with equal sides of 0.173 m.*

inaccurate counter-masses that are 0.188 kg too lightweight or of a payload of 0.107 kg on the platform. The results in Figure 7 show that the shaking forces increase from maximum values of 33 N along x and 30 N along y (column three) to maximum values of 57 N along x and 37 N along y (column two). This means an increase of shaking forces of 73% along x and 23% along y. The difference in shaking force along x is 57 – 33 = 24 N and close to the expected 20 N shaking force for the 3.28% balance inaccuracy. The maximum shaking moment shows to be reduced from 0.64 Nm (column three) to 0.56 Nm (column two), which is a reduction of 13%.

Due to the PID-controller that allowed the manipulator to move not perfectly along the desired trajectories, from the results in Figures 6 and 7 the sensitivity to motion inaccuracy can also be inferred. For imperfect motion along the orthogonal axes, Figure 6 shows that a shaking moment exists, however it remains relatively small. The sensitivity to rotation of the platform is shown too. Small rotations of the platform can already contribute significantly to the shaking forces, since the measured shaking forces of the balanced manipulator in Figures 6 and 7 are not zero as expected.

Altogether it can be concluded that small inaccuracies of the counter-masses, of unbalanced payload on the platform, and of platform rotations can already lead to considerable vibration for high-speed manipulations, although they remain significantly lower as compared to the unbalanced manipulator. Therefore, high accuracy in the design, production, and control of a balanced manipulator is important for optimal dynamic balance.

Actuator torques

The measured actuator torques in Figure 8 show that the torques required to move the balanced manipulator are higher than the torques of the unbalanced manipulator. The maximum values of the torques τ_1, τ_2, τ_3, and τ_4 of the unbalanced manipulator are 31, 35, 30, and 29 Nm, respectively, and of the balanced manipulator they are 52, 53, 47, and 44 Nm, respectively. This means that for the balanced manipulator they are 1.68, 1.51, 1.57, and 1.52 times the torques of the unbalanced manipulator, respectively, which is on average 1.6x higher.

From the theoretical results in column three in Figure 8, the maximum torques τ_1 and τ_2 are both 1.42 times higher, being 27 Nm, and the maximum torques τ_3 and τ_4 are both 1.47 times higher, being 22 Nm, which is on average 1.4x higher for the balanced manipulator. The actuator torques from the theoretical results are lower than the measured torques, which may be caused by the high torques that the PID-controller calculates to correct the output motion, and by friction, which was not included in the calculations with the inverse dynamic model.

Bearing forces

The bearing forces shown in columns one and two in Figure 9 were derived from the simulation of the real motion following the mentioned triangular trajectory. For simulation of precise motion along the triangular trajectory with equal accelerations, columns three and four of Figure 9 show the bearing forces of which the shapes and size are comparable with columns one and two. From both simulations it is found that the maximum bearing forces in A_1 and A_2 are 73% lower and in A_3 and A_4 they are 69% lower for the balanced manipulator. The maximum forces were calculated as max $\sqrt{(F_x^2 + F_y^2)}$ in each bearing. The lower bearing forces imply that the balanced manipulator has increased stiffness characteristics.

Conclusion

A prototype of a dynamically balanced redundant planar 4-RRR parallel manipulator in an experimental setup was designed and presented for evaluation and comparison with the unbalanced manipulator. The prototype manipulator successfully performed high-speed motion with low base vibration. Experiments showed that the balanced manipulator has about 97% lower shaking forces and a 96% lower shaking moment for motion along the orthogonal axes. For motion throughout the workspace, the balanced manipulator showed about 93% lower shaking forces and 16% lower shaking moment. Since the PID-controller allowed small rotational motion of the platform, causing shaking forces, it is expected that these values are reduced further with improved control of the rotation of the platform.

A relatively small balance inaccuracy of 3.28%, representing too light counter-masses or an unbalanced payload on the platform, was shown to increase the shaking forces considerably, while they still remain significantly lower as compared to the unbalanced manipulator. For a manipulator with optimal dynamic balance, accurate design and production therefore are important. The actuator torques of the balanced manipulator were shown to be about 1.6x higher than for the unbalanced manipulator and the bearing forces of the balanced manipulator were shown to be about 71% lower than for the unbalanced manipulator.

Acknowledgement

For their collaboration and support, the author likes to extend his appreciation to the industrial partners in the dynamic balance research: Stamhuis Lineairtechniek, Control Techniques (now part of Emerson Industrial Automation), Masévon Technology, Ternet, Blueprint Automation, and Penta Robotics. ■

REFERENCES

[1] Van der Wijk, V., "Methodology for analysis and synthesis of inherently force- and moment-balanced mechanisms – theory and applications", Ph.D. thesis, University of Twente, ISBN 978-90-365-3630-1, DOI 10.3990/1.9789036536301 (2014).

[2] Van der Wijk, V., Krut, S., Pierrot, F., Herder, J.L., 2013, "Design and experimental evaluation of a dynamically balanced redundant planar 4-RRR parallel manipulator", *Int. J. of Robotics Research* 32(6) pp. 744-759.

[3] Van der Wijk, V., Herder, J.L., "Synthesis method for linkages with center of mass at invariant link point - pantograph based mechanisms", *J. of Mechanism and Machine Theory*, Vol. 48, pp. 15-28 (2012).

[4] Van der Wijk, V., Krut, S., Pierrot, F., Herder, J.L., "Manipulator comprising a fixed base and a movable platform, with four motor-driven chains of articulated links", Patent WO2012/173471A1 (2012).

[5] Van der Wijk, V., Demeulenaere, B., Gosselin, C., Herder, J.L., "Comparative analysis for low-mass and low-inertia dynamic balancing of mechanisms", *Mechanisms and Robotics* 4(3, 031008) (2012).

[6] Corbel, D., Gouttefarde, M., Company, O., Pierrot, F., "Towards 100G with PKM. Is actuation redundancy a good solution for pick-and-place?", *Proc. IEEE Int. Conf. on Robotics and Automation*, Anchorage, USA (2010).

'Fabricated', The New World of 3D Printing

This well-written paperback (302 pages; £19) explores in an interesting and realistic style the wide-ranging modern world of digital additive manufacturing (AM) in terms of people and processes. In particular, it offers an insight into the technology of three-dimensional micro- and macroprinting. This 3DP process – which is coming of age at the speed of light as could recently be seen at the RapidPro 2014 event in Veldhoven, the Netherlands – has already grown beyond the prototyping stage.

The book puts the nowadays rather over-promoted DIY-hype in the right perspective without downgrading this potentially strong technological innovation. It also addresses the many drastically changing economical, technological, legal, ethical, environmental, health and safety issues, and industrial challenges and implementations, raised by an upcoming open self-producing society – whether industrial or 'home professional' – with 'copycat features'. These important aspects are touched upon in a broader sense than is generally the case.

For the more technically interested readers, 3D-printing one-of-a-kind products layer-wise directly from 3D CAD files – in plastics, ceramics, metals and, already quite common, (bio) materials – is worked out in its numerous different core appearances. The selectively depositing or binding technology is evolving at such a rapid pace – into 'everyday' medical, dental, and general public applications (even man-on-the-moon parts and confectionery) – that some innovative industrial developments could not be mentioned.
One 'out of the book' example is a brand-new 5-axis Lasertec machining centre as a hybrid platform for 3D laser cladding in combination with intermediate, precise milling to mirror-like qualities. This is achieved with up to 20 times faster nozzle-deposited metal powder (compared to traditional powder bed 3DP) for high-tech repair and refurbishing applications, low-wear or corrosion-free cladding (even on new moulds, tools and parts) and low-volume, high-end, functionally intricate geometries with a high added value.
Three dimensional printing of parts on a micro- and precision scale is hardly touched upon, as this is the realm of just a few specialists nowadays.

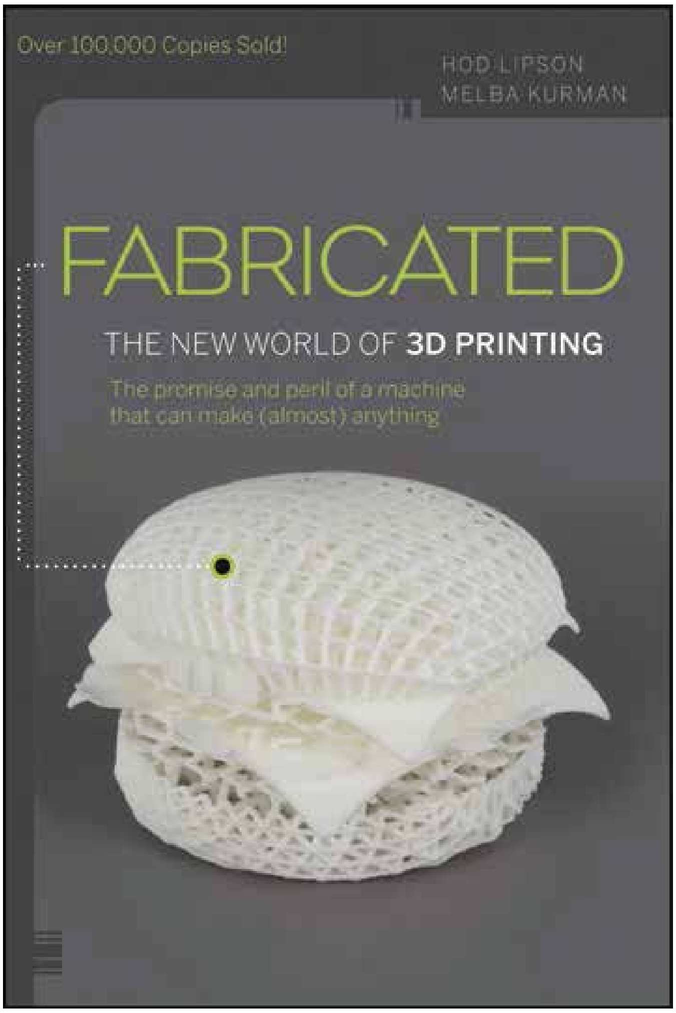

Hod Lipson and Melba Kurman, "Fabricated, The New World of 3D Printing", ISBN 978-1118350638, is available in print and as an e-book (www.wiley.com).

As to production, the two professional authors (Hod Lipson, professor at Cornell University, and Melba Kurman, technology writer/analyst) quite rightly question the so-called disruptive power of generative 3DP when comparing AM to conventional subtractive machining such as milling, grinding and EDM. This makes perfect sense if we look at the actual practice in general metalworking, tool and die shops, for example. In small series and mass production, work is done with a wealth of ISO- and DIN-validated materials, with tried-and-tested reproducible technologies, specific product design and production strategies, with high precision, highly productive machine tools, and so on.
For 3DP to reach a comparable techno-economical level, acceptance and validation in industry will take at least a decade or more, even in already feasible one-of-a-kind or small series production. Finishing of 3D objects, parts and instruments to challenging geometric and surface qualities will require traditional chipping for a long time to come. It is clear that, aside from the breakthrough in use at the people's home or in the classroom, 3DP is more of a boundary-shifting technology than a disruptive one.

While reading, the futuristic view unfolds that in the end – bearing in mind that "predicting is a crapshoot" – it should bring us more freedom in controlling:
- in terms of shape (complexity: e.g. internal cooling features, mimicking nature in extremely light but sturdy objects);
- in terms of composition (a graded mix of metal and plastics, in colour, conductive and insulating, soft and hard); and even
- in terms of actual – self-healing or active – behaviour of physical objects.

Combining available computing strength, easy scanning instruments and a secure internet – opening up an immense vat of useful content – will in the end also lead to economic freedom in production, both in scale and location.

However, professionally a complete paradigm shift – with an innovative, unconventional mind-set, a complete new set of practical or even automatic (design) rules, more robust devices and standardised materials – will be an absolute prerequisite to make – on a case-by-case basis – 3D printing (in industry circles aptly dubbed additive manufacturing) more mainstream.

Quite a number of recent references are noted at the end, evoking new ideas and insights for a 3D printing future world.

An absolute must for those interested in an informative mix of the many practical and imaginative aspects of this intriguing 'cloud manufacturing-process' of the future!

(review by Jan Wijers, production processes freelancer)

Field Guide to Displacement Measuring Interferometry

This field guide, published by the international society for optics and photonics, SPIE, delves into a subfield of optical metrology that is prevalent in many precision systems. Precision systems that require accurate positioning knowledge use displacement measuring interferometry either through direct measurement or calibration of alternative metrology systems. Displacement measuring interferometry offers high-accuracy measurements with a wide bandwidth and direct traceability to international length standards.

The aim of this field guide (ISBN 978-0819497994, 154 pages, $29 (SPIE members), $34 (non-members)) is to provide a practical treatment of the fundamental theory of displacement interferometry along with examples of interferometry systems and uses, to outline alignment techniques for optical components, and to discuss measurement uncertainty with a practical example.

For practising engineers, it will serve as a refresher manual for error sources and uncertainty budgets. For researchers, it will hopefully bring new insight into ways in which this technology can be useful in their field. For new engineers, researchers, and students, it will serve as an introduction to basic alignment techniques for breadboard-based optical systems.

The author, Jonathan D. Ellis, is Assistant Professor of Mechanical Engineering and Assistant Professor of Optics in the Department of Mechanical Engineering at the University of Rochester, NY, USA. He obtained his Ph.D. in Mechanical Engineering from Delft University of Technology, the Netherlands, in 2010.

(This publication was brought to the editor's attention by René Klaver, Heidenhain; his input is gratefully acknowledged.)

SPIE.ORG/X647.XML

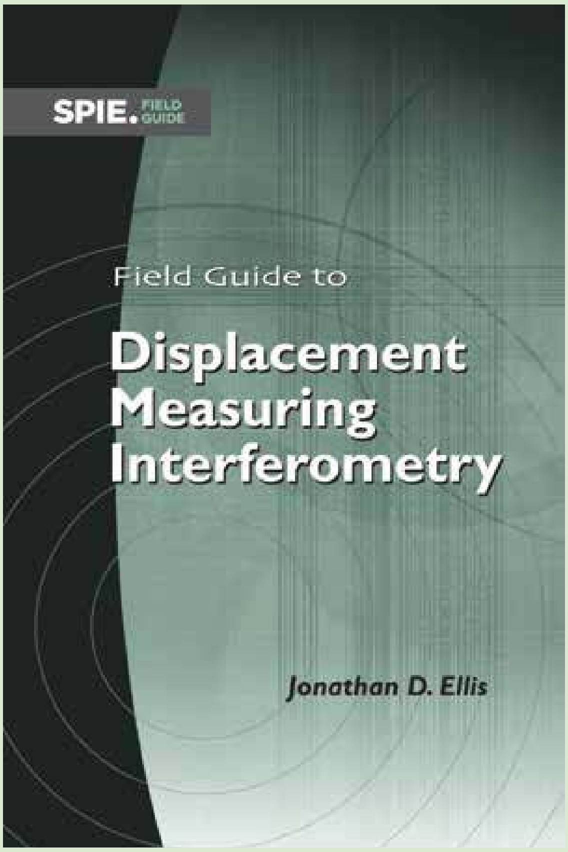

Table of Contents

The Design of High Performance Mechatronics, second edition

In 2011, "The Design of High Performance Mechatronics" was published as a comprehensive handbook. Written especially for mechatronic designers and architects, it provided an extensive overview of all technical subjects needed for conceiving and creating a mechatronic high-precision motion system. This year, the second revised edition was published, extended in size (from 750 to 900 pages), number of authors (Adrian Rankers joined the team), and content.

In their preface, the authors write: "It gradually became clear that [besides typos and language issues] also some unbalance existed in the chapters, mainly regarding the basic background material on mechanics and dynamics. The book was initially mainly intended for mechanical engineering students with B.Sc.-level knowledge. It appeared, however, that students from other disciplines would also attend the related courses and this made us decide to add some basic mechanics in this second edition."

Further, the part on modal analysis deserved a much more in-depth treatise in view of the frequent application in controlled mechatronic systems. Another addition is concerned with discrete-time control. The errata of the first and second edition are noted at a dedicated website.

WWW.IOSPRESS.NL

ERRATA.RMSMECHATRONICS.NL

■ *Robert Munnig Schmidt, Georg Schitter, Adrian Rankers and Jan van Eijk, "The Design of High Performance Mechatronics – High-Tech Functionality by Multidisciplinary System Integration", IOS Press, ISBN 978-1-61499-367-4 (print), 978-1-61499-368-1 (online), US$195 / €135 / £115.*

Frencken

PRODUCT DEVELOPMENT & ENGINEERING
COMPONENT MANUFACTURING
HIGH LEVEL ASSEMBLY
GLOBAL SUPPLY CHAIN MANAGEMENT
MOTION CONTROL

WWW.FRENCKENGROUP.COM

GLOBAL
HIGH TECH
SERVICE
PROVIDER.

PARTICIPANT HIGH-TECH SYSTEMS 2014

ULTRA-HIGH PRECISION METROLOGY OF 3D SURFACES

By designing and developing an interferometer with integrated environmental compensation, IBS Precision Engineering and the University of Huddersfield have developed an ultra-high-precision metrology tool that is suitably robust for application within a production environment. To show the accuracy of the Wavelength Scanning Interferometry (WSI) technology developed, measurement results have been compared with those of a 3D coordinate measuring machine having a traceable measurement uncertainty proven to within 11 nm.

IVO HAMERSMA AND MICHIEL BAAS

Using highly accurate inline (optical) measurement tools on a shop floor or in a production environment can be challenging, as the requirements on positioning and stability are demanding. In collaboration with the University of Huddersfield, UK, IBS Precision Engineering has developed a new optical interferometry system for fast and high-precision areal surface measurements of micro- and nanoscale structures. The technique developed is based on the principle of Wavelength Scanning Interferometry (WSI). Coupled with the implementation of a novel vibration compensation system, this creates the possibility to use high-precision lab metrology in a production environment.

The technique involves capturing a set of interferograms across a range of wavelengths. Using this data, a height map of (discontinuous) areal surfaces can be produced using the phase shifts generated between the interferograms. Using wavelength scanning to access the phase shift excludes the need for mechanical movement of the measurement set-up. This, in turn, makes the system more suitable for integration into noisy environments without the need for large and/or complex isolation systems.

The WSI system is able to measure both discrete step heights and surface quality. It can be used for inline defect detection and characterisation, optical surface and structure

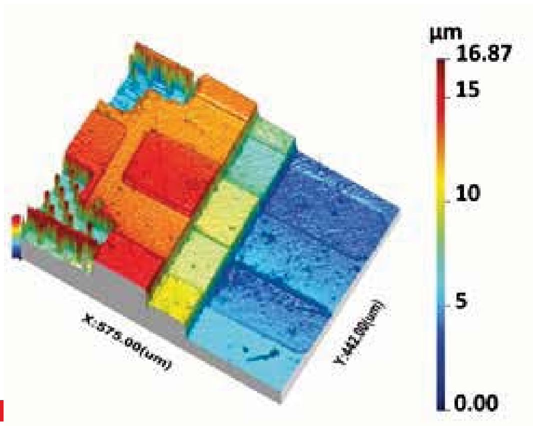

1 *Measurement of a multi-step IC.*

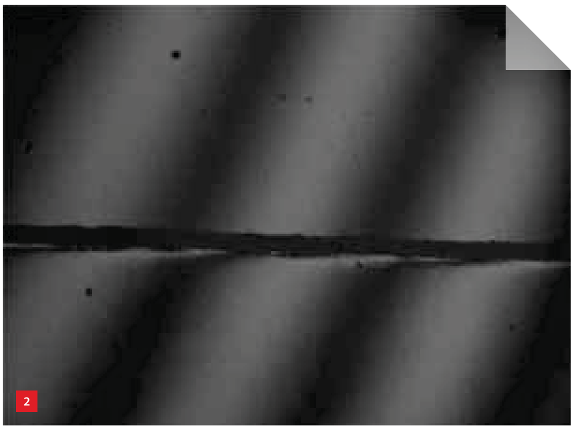

2 *Parallel fringes indicating tilt of the surface. The small horizontal shift of fringes indicates a step.*

AUTHORS' NOTE

Ivo Hamersma and Michiel Baas are both working as a system/metrology engineer at IBS Precision Engineering, based in Eindhoven, the Netherlands. Ivo Hamersma received his M.Sc. in Mechanical Engineering from Eindhoven University of Technology and is focussing on opto-mechatronic measurement solutions. Michiel Baas is focussing on both machine tool calibration and the 3D CMM Isara 400. He obtained his M.Sc. in Mechanical Engineering from Delft University of Technology, the Netherlands.

hamersma@ibspe.com
ibspe.com

measurement, 3D surface topology measurement, MEMS/NEMS inspection and more. A measurement of a multi-step IC is shown in Figure 1.

Interferometry

In the interferometric system, an incoming beam of a fixed wavelength is split into two beams to give a measurement and a reference beam. A reference target and the object to be measured reflect the beam, where they are recombined in the beam splitter. The recombined beam is imaged by the camera. The phase shift between the two beams results in interference fringes (Figure 2), which may be used to derive height information regarding the measured object.

By using imaging lenses in the measurement and the reference beam, the interferometer can also be used for surface contour measurements and topography. This layout is known as a Linnik interferometer.

WSI principle

In order to obtain height information over a distance of more than a single wavelength, interferograms of multiple phase shifts are required. One method to generate a phase shift is to alter the distance of the measurement beam, by moving the object with respect to the interferometer.

For the WSI, the phase shift is generated by scanning the wavelength over a fixed interval. Using the wavelength shift, the WSI system does not need any movements to generate multiple phase shifts. The total phase shift as introduced by the change in wavelength, indicated in Figure 3, can then be obtained from the intensity signal using Fourier transforms. The height of the point represented by the pixel can be calculated by:

$$h(x,y) = \frac{\Delta\varphi(x,y)}{4\pi\left[\frac{1}{\lambda_{max}} - \frac{1}{\lambda_{min}}\right]} = \frac{\#\ periods}{2\pi\left[\frac{1}{\lambda_{max}} - \frac{1}{\lambda_{min}}\right]}$$

Here $h(x,y)$ is the height of the specific point x,y and $\Delta\varphi(x,y)$ the calculated phase shift of the pixel over the scan range. λ_{max} and λ_{min} are the upper and lower wavelengths of the scan range, respectively.

Vibration compensation

To enhance the performance of WSI technology in a shop-floor environment, active vibration compensation is integrated in the design. A second monochromatic light source, that shares a common optical path with the WSI, is used to monitor and compensate for the displacement of the object. In Figure 4, the coupling of both light sources into the interferometer is shown schematically. Then, the piezo is actuated to compensate for vibrations of the object.

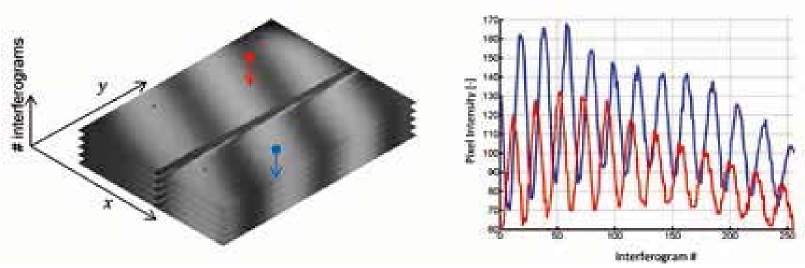

3

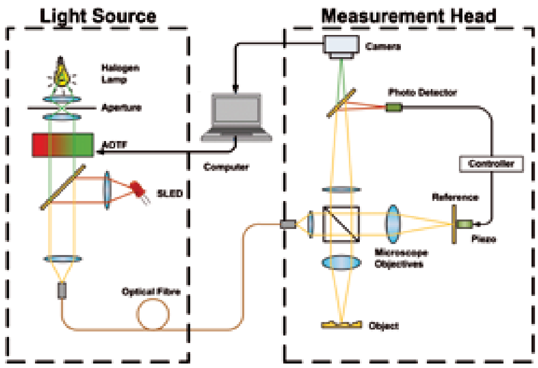

4

5

3 *Measurement set of step height with representation of the 3D image array (left) and the signal of two pixels over the scanned wavelength (right).*
4 *Schematic layout of the WSI set-up.*
5 *Prototype of the WSI.*

The vibration compensation relaxes the requirements on the stability of sensor and object, which enhances the flexibility of the design for integration. This creates the possibility to integrate a high-end system for online or in-process measurements on a shop floor. To prove these features, a prototype has been realised, as shown in Figure 5.

WSI specifications

In the design of the WSI sensor, the user is given the possibility to change the magnification of the system by changing the microscope objectives. An autofocus function is implemented to improve the usability of the measurement system.
As the measurement principle of the WSI is based on the wavelength variation, the height resolution does not change when the magnification is changed. Other lens-specific parameters, such as vertical range (depth of focus) and lateral range (field of view) do vary. A range of objectives, from 2x up to 50x (even 100x), can be used. In Table 1, an overview of specifications of the WSI is given.

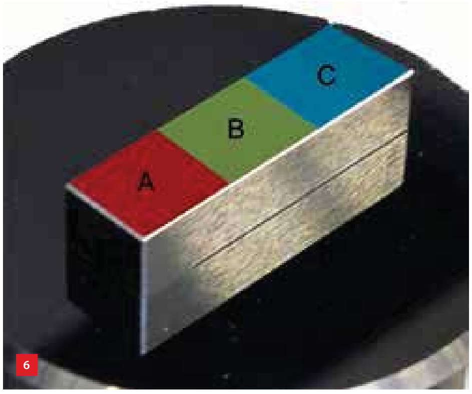

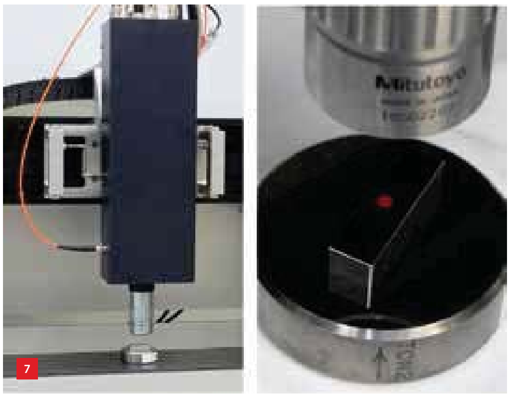

6 *Bridge gauge layout.*
7 *The WSI mounted on the measurement set-up (left), and the measurement set-up of the bridge gauge, showing the microscope objective and measurement spot (right).*
8 *Measurement results using the WSI on the two step heights in the bridge gauge, with the step AB (left) and BC (right).*

Comparison artefact

To qualify the accuracy of the developed technology, data has been compared for measurements taken on an artefact by both the WSI technology and that of a coordinate measuring machine (CMM) with traceable uncertainty proven to 11 nm for a flatness measurement.
Here, a bridge gauge is used as an artefact. This bridge gauge contains three surfaces, where a step in height is defined between each surface. This is depicted in Figure 6.

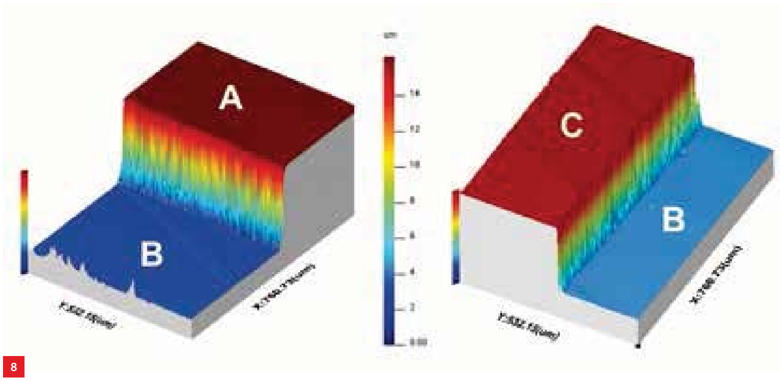

WSI Measurement

In Figure 7 the measurement set-up for the WSI measurement is shown. Here, the WSI system is mounted on a horizontal translation stage to be able to move over the sample. A z-stage is used to autofocus the WSI with respect to the object.

Using the WSI, each step was measured in a single measurement. The A-B step was measured first, then the WSI system was repositioned, after which the B-C step was measured. Both measurements were done using a set of 5x objectives. The measured step height data is shown in Figure 8.

Table 1. Specifications of the WSI for a 2x objective.

Specification	Value	Unit
Vertical range (lens-dependent)	96	µm
Vertical resolution	< 2	nm
Vertical accuracy	~15	nm
Lateral range (lens-dependent)	2.8 x 2.8	mm^2
Lateral sampling	1,000 x 1,000	pixels
Lateral resolution (lens-dependent)	5	µm
Measurement time	< 1	s
Autofocus time	< 1	s

For comparison, both measurements are levelled with respect to the surface B. The step height is calculated by measuring the distance between the average heights of each surface. This gives a step height of 12.649 µm for step AB and 12.479 µm for step BC. With the measurement completed on the WSI system, the artefact was transferred to the Isara 400 CMM and step height data once again collected.

Comparison with Isara 400

In this study, the Isara 400 coordinate measuring machine has been used as a reference measurement system for assessment of the WSI measurement technology. To verify the accuracy of the Isara 400, a Ø150 mm Zerodur flat-mirror reference artefact has previously been measured. The flatness of this mirror was measured using Fizeau interferometry at Germany's national metrology institute, the Phykalisch-Technische Bundesanstalt (PTB). The result of this flatness measurement is directly traceable to international standards. The theoretical 1D measuring uncertainty for the full measuring volume capability of the Isara 400 (400 x 400 x 100 mm^3) has been estimated at 57 nm. For the PTB sample measured, with an area of approximately Ø150 mm, it was found that 95.5% of the data points match to less than 11 nm with the PTB calibration [1]. For the artefact used in this assessment the measurement area was 36 mm^2 per surface.

Measurement set-up

Figure 9 shows the Isara 400 3D ultra-precision CMM and the measurement set-up on the machine. A CAD model of the bridge gauge is imported in the CMM software and five points are probed manually on the part for alignment. Next, the rest of the measurement is programmed and executed as an automated sequence.

After the grid measurement is completed, the measurement data is levelled to surface B. Each of the three surfaces is measured with 950 points. The step heights are calculated by levelling all surfaces to the surface B and comparing the mean heights. This gives a step height of 12.631 µm for the step AB, where a height of 12.495 µm is measured for the BC step. Figure 10 shows the acquired data as well as a representative cross section.

Results

Comparison of the measurement data between the WSI and the Isara 400 shows a maximum deviation in step height measurement down to 18 nm. The deviation is consistent with the combined measurement uncertainty of the Isara 400 and the WSI. This shows that the WSI can be used as a fast and high-accuracy metrology instrument to measure micro- and nanoscale surfaces.

Table 2. Measurement comparison between the WSI and the Isara 400.

Step	WSI	Isara 400	Difference
A-B	12.649 µm	12.631 µm	18 nm
B-C	12.479 µm	12.495 µm	16 nm

Conclusion and outlook

The results as presented in this article show that the WSI is an outstanding tool to be used for high-accuracy areal measurements, such as 3D surface topology and MEMS/NEMS inspection. Active vibration compensation and autofocus functionality improve the usability of the sensor in a shop-floor environment.

As part of the NanoMend project, the WSI system will be implemented at the Centre for Process Innovation (CPI) in the UK as a demonstrator sensor for the detection of defects in polymer film [2]. This will be a showcase of the fast, large-range, nanometer-resolution and robust capabilities of the WSI.

Acknowledgement

Part of the development of the WSI has been done within the EU FP7 NanoMend project. The authors would like to thank the EC for funding this work (NanoMend NMP4 LA-2011-280581). ■

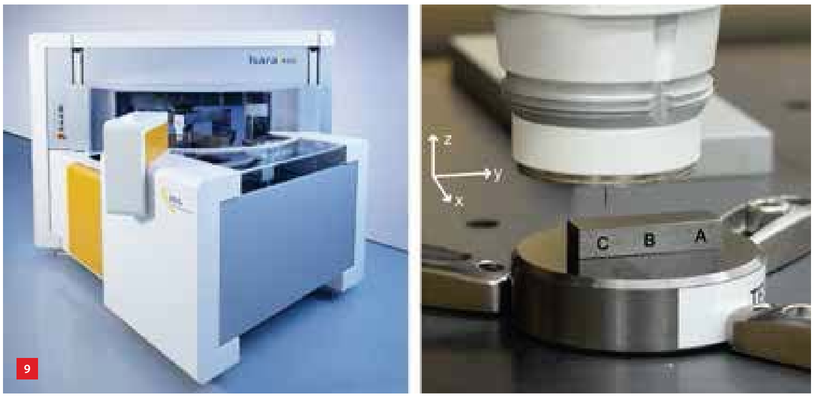

9 *The Isara 400 3D ultra-precision CMM (left) and the measurement set-up of the bridge gauge, showing the Triskelion touch probe (right).*

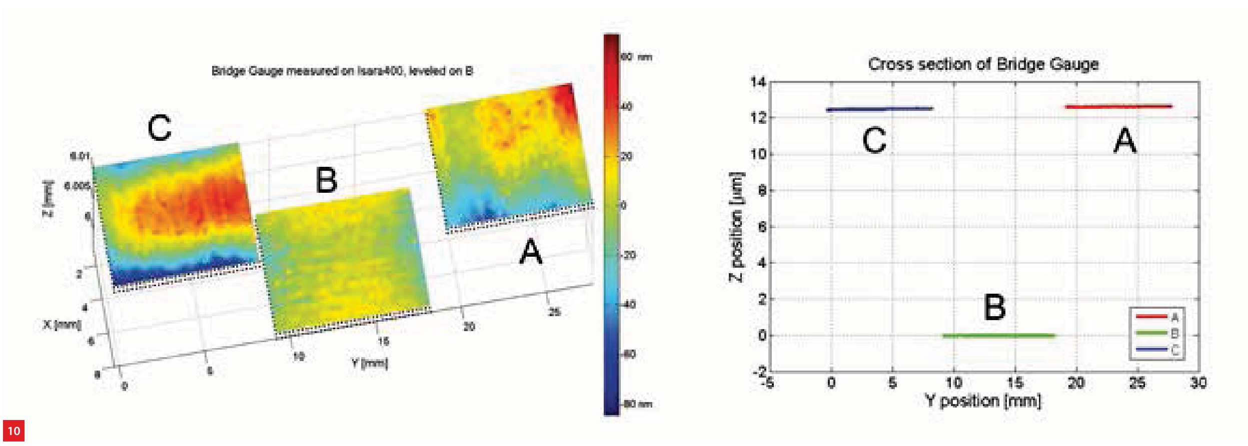

10 *Measurement results of the bridge gauge on the Isara 400 with surface representation (left) and cross-section of the surfaces (right).*

REFERENCES

[1] I. Widdershoven, M. Baas and H. Spaan, "Ultra-precision 3D coordinate metrology results showing 10 nm accuracy", *Proc. 11th Int. Symp. of Measurement Technology and Intelligent Instruments (ISMTII)*, July 2013.

[2] http://nanomend.eu/2014/02/nanomend-develop-pilot-scale-ultra-barrier-defect-detection-tool

THE HIGH TECH INSTITUTE

LEADERSHIP IN TECHNOLOGY AND INNOVATION

Leadership & Communication

How to deal with the 7 biggest communication challenges in innovation and technology

Do you recognise that clear communication in projects can be difficult? Do you want to improve your influence without power and get your message across? Do you want to learn how to delegate and coach effectively? In 2 modules of 3 days that can be followed seperately you will be confronted with the 7 biggest communication challenges you face in your daily work and get the tools to deal with them. This course is 100 percent practical and hands-on because we will work with cases directly coming from your personal work. You will learn for example:

- peoples logic (how to motivate others);
- how to coach and delegate work;
- how to be hard on content and soft on relation;
- convincing your stakeholders and dealing with resistance in group meetings;
- being able to influence without power.

Course code: 7-CC MODULE I
Location: Eindhoven
Course price: 1,795 euros excl. VAT
Duration: 3 consecutive days + 1 evening
Dates: 10th - 12th June 2014

Course code: 7-CC MODULE II
Location: Eindhoven
Course price: 1,795 euros excl. VAT
Duration: 3 consecutive days + 1 evening
Dates: 27th - 29th October 2014

Mechatronics

Design for ultra high and ultra clean vacuum

In the course "Introduction in ultra high and ultra clean vacuum", the trainees have been acquainted with the basics of vacuum technique. Subsequently, in this module they learn how to make a rigid design, applicable for vacuum conditions. One of the key items is to work on exercises in workshop like conditions, guided by 2 trainers. The last day will be dedicated to the construction, assembly and testing of vacuum systems. The course "Design for ultra high and ultra clean vacuum" is meant for employees of BSc and higher level responsible for constructions in ultra clean vacuum in any way. These employees could be in research and development, (production) engineering, purchase, management, et cetera.

Course code: UHV2
Location: Eindhoven
Price: 1,695 euros excl. VAT
Duration: 3 days in a period of 2 weeks
Dates: commences 22nd May 2014

Meet us at stand 30 and the reception at High-Tech Systems on 7 and 8 May

www.hightechinstitute.nl

SUMMER SCHOOL OPTO-MECHATRONICS 2014

For the seventh time, DSPE and The High Tech Institute organise the Summer school Opto-Mechatronics, from 16 to 20 June 2014 in Eindhoven, the Netherlands. Once again, it is the place to be for anyone working in the field of precision engineering and wanting to learn and experience from experts how to design actively controlled opto-mechanical instruments.

Summer school Opto-Mechatronics
Precision Technology

The Summer school Opto-Mechatronics 2014 comprises five days of intensive course, taught by excellent (Dutch) professors and scientists in the field of precision engineering, who work at TU Delft, TU Eindhoven, ASML, Philips, TNO, ESO and Mechatronics Academy, combined with hands-on training. Participants will come from universities and high-tech large companies and SMEs. Last year's edition attracted participants from five different nationalities, twelve different companies (including Philips, ASML, Segula Technologies and Physik Instrumente) located in three European countries, and a range of positions (e.g. an optical engineer, a Ph.D. student, a design engineer, a junior architect, a chief researcher). The programme includes social events and venue is TNO at the university campus in Eindhoven.

Last year's Summer school Opto-Mechatronics was attended by a diverse group of participants.

Programme

Monday 16 June 2014:
"The BIG Picture" & Systems Engineering
Opto-mechanical instruments are always co-existing with other equipment. So, before starting their design, the essence of the systems engineering has to be considered. What is critical and what are the margins? How to approach such a project and how to gain insight in the background of the requirements?

Tuesday 17 June 2014: Optical Design
The case starts with an introduction to the optical design and its use in optical aperture synthesis applications. Next, in teams, several delay line designs will be compared, in order to select the best design with respect to the optical requirements. Also, an effective optical design has to be found for measurement of the optical path differences. Zemax will be used to analyse the optics in the delay line. Further work pertains to wave-front analysis and pupil imaging while moving the delay line, and assessment of alignment accuracy.

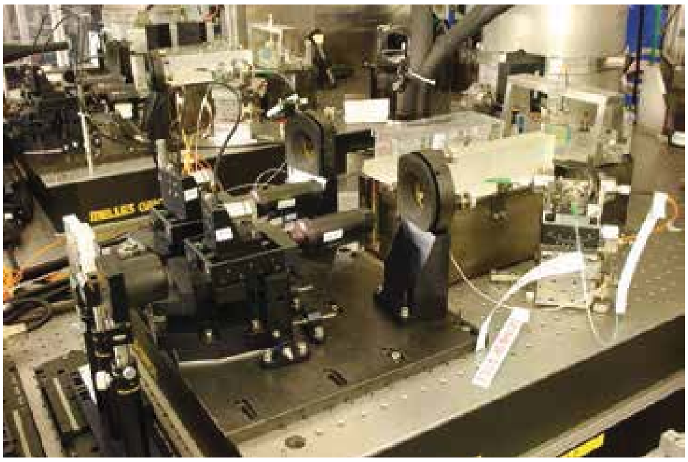

The leading thread in the Summer school is the design of an optical delay line.

Wednesday 18 June 2014: Control Design
Based on the functional requirements of the optical delay line, the challenges for control are discussed. These include actuation for a high dynamic range, servo behaviour, vibration rejection, sensor noise, closed-loop stability and others. An introduction of suitable control design methods is presented to achieve nanometer positioning accuracy.

Thursdag 19 June 2014:
Opto-Mechanical Design
High-quality mechanics will guarantee best performance in terms of optical quality/ stability and control performance. Therefore, lightweight and stiff structures are crucial. The design of the existing ESO delay line will be used to explain the requirements for such a structure. Emphasis will be put on the interactions with the other key technologies needed (optics, control and electronics) and on the mechanical design itself. The participants will be challenged to participate by designing, in a team effort, a specific part of the cat's eye (optical section of the delay line) using their own experience and the information provided.

■ *The programme of the Summer school includes social activities.*

Friday 20 June 2014:
Actuation, Sensing & Dynamics
Designing an actively controlled delay line that is stable enough to perform interferometry over large distances, is far from trivial. Some still missing elements will be presented that are necessary to realise high-performance active positioning and control systems for optics. Following an overview on electromagnetic and piezoelectric actuators, optical position measurement systems and capacitive sensors, attention will be given to the performance-determining mechanical system dynamics and vibration isolation. The new field of adaptive optics will also shortly be touched upon. ■

Information and registration:
WWW.SUMMER-SCHOOL.NL

ROBUSTNESS IN EMBEDDED SOFTWARE FOR AUTONOMOUS ROBOTS

The European BRICS project aims to bring about a long-lasting change in robotics research and development in industry as well as in academia. It wants to change the current situation of non-interoperable, monolithic and single-sourcing robotic components into a situation that other domains have already reached: cost-effective access to interoperable infrastructure components, which can create a thriving ecosystem of innovative products and services. This article focuses on techniques that could be used to increase the level of robust autonomy of robots.

JAN BROENINK, YURY BRODSKIY, DOUWE DRESSCHER AND STEFANO STRAMIGIOLI

AUTHORS' NOTE

Jan Broenink, associate professor of embedded control systems, Douwe Dresscher, Ph.D. student, and Stefano Stramigioli, professor of advanced robotics, are members of the Robotics and Mechatronics group at the University of Twente, the Netherlands. Yury Brodskiy obtained his Ph.D. within this group; he is now a researcher at KU Leuven University in Leuven, Belgium.

www.ce.utwente.nl

Introduction

Robotic systems and applications are going to become a key technology within the next 10 to 15 years to address two socio-economic megatrends: the overaging society and the competitiveness in the global markets. To address the most urgent needs of an overaging society, a multitude of service robots will have to be developed in a rather short period of time. To persist in an increasingly harsh competition with low-wage countries, the innovation and production cycles in Europe have to be shortened significantly, requiring new and flexible automation solutions.

In spite of the scientific and technological achievements of the past three decades, the development of new, complex robot systems and applications remains a challenge requiring significant time and effort. Currently, such developments are typically highly specialised, unique, and 'from scratch'. Little attention is paid to the creation of easily configurable, re-usable, interoperable components and solutions. Technological divergence prevails. This leads to high development costs and times, long innovation cycles, moderate system robustness, and a significant waste of resources.

Robot developers in academia and industry urgently need research platforms and an integrated development environment to be able to cut the development cycles for new robot systems significantly. In areas such as telecommunications, the automotive industry or embedded systems, a great deal of progress has been made to design such integrated development environments. Robotics must follow a similar strategy in order to develop the technology necessary to meet the challenges mentioned above.

Improving reliability

The BRICS project (Best Practice in Robotics, a collaborative project in the Seventh Framework Programme of the European Union) aims to bring about a long-lasting change in robotics research and development in industry as well as in academia: it wants to change the current situation of non-interoperable, monolithic and single-sourcing robotic components into a situation that other domains have already reached: cost-effective access to interoperable infrastructure components, which can create a thriving ecosystem of innovative products and services.

Research within BRICS, [1] [2], is aimed at finding ways to improve the reliability of a robot, with a focus on its motion control software. Robot motion control ensures the ability to proceed with a designated task, and it is one of the vital parts of a robot, where non-functional requirements such as robustness and reliability are essential for a high quality of the overall system. Several threats to the reliability and safety of the motion control software can be identified and addressed: the quality of software implementation, the external faults from a connection to the physical domain such as failures of a sensor, and the external faults from a connection within the cyber domain such as communication with other components.

A modelling approach to software development can be advocated as a means to improve the quality of the software produced. The proposed approach to software development uses 'uniform' modelling of the software components to improve their reliability. The need to model software from different perspectives is emphasised here – the software practice of separation of concerns is used to identify different perspectives from which a software component has to be modelled.

Robustness of robot autonomy

The development of a robot that can perform its duties for a long time in an unstructured environment with limited human assistance is of particular interest to the robotic community. The BRICS project addresses this interest by developing the methodology, the framework and the tool chain for such applications. One of the important facets of such a methodology is support for a controllable investment into robustness of robot autonomy.

The ability of a robot to deal with unexpected situations is an essential requirement for robot-human co-existence. While quite separate from demanding functional requirements, this ability of robust autonomy is a barrier that separates a service robot at home from a prototype in the lab. We have defined robust autonomy as the ability of a robot to deal with abnormal situations with minimal human involvement. The models of abnormal event management can be used to analyse this ability.

A three-stage assessment approach reflects separation of concerns in the system:

- Fault detection represents the context-based information acquisition and analysis.
- Decision and action selection reflect the amount of responsibility the robot is allowed to take.
- Action implementation indicates the robot's ability to fulfil its goals.

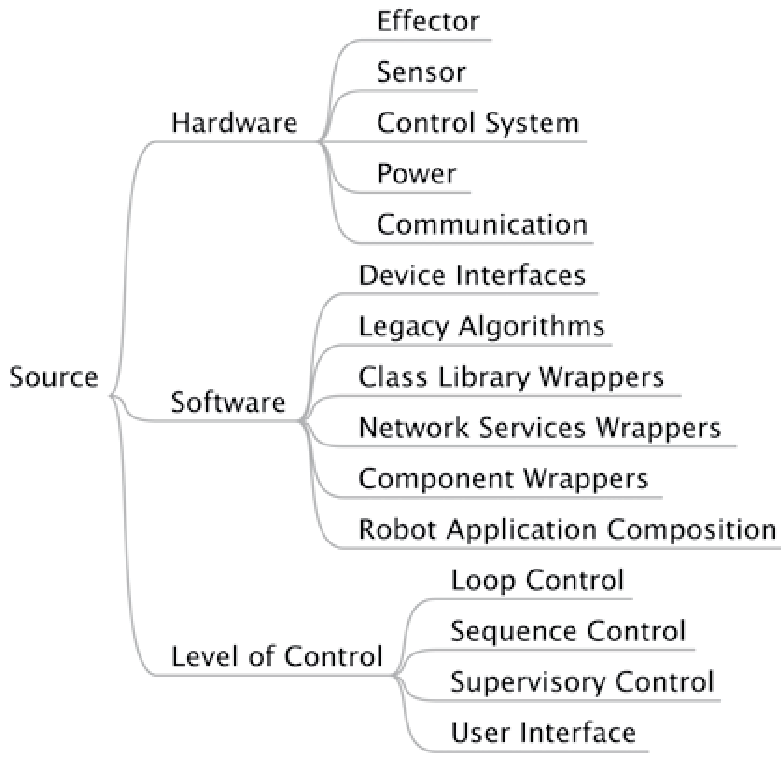

1

1 *Taxonomy of faults.*

Fault forecasting

To identify the rates of human guidance required by the system, a systematic analysis of potential abnormal events can be made. Fault-forecasting techniques for itemising and assessing probability and system reaction to abnormal events include:

- Scenario-based analysis: Failure Mode Effect and Criticality Analysis, Software Architecture Reliability Analysis Approach.
- Cause and effect analysis: Fault Tree Analysis, Event Tree Analysis.
- Risk assessments: Stress Strength Analysis, Reliability Prediction.

In this event-based approach, the sources of the failure can be analysed from three different perspectives: hardware, software organisation and control organisation; Figure 1 presents a taxonomy of faults. The result of performing a fault-forecasting analysis is a knowledge base that contains interrelations between the components, functions, events and failures. This knowledge base can be utilised in two different ways: as major guidelines for system redesign to support the robust autonomy concept and as part of automated fault-tolerance algorithms.

On the other hand, a lifetime performance approach can be followed for determining system autonomy. This involves a concept for estimating the level of system lifetime autonomy, based on statistical behaviour of the robot, which will be formally described in order to arrive at an elegant, effective measuring method that can be used to infer the robust autonomy in a quantitative way.

Design guidelines

The development of a robot should be structured in such a way that decisions affecting non-functional requirements such as robust autonomy are highlighted. The engineering process can be described as a combination of design procedures and artefacts (deliverables). An artefact is the most explicit way to ensure that the requirements are met. Therefore, it is good practice to include robust autonomy requirements in it.

The developments in the dependable computing research field and safety-critical system design provide numerous techniques that are applicable to robust robot autonomy. A review is presented here, covering the initial guidelines and challenges for the architecture that will support the autonomous and robust behaviour of the system, and the taxonomies of algorithmic solutions for robust autonomy.

One of the main trends in robotics is to ensure component reuse and functionality encapsulation. From the field of secure and dependable computing, this trend is supported by means of increasing dependability. The main emphasis created by such an approach is the development of dependable components. Components with a low dependability level and without special precautions will jeopardise the dependability of the entire system.

It is often a requirement in robotics to construct a reliable system from less reliable components, which is a typical challenge of safety-critical systems. Limited human interventions in a robot workflow make the ability of detecting and recovering from failure of a component at the system level an essential feature for a robot to ensure its robust autonomy.

Dependable components encapsulate certain types of functionalities, making them reusable; however, fault tolerance is enclosed and fused with component functionality. Separation of the normal execution flow from exception handling allows the creation of more reliable, more understandable and more reusable systems.

To complicate matters further, convoluted states of a robotic system created at different levels of abstraction produce a set of complex abnormal situations. A recovery process required to let the system return to an error-free state needs to be more involved and requires cooperative efforts of several components.

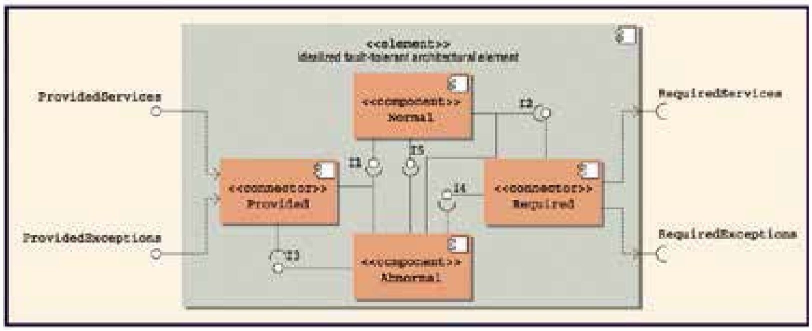

2

2 *Idealised fault-tolerant component software [3].*

Cooperative recovery

These requirements (to tolerate failure of the component at system level, to separate exception handling and to create a more complex recovery process) present the idea of cooperative recovery. From a component point of view, cooperative recovery is a process by which a system (component) is transferred to an error-free state by a sequence of environmental states (actions of cooperative components). For example, software rejuvenation is a solution that allows the removal or prevention of component failure.

One of the concepts of component-based development is a hierarchical organisation of the system. This concept implies the combination of the components used to create a new component with more complex behaviour. The hierarchical architecture of the components reinforces the concept of cooperative recovery. At each hierarchical level, components capable of cooperative recovery will create a level of protection for the system.

The development of a system that would support cooperative recovery consists of the analysis of existing solutions and limitations, synthesis or adaptation of the solutions, and evaluation. There are several facets of the fault-tolerance process that need to be reviewed:

- architectural problem – how the components should be organised to support cooperative recovery;
- detection problem – how the failure could be detected/ recognised outside of the component;
- recovery problem – how the recovery process should be organised.

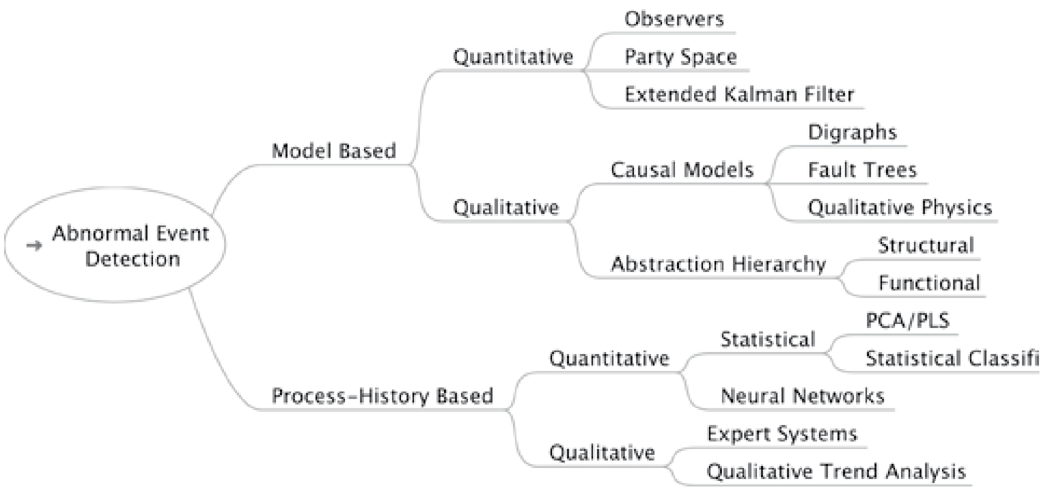

3 *Taxonomy of detection systems [4].*

Architectural problem

Cooperative component recovery should be supported by a proper system architecture. The addition of new parallel types of behaviour to the system will increase its complexity, eventually reducing the system's maintainability and jeopardising its dependability. Moreover, a requirement to interrupt the normal workflow in case of fault activation or to enter a special state demands a mechanism of switching execution paths, which also contributes to system complexity. There are three topics that address the complexity issue: organisation of a single component, system partitioning and flow of execution control.

There are several requirements for the organisation of a single component. To ensure reusability and avoid the introduction of unnecessary complexity in the system component, it must have a clearly defined boundary. The behaviours of the components should be encapsulated, as should fault handling mechanisms. This is achieved through defined interfaces for normal and abnormal workflows.
For an abnormal workflow, a component should receive the information about the failures in cooperative components and distribute information about faults it cannot handle. Internally, the component should also support a separation of exception handling from normal flow. An example of the component architecture that meets these requirements is presented in Figure 2.

The idealised fault-tolerant component/element (iFTE) has four types of external interfaces:

- ProvidedServices, which is responsible for the provision of (fault-tolerant) services.
- SignalledExceptions, which is responsible for signalling either interface or failure exceptions.
- RequiredServices, which specifies the required services.
- ReceivedExceptions, which specifies the external exceptions that need to be handled.

The decomposition of the system into recoverable units is a trade-off between error confinement and development overhead. Figure 2 shows that each component responsible for normal behaviour is supported by three other components. Although it is possible to create an iFTE for every system component, it might not be beneficial. This is because the development and computation overhead created by additional components requires additional resources, possibly making the component unusable. On the other hand, decomposition of the system into smaller elements allows better fault isolation, thus increasing fault tolerance.

A solution can be provided by partitioning the system into recoverable units (RUs) based on minimisation of function calls between the RUs. The main limitation of the proposed solution is scalability, since the system should be analysed at run time and the decomposition is based on the solution of a set partitioning problem. Another part of the solution is to create another view of the system that will explicitly represent RUs and communications between them.

Control of the execution flow based on the element failures is similar to exception handling mechanisms developed in software engineering. The control of the execution flow is rarely supported by component level abstraction. Therefore, further investigation is required to identify the best practice in that area.

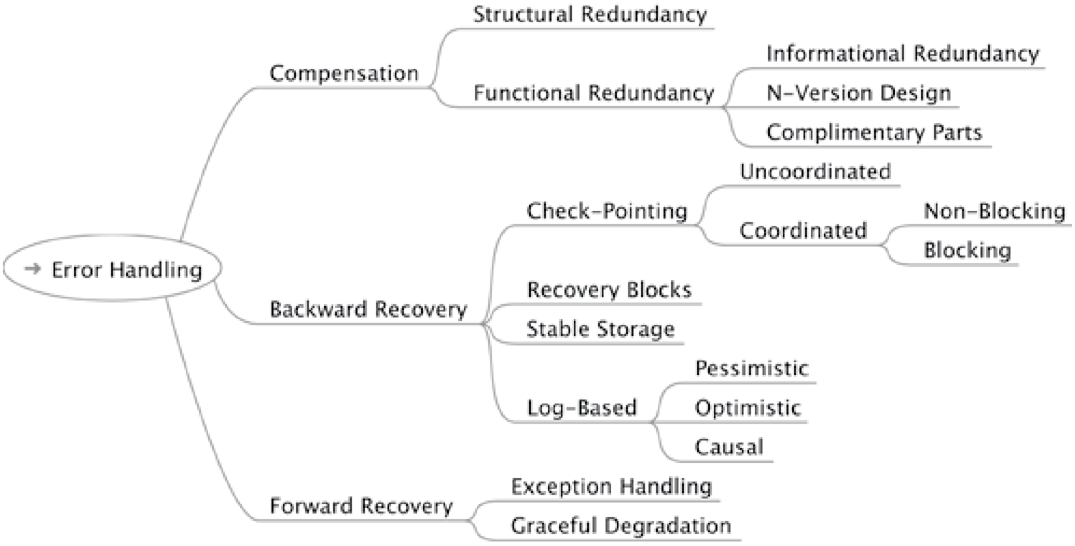

4 *Taxonomy of recovery types.*

Detection problem

The detection of a component failure addresses the signalling of system failures. From the detectability point of view, there are two types of failures: signalled and unsignalled. The signalled failures are detected inside of the component and indicated for users. If such indication does not occur, the failure is called unsignalled. The development of a detection mechanism is directed at creating components that will reduce the set of unsignalled failures in the system. Figure 3 presents a taxonomy of detection systems used in chemical engineering.

Based on the knowledge used in the system, there are three main types of fault detection and isolation systems, namely:

- A model-based system, created on the assumption of a priori knowledge about the component. The components are presented as white boxes, whose internal execution can be described and monitored.
- A process history-based system, which is created based on the assumption that the only accessible information is the process history.
- Hybrid systems, combining both types of information.

Several comparative studies have been performed in order to identify optimal detection algorithms for the task in hand. The detection system should be structured in the same way as was presented in the section on the architectural problem. Each detection element is responsible for one RU. Increasing the complexity of the RU will increase the complexity of the detection algorithm and reduce the quality of isolation.

Recovery problem

From the point of view of dependable computing, a recovery process is a transformation of the system state that contains errors or faults into a state without detected errors and without faults that can be activated again. Fault handling is a process that prevents faults from further activation. Error handling is a process of eliminating errors from the system state. The ability of the robot to respond to exceptional situations to a large extent depends on recovery processes. Recovery algorithms are aimed at transferring the system into a correct state after the fault has been activated, in three different ways: compensation, forward recovery and backward recovery; see the taxonomy in Figure 4.

Compensation is an online replacement of the failed component with a redundant one. Such a system does not lose any functionality in case of a component failure. There are two possible types of redundancy: replication of the element (structural redundancy) or replication of its function (functional redundancy).

Backward recovery is a process of transferring the system to a known error-free state. There are two distinct types of backward recovery: recovery blocks and check-pointing. Recovery blocks contain three elements: the functionality, the checking mechanism and a rollback procedure. In check-pointing, system states are recorded to be replayed in case of system failure.

5a

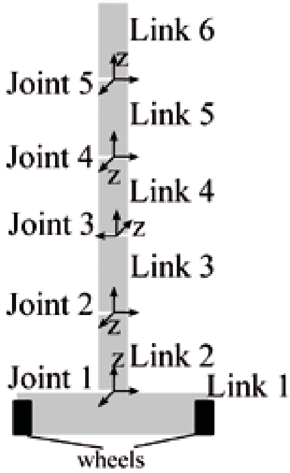

5b

5 *The robotic manipulator platform.*
(a) The youBot.
(b) Schematic representation.

Forward recovery is a process of masking the failure of the component. The system interrupts the normal workflow and attempts to provide the service by an alternative execution process. Depending on the system's ability to achieve the goal, there are two types of forward recovery: exception handling and graceful degradation.

Use case

In the BRICS project, a use case implementation was elaborated concerning a signalling system that is used to increase the robot's level of autonomy. The detection system was designed to signal failures in effectors and related sensors. It creates functional redundancy on perception utilising the prior knowledge of the system dynamics. The technique could be reused to create fault-tolerant control or to enforce fail-safe behaviour of a manipulator with interaction control.

The detection system is included in the robot loop control. It is a separate behaviour that works in parallel with normal control. For this use case, we have selected a mobile robotic manipulator (youBot-like) consisting of a robotic arm and a base driven by four Mecanum wheels; see Figure 5a. Such a platform provides most of the common elements of a modern robot designed for performing a variety of tasks. The kinematic structure of the youBot robotic manipulator is shown in Figure 5b.

The manipulator has six links connected in series by five actuated rotational joints. The four Mecanum wheels are mounted in a parallel construction to the first link of the robotic actuator to make it mobile. For construction of the model of the platform, see [1].

The development of a detection system begins with the systematic analysis of possible abnormal events in the system. There are two types of failures that should be considered at loop-level control: sensors and actuators. Actuation failures are most likely to originate in joints or wheels, because with a non-prescribed workload, the links have negligible probability of destruction, whereas MTTF (mean time to failure) for a joint is in the range of 5,000 hours.
Presuming that a set of sensors in a joint is limited to a position/velocity and a current sensor, there is no possibility to increase the isolability of the system. Therefore, the detection system we develop will have 'joint failure' as a base event.

The final step towards fault-tolerant control is the design of a recovery action. We use the kinematic redundancy present in the youBot to compensate for joint failure. This way, the tool tip can be positioned and manipulation tasks can be performed with a broken wheel-drive or joint-drive. The reconfiguration of the controller is required to exploit this idea.

The youBot's arm is an open kinematic chain. As such, the actuators have to be at least fail-safe to maintain operation. For the existing hardware, the only response possible in case of failure detection is stopping the operation. The reconfiguration process for the robot with fail-safe

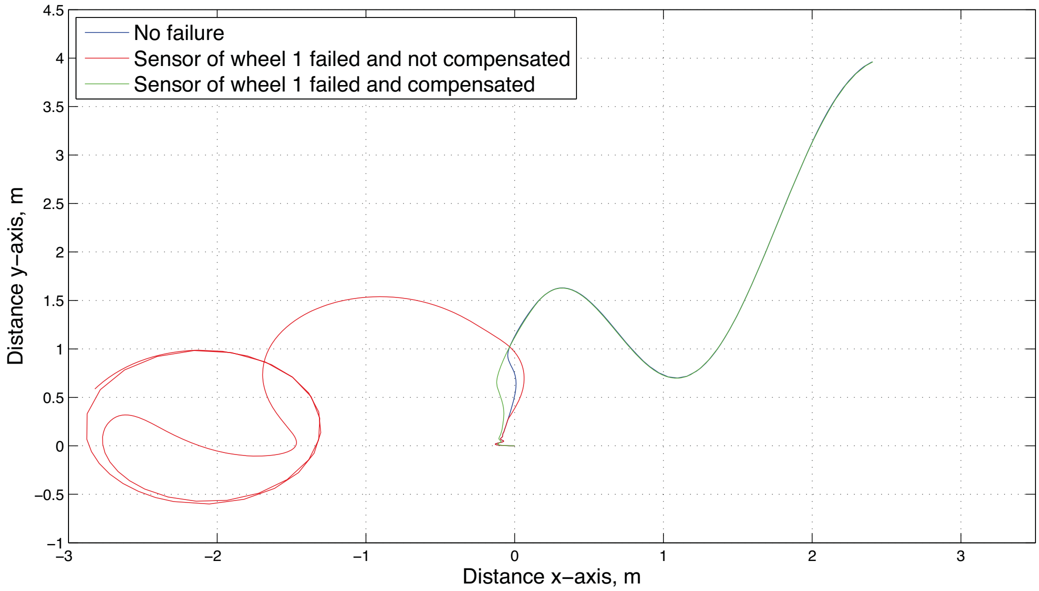

6 *Trajectory of the youBot base during trajectory tracking with tool tip.*

actuation is of most interest; in our simulation study, the joints are therefore considered fail-safe (they have brakes).

As part of reconfiguration, the sensor readings of the failed joint should be fixed to the last correctly estimated measurement to determine the configuration of the kinematic chain. The control signal is set to zero. A joint with engaged brakes is indistinguishable from a rigid connection, so two links connected by this joint can be considered as a new single link.

The youBot's base is a parallel structure and can be considered as a kinematic loop. Thus, fail-safe operation of the wheel-drive requires free rotation of the wheel. A wheel with a brake impairs the mobility of the robot by constraining motion of the wheel. During reconfiguration, the wheel actuator is powered down to minimise the friction induced by the uncontrollable wheel. The sensor information from this wheel is ignored, and the three sensors on the other wheels are used to compute the odometry. Actuation of three Mecanum wheels of the base allows omni-directional movement [5], completely preserving initial mobility of the base.

At this stage of the project, the use case was restricted to simulations, which were performed using the 20-sim tool [6]. Faults were injected to test the performance of the fault detection and recovery procedures. In simulation, the youBot had to perform trajectory tracking with the tool tip. Two types of simulation are recorded: with and without stand-by brakes on joints of the youBot arm. In case of no brakes on the joints, the reconfiguration performs power down, instead of engaging the brake.

A single failure was injected at $t = 1.0$ seconds after the start of performing the task, then the youBot was followed for 40 seconds, during which it had to track a predefined trajectory. Prior to these simulations, the performance of the youBot without failures was recorded in such a way that a possible performance drop could be assessed.

The trajectories of the youBot base during the task execution are presented in Figure 6. Three trajectories are shown, namely during nominal execution, after fault injection without (not compensated) and with the proposed fault-tolerant control (compensated). With fault-tolerant control, the base follows a trajectory similar to the nominal case, while without it the robot moves in a different direction.

In Figure 7, the tracking error of the trajectory of the tool tip during its tracking task is illustrated, which is represented by the distance between tool tip and desired position on the trajectory. The nominal case without failure has a non-zero tracking error because of the simulated friction which is not compensated by the controller. It can be seen that, in case of failure, the error grows rapidly if no compensation is present. With fault-tolerant control, however, the error converges to a small value similar to the nominal case. The difference between nominal case and fault-tolerant control is due to the deviation in the sensor

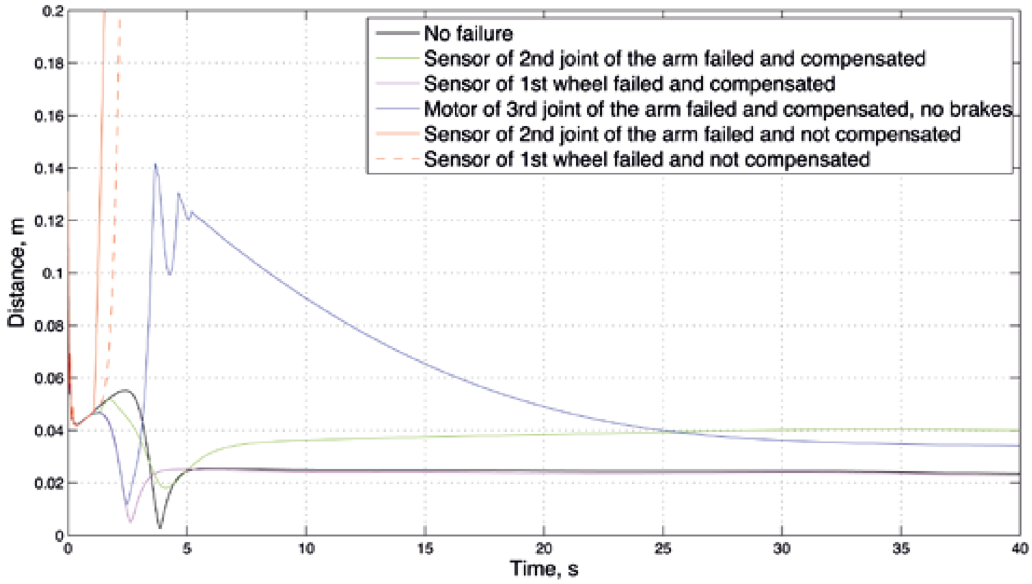

7 *Trajectory of the tool tip during its tracking task.*

measurements introduced by the fault before it was detected.

Conclusion

This article provides an overview of techniques that contribute to the increase of robust autonomy in robots, covering three main steps in the development process: a) specifying the requirements; b) analysing system behaviours; and c) adding new functionalities.

For specification purposes, the requirements for robust autonomy were made explicit from two different perspectives: an event-based approach with which single-event behaviour can be treated as a basis for determining the level of autonomy in the system; and a lifetime performance approach for determining system autonomy. These requirements can be applied in order to determine when new functionality is needed.

The essence of robust autonomy is interaction between robot and environment. Through the systematic analysis of this interaction, the functionalities that will provide a robot with autonomous characteristics can be discovered. An overview of the techniques that support such analysis was presented, as well as a proposal for an extension to the existing taxonomy of the failures, to make it more applicable to robotics.

New functionalities directed at increasing the level of autonomy in the robot consist of two major elements: detection and recovery systems. Their taxonomies allow a designer to select an appropriate approach based on the available system resources and knowledge. Adding new functionalities to a system brings up the question of increased complexity of the system and reusability of the components. In the proposed design guidelines, the architectural approaches to counteract these problems are reviewed. ■

REFERENCES

[1] Brodskiy, Y., Dresscher, D., Stramigioli, S., Broenink, J., and Yalcin, C. (2011), "Design principles, implementation guidelines, evaluation criteria, and use case implementation for robust autonomy", BRICS deliverable D6.1, 2011.

[2] Brodskiy, Y. (2014), "Robust autonomy for interactive robots", Ph.D. thesis, University of Twente, the Netherlands (https://www.ce.utwente.nl/aigaion/attachments/single/1174).

[3] Lemos, R. D., de Castro Guerra, P. A., and Rubira, C. M. (2006). "A fault-tolerant architectural approach for dependable systems", *IEEE Software*, pp. 80-87.

[4] Venkatasubramanian, V., Rengaswamy, R., Yin, K., and Kavuri, S. N. (2003), "A review of process fault detection and diagnosis", *Comp. Chem. Eng.*, 27(3), pp. 293-311.

[5] Siciliano, B., and O. Khatib (2008), *Springer Handbook of Robotics*, Springer, Berlin/Heidelberg. (p. 167)

[6] www.20-sim.com (Controllab Products, a University of Twente spin-off company).

INFORMATION

WWW.BEST-OF-ROBOTICS.ORG

HIGH-TECH SYSTEMS

TUESDAY 6 MAY 2014
TOURS

MORNING PROGRAMME

	Precision Tour	Ecosystem Tour	Additive Manufacturing Tour
08:30	Registration, 's-Hertogenbosch		
10:00	Frencken and KMWE	High Tech Campus	AddLab
12:30	Lunch at High Tech Campus, Eindhoven		

AFTERNOON PROGRAMME

	Precision Tour	Thin Layer / Printing Tour	Vacuum / Clean Tour
14:00	FEI and MI-Partners	Holst Centre and SMIT OVENS	Clean Pack Centre and Roth&Rau
17:00	Dinner, 's-Hertogenbosch		

Entrance fee: € 195 VAT excluded. An entrance ticket includes entrance to the tour programme, transport, lunch and dinner.

WEDNESDAY 7 AND THURSDAY 8 MAY 2014
BROKERAGE EVENT

Meet the right partner at the right place

Supported by enterprise europe network — Business Support on Your Doorstep

High-Tech Systems 2014 especially welcomes international visitors. Open innovation and collaboration are at the heart of Dutch high tech industry. The industry is particularly open-minded towards cooperation with international partners to strengthen its business.

Take part in the High-Tech Systems 2014 Brokerage Event, Wednesday 7 and Thursday 8 May 2014.

For more information and registration: www.b2match.eu/hts2014

TUESDAY 6 MAY 2014
WORKSHOPS

ALL-DAY WORKSHOPS

09:30 - 17:00	State of the art industrial motion control in the US € 495
09:30 - 17:00	Piezoelectric Materials and Applications € 395

MORNING WORKSHOP

09:30 - 12:30	Recent advances in modern optical microscopy € 295

AFTERNOON WORKSHOPS

14:00 - 17:00	Illumination for vision and in optical systems € 295
14:00 - 17:00	Hands-on introduction in the multi-view method for High Tech Embedded Systems - CAFCR € 295

An entrance ticket includes: lunch, drinks and entrance to the exhibition and conference on 7 and 8 May 2014. Entrance fees are exclusive of VAT.

WEDNESDAY 7 AND THURSDAY 8 MAY 2014
ROBOT FOOTBALL

First appearance of new robot football teams

Visit the robot football pitch in Hall B

The robot football teams of ASML, VDL-ETG and the combined Turtle-5k-team (ACE, Frencken, VEDS and TU/e) will make their first appearance at High-Tech Systems 2014. The teams will compete in several games and contests.

WEDNESDAY 7 MAY 2014 PROGRAMME

	High-level supply chain	Vacuum & Ultra clean	System architecture	Design & Modelling
09:30	**KEYNOTE** From specifications to strategy; an evolved perspective on supplier relations **Paul van Attekum, ASML**			Against all odds; the price to be first on the market **Jeroen Slobbe, TDC**
10:00				Tools for thermo mechanical design **Fred van Keulen, TU Delft**
10:30	Break			
11:30	Module driven supply chain in a mature and competitive high-tech industry **Jeroen de Groot, Assembléon**	Vacuum systems in the high-tech domain: what the stories often do not tell **Sven Pekelder en Gerrit van der Straaten, Settels Savenije van Amelsvoort**	Automated mixed palletizing in distribution centres **Joost van Eekelen, Vanderlande**	Adoption of model-based development for machine controller software **Johan Van Noten, FMTC**
12:00	How to innovate with others **Ton van Mol, Holst Centre**		Challenges of a new platform during market introduction **Henk-Jan Zwiers, Mutracx**	Model-based design exemplified by a self-correcting strategy for manufacturing of small parts **Christian Henke, Fraunhofer IPT**
12:30	Lunch			
14:00	Creating agility by using open innovation and partnerships with key suppliers **René van Wijk, NTS**	Linear motors in vacuum **Erwin Hofsté, Tecnotion**	Platform development: architecture meets reality **Hugo van Leeuwen, FEI**	HIL-testing of a towing tank **Christian Kleijn, Controllab**
14:30	From B2P to B2S **Gustaaf Savenije, VDL-ETG**	Ultra clean vacuum: it is not about how low you can go **Norbert Koster, TNO**	New system architecture challenges in the connected world **Ben Pronk, Philips Innovation Services**	Fibre rope winch modelling and design **Niels Nijenmanting, Reden, Jeroen Braadbaart, IHC**
15:00	Break			
16:00	How a target based approach and developers DNA result in highly competitive solutions for demanding OEM's **Pieter Janssen, Prodrive**	Innovations in the area of precision cleaning **Cees van Duijn, VDuijn-PE-Support**	How ASML's system engineering enables the design and build of total systems **Tom Castenmiller, ASML**	Space qualified design and vibration analysis of a thin membrane **Johannes Dercksen, SRON**
16:30	Simultaneous product and process development **Geert Ostyn, Picanol**	Vacuum system development for Mapper's lithography tool **Bas van Gelder, Mapper**	How interface driven system architecture leads to high-quality systems **Paul Zenden, Sioux**	How does the 'no compromise' philosophy influence the engineering process at Donkervoort **Renso Kuster, Cadmes**

This track is sponsored by settels savenije van amelsvoort

Connected innovation

	Connected innovation
11:30	Robotic flexible endoscope **Jeroen Ruiter, Demcon**
11:50	Ultra-fast scanner: a joined innovation project **Hans Spitshuis, CCM**
12:10	Corporate social responsibility throughout collaboration **Frank Steeghs, ACE**
12:30	Lunch
14:00	Working together to bring a new disruptive technology to the market **Henk-Jan Zwiers, Mutracx**
14:20	Multi-beam laser dicing for the semiconductor industry **Guido Knippels, ASM Alsi**
14:40	Without cooperation no business **Huib Heezen, Solaytec**
15:00	Break
16:00	Pulsed laser deposition for new generation thin film applications **Arjen Janssens, Solmates**
16:20	How connected innovation works for Phenom **Emile Asselbergs, Phenom World**
16:40	The Sorama Cam Pilot: sound imaging and sound connections **Rick Scholte, Sorama**

This track is organised in cooperation with High Tech NL

THURSDAY 8 MAY 2014 PROGRAMME

	Robotics	Agro & Food	Ultra precision	Design & Modelling
09:30	Twente humanoid head – the second generation is agile Theo de Vries, Imotec	Rapid 3D reconstruction of plants and the benefits for phenotyping and robotics Rick van der Zedde, Wageningen UR	DUV immersion lithography: the next step Hans Butler, ASML	Thermo elastic robustness of electro optical system in harsh thermocyclic environment Michel Azouley, In Summa
10:00	Using interactive haptic simulation to simulate robotic maintenance for Iter Cock Heemskerk, HIT	Spectroscopy in fruit business Henk Reitsma, Greefa	Maskless lithography developments Laurent Pain, CEA-Leti	CFD simulation of a heater for blood with high temperature stability Harmen Krediet, Demcon
10:30	Break			
11:30	Service robotics for personal and professional use Birgit Graf, Fraunhofer IPA	3D grippers, also a reality in the food industry Karel Van Hoecke, Van Hoecke	Precise wafer positioning for Mapper's lithography tool Paul Scheffers, Mapper	Topology optimization: maximum performance, minimal restrictions Matthijs Langelaar, TU Delft
12:00	Turtle-5k: How and why we developed a soccer robot for everybody Niels Koenraad, TU Eindhoven	Mechatronical challenges in fruit sorting Christiaan Fivez, Tomra	Industry driven academic research on thermal aspects in high-tech systems Gert van Schothorst, Philips Innovation Services	Integral optimization of structure and controller for motion systems Gijs van der Veen, TU Delft
12:30	Lunch			
14:00	A novel master-slave system for reconstructive microsurgery Raimondo Cau, TU Eindhoven	Smart weighing in poultry processing Gerrit Reintjes, Marel	Gaia: Galactic census through ultra stable mechanical design and control Teun van Dool, TNO	Automatic design of complex processes Amin Mannani, Alten
14:30	Haptic shared control – from design philosophy to applications David Abbink, TU Delft	Can you automatically harvest asparagus? Fred Hugen, Imix	Manufacturing of ultra high precision mechanical and optical components Mathieu Breukers, VDL-ETG	Model-based gearbox optimization Kristof Berx, FMTC
15:00	Break			
16:00	The smartest move in big industries between high-tech engineering and intra-logistics Patrick Verkerk, Frog	Milking plants with electorspraying Jeroen Rondeel, Wetering	Parallel scanning probe microscope comes of age Hamed Sadeghian, TNO	How predictive modelling can facilitate an intuitive approach in robot design Arend-Jan Beltman, CCM
16:30	Swarm robotics, theory or practice? Anne van Rossum, Almende	Most common pitfalls in the development of agro & food systems Wouter de Heij, Top	Optical fiber technology for biomaterial research Niek Rijnveld, Optics11	Parametric multiphysics simulation approach in inkjet unit design at Océ Wybo Wagenaar, Infinite

This track is organised in cooperation with
Powered by DUTCH TECHNOLOGY

Subject to changes

HIGH-TECH SYSTEMS

7 and 8 May 2014 | 1931 Congrescentrum Brabanthallen 's-Hertogenbosch | The Netherlands

www.hightechsystems.eu | #HTS14

WEDNESDAY 7 MAY AND THURSDAY 8 MAY 2014

EXHIBITION

STAND	EXHIBITOR
1	Kamer van Koophandel
3	Imotec Stichting Applied Piezo
4	TMC Group
5	YASKAWA Benelux
6	AIS Automation Dresden
7	I.B. Kracht
8 - 9	ATR Industrie-Elektronik R&D Elektronik Standort Niederrhein WFMG - Wirtschaftsförderung Mönchengladbach
10	Philips Innovation Services
11	Dutch Precision Technology (DPT)
12	Masévon and Vernooy Vacuum Engineering
13	Newport Spectra Physics
20 - 21	Altran
22	Silicon Europe
23	ENTER
24	TOPIC Embedded Products
25	Beckhoff.nl / IAL
26 - 27	CCM Centre for Concepts in Mechatronics High Tech NL Sorama
28	Variass Group
30	The High Tech Institute
31	Segula Technologies Nederland
32	Reden
33	3T
34	MathWorks
37	Venne Electronics
40	Renishaw Benelux
41	Claytex
43	TNO
44	Framo Morat
47	FMTC - Flanders' DRIVE
49	ACE Ingenieurs- & Adviesbureau
50	elero Elmekanic halstrup-walcher isel Germany mechOnics Steinmeyer Mechatronik Transfer DSW
58	Robot football
61 XL	Prodrive Technologies
62	Fontys Hogescholen
63	Opleidingen HBO Mechatronica
64	Festo
65	Vario*Drive*
66 XL	Nobleo Technology
67	Greentech Engineering | Pezy Group
68	KMWE Precision
72	NTS-Group
73	SCHUNK Intec
77	Sioux
78	ASML
79	Duranmatic
80	Nijdra Group
81	Irmato
82	Alten Mechatronics
83	TEVEL
84	Tecnotion
85	HEIDENHAIN
86	DEMCON
87	MTA
88	Ceratec Technical Ceramics
89	Sensitec
90	MAPPER Lithography
91	Data Vision
92	SICK
93	Euro HÜBNER Benelux PWB encoders
94	DVC machinevision
95	ETEL
96	IBS Precision Engineering
97	Oriental Motor
98	Hittech Group
107	Brainport Industries
108	Dutch Society for Precision Engineering

EXHIBITOR	STAND
3T	33
ACE Ingenieurs- & Adviesbureau	49
AIS Automation Dresden	6
Alten Mechatronics	82
Altran	20 - 21
ASML	78
ATR Industrie-Elektronik	8 - 9
Beckhoff.nl / IAL	25
Brainport Industries	107
CCM Centre for Concepts in Mechatronics	26 - 27
Ceratec Technical Ceramics	88
Claytex	41
Data Vision	91
DEMCON	86
Duranmatic	79
Dutch Precision Technology (DPT)	11
Dutch Society for Precision Engineering	108
DVC machinevision	94
elero	50
Elmekanic	50
ENTER	23
ETEL	95
euro HÜBNER benelux	93
Festo	64
FMTC - Flanders' DRIVE	47
Fontys Hogescholen	62
Framo Morat	44
Greentech Engineering | Pezy Group	67
halstrup-walcher	50
HEIDENHAIN	85
The High Tech Institute	30
High Tech NL	26 - 27
Hittech Group	98
I.B. Kracht	7
IBS Precision Engineering	96
Imotec	3
Irmato	81
isel Germany	50
Kamer van Koophandel	1
KMWE Precision	68
MAPPER Lithography	90
Masévon and Vernooy Vacuum Engineering	12
MathWorks	34
mechOnics	50
MTA	87
Newport Spectra Physics	13
Nijdra Group	80
Nobleo Technology	66 XL
NTS-Group	72
Opleidingen HBO Mechatronica	63
Oriental Motor	97
Philips Innovation Services	10
Prodrive Technologies	61
PWB encoders	93
R&D Elektronik	8 - 9
Reden	32
Renishaw Benelux	40
SCHUNK Intec	73
Segula Technologies Nederland	31
Sensitec	89
SICK	92
Silicon Europe	22
Sioux	77
Sorama	26 - 27
Standort Niederrhein	8 - 9
Steinmeyer Mechatronik	50
Stichting Applied Piezo	3
Tecnotion	84
TEVEL	83
TMC Group	4
TNO	43
TOPIC Embedded Products	24
Transfer DSW	50
Variass Group	28
Vario*Drive*	65
Venne Electronics	37
WFMG - Wirtschaftsförderung Mönchengladbach	8 - 9
YASKAWA Benelux	5

There are still a few stands available. Interested? Please contact Techwatch Events at events@techwatch.nl.

FLOOR PLAN

NEW

Inspiring pitches on high tech topics

Wednesday 7 May 2014

- **Industry 4.0**
- **Innovations in the manufacturing industry**

Thursday 8 May 2014

- **Additive manufacturing**
- **Co-development**

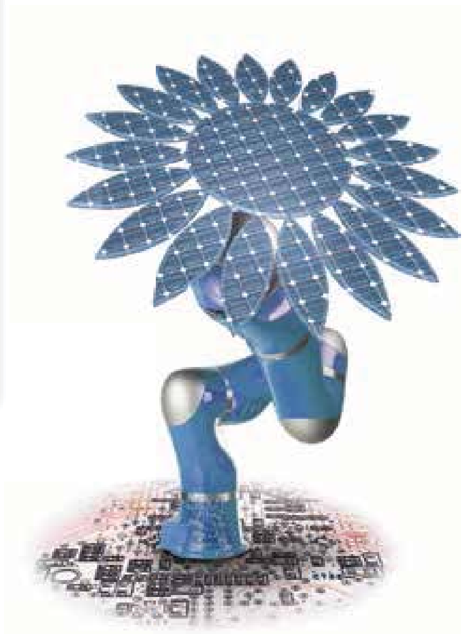

DSPE

YOUR PRECISION PORTAL

DUTCH SOCIETY FOR PRECISION ENGINEERING

DSPE Conference 2014

Conference on Precision Mechatronics

Conference Hotel De Ruwenberg, Sint Michielsgestel
2-3 september 2014

Presentations

Discussions and networking

Sharing ideas and experiences

Posters and demonstrations

Meeting peers in precision mechatronics

EARLY BIRD BONUS!

If you register before May 15 2014, you will receive one of these books:

- Displacement Measuring Interferometry
- Piezoelectric Materials and Applications

Conference by & for technologists, designers and architects in precision mechatronics. This conference is targeted at companies and professionals that are member of:

- Dutch Society for Precision Engineering
- Brainport Industries
- Mechatronics contact groups MCG and MSKE
- Selected companies/academia

Revolution vs. Evolution

This year's theme is 'Revolution vs. Evolution', because progress is always a mix of evolution (optimization) and revolution (disruptive technologies). Therefore it is crucial to learn from each others evolutionary steps, but also to discuss the revolutionary steps in requirements, material science, manufacturing science, computer intelligence, design approaches, ... we are facing today and tomorrow.

Be part of the inspiring community

"Informal, inspiring, enjoyable, relaxed, pleasant, open atmosphere, reunion, amazing community, a warm bath of exchanging interesting technical knowledge and networking, fun, good mix of people from different companies" were some of the remarks of the successful 2012 edition.

Important dates

May 15, 2014	Deadline Early Registration Bonus
July 1, 2014	Deadline for submission final papers / extended abstracts
Sept 2-3, 2014	Second DSPE conference on precision mechatronics

Conferencepartner

Brainport Industries

www.dspe-conference.nl

Erratum

In the previous issue of Mikroniek, references to Figures 8 and 9 in the report on the 2013 Precision Fair were swapped around in error. The text should have read as follows:

Precision measuring

No precision products can be made without accurate measuring. Many well-known measuring machine suppliers presented their large coordinate measuring machines (CMMs), such as the Nikon Altera 15.10.8 (see Figure 8). Nikon Metrology claims to be the only manufacturer to guarantee the accuracy of its CMMs for ten years. At the opposite end of the spectrum to this large CMM with an X stroke of 1,500 mm is the Dino-Lite digital microscope (see Figure 9), exhibited by Schut Geometrische Meettechniek.

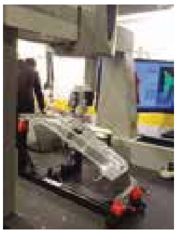

■ *Figure 8. The Nikon Altera 15.10.8 CMM. The deviations (with respect to CAD data) of the real product that is being measured are displayed on the right.*

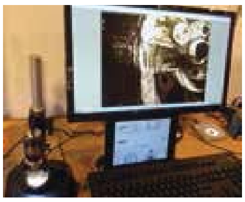

■ *Figure 9. The Dino-Lite digital microscope, marketed by Schut Geometrische Meettechniek.*

New miniature incremental optical encoder

Renishaw, the global metrology specialist, launches ATOM™, an innovative non-contact optical linear and rotary incremental encoder system that combines miniaturisation with leading-edge dirt immunity, signal stability and reliability. The new encoder achieves unmatched performance as a consequence of a design that avoids the many compromises traditionally associated with miniaturised encoders, according to Renishaw.

ATOM, which is available in sizes as small as 6.8 mm x 12.7 mm x 20.5 mm, is the world's first miniature encoder to use filtering optics with Auto Gain Control (AGC) and Auto Offset Control (AOC). This advanced technology provides excellent signal stability and exceptional dirt immunity, Renishaw claims.

The ATOM readhead is available in a range of formats and delivers excellent accuracy with low Sub-Divisional Error (SDE), low jitter, high signal stability and long-term reliability. ATOM offers speeds to 20 m/s (29,000 rpm on a 17 mm disc) and resolutions to 1 nm (0.004 arcsec on a 108 mm disc) with a range of linear and rotary (angle) scales available in stainless steel and glass. The readhead also includes a set-up LED to allow quick and easy installation and an auto-calibration routine to enable faster optimisation.

The compact ATOM incremental encoder is supplied in hi-flex cable and Flexible-Printed Circuit (FPC) variants with both 20 µm and 40 µm scale options. The side-exit FPC version reduces the overall package size and allows integration with PCBs. Customers can also choose from a range of high-accuracy linear glass spars to 130 mm in length, stainless steel tape to 10 m and rotary glass disc scales from 17 mm to 108 mm in diameter.

Applications for ATOM's ultra-compact readhead include laser scanning, coordinate measurement systems, semiconductor and flat-panel display production, motor drive systems, microscopy and the scientific research sector.

Recently, Renishaw Benelux has opened offices on the High Tech Campus in Eindhoven, the Netherlands.

WWW.RENISHAW.COM

Additive Manufacturing Academy launched

Fontys University of Applied Sciences, Mikrocentrum and Additive Industries, all based in Eindhoven, the Netherlands, have joined forces to coordinate education in the field of Additive Manufacturing (AM). Additive Manufacturing Academy (AM Academy) aims to bring the Dutch industry's knowledge of 3D printing to 'World Class' level by developing a coherent range of courses, training sessions, workshops and master classes in the area of industrial 3D printing / AM. All issues are addressed, from 3D design and engineering through material selection to the actual printing process and finishing, testing and qualification.

AM Academy is a not-for-profit initiative of three partners. Within its Centre of Expertise, Fontys University of Applied Sciences focuses on hands-on training in the new objeXlab. Additive Industries organises master classes for decision makers from the manufacturing and other industries. Mikrocentrum extends its existing portfolio of AM courses for industry. "By joining forces and gaining insight into the offering at all levels, we are able to fill in the white spots and prevent overlap", says Arno Gramsma of KMWE 3DP, who is involved in new initiatives on behalf of industry.

WWW.AM-ACADEMY.NL

Picometers in capacitive measuring technology

Lion Precision has launched the latest capacitive measuring technology delivering resolutions down to 50 pm and a bandwidth up to 50 kHz. Application areas of the CPL490 system include high-density hard-disk drives where spindles are required to turn with near-zero amounts of error motion (wobble).

■ *The CPL490 system.*

Previous technology was incapable of seeing the tiny movements when the spindles were turning at operating speeds. The CPL490 has now opened a viewing window into the dynamic pico-world enabling spindle manufacturers and designers to take the next step in precision. Many other industries, including semiconductor and electron microscopy, require measurement of position with similarly increasing precision.

At 15 kHz bandwidth, the resolution is 7 parts-per-million of full-scale range, which is as low as 50 pm. A bandwidth up to 50 kHz is supported, meaning that measurements of tiny displacements at very high speed are now possible – at this remarkably high frequency for capacitive sensors, the precision is still better than 0.3 nm.

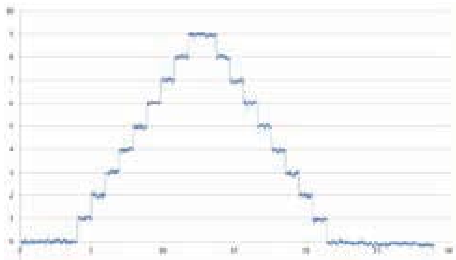

■ *Steps of 1 nm on InSituTec stage measured with the CPL490 system over a 30 second time period.*

IBS Precision Engineering, based in Eindhoven, the Netherlands, is the distributor of Lion Precision's capacitive and eddy-current non-contact measuring systems in Europe.

WWW.LIONPRECISION.COM

WWW.IBSPE.COM

New FOM group has started at ASML

FOM (Foundation for Fundamental Research on Matter) and ASML have signed a collaboration agreement for a new FOM research group in the field of fluid dynamics, located at ASML in Veldhoven, the Netherlands. The group will focus on the behaviour of small tin droplets, which emit extreme UV light (EUV) under the influence of laser light. ASML uses the tin droplets for EUV lithography, a technique used in the production of computer chips. The new group is associated with the Physics of Fluids group of Professor Detlef Lohse at the University of Twente. The collaboration is taking place in the form of an Industrial Partnership Programme (IPP).

The advantage of EUV light is its very short wavelength – down to 10 nanometers – with which extremely small structures can be produced. In the EUV lithography machines of ASML a very powerful laser is fired onto miniscule tin drops. This brings the electrons in the tin atoms to a higher energy level after which they emit extreme UV light of exactly the right wavelength. Special mirrors in the machine focus the light on the wafer. Contamination is one of the problems with this technique. If a tin aerosol precipitates on the mirrors then these no longer function and the light is dispersed. The new group will investigate how to minimise the spattering of the drops.

WWW.ASML.COM

WWW.FOM.NL

Ter Hoek Vonkerosie introduces Laser MicroJet

Ter Hoek Vonkerosie, based in Rijssen, the Netherlands, has extended its precision machining capabilities with the Laser MicroJet® technology from Synova. This precision technology combines a laser beam with a water jet, which eliminates heat-affected zones that arise during wire eroding. Compared to wire erosion, the Laser MicroJet produces a lower surface quality of the cut, but accuracy and speed are superior. Moreover, there are materials that are suitable for laser microjetting and not for wire eroding.
Swiss company Synova is a manufacturer of advanced laser cutting systems for the semiconductor, electronic, automotive, solar, medical, watch and diamond industries. Through its proprietary Laser MicroJet® (water jet-guided laser) technology, it enables accuracy, speed and flexibility improvements in numerous precision manufacturing processes, paving the way for a considerable number of new applications in the domain of sensitive material micro-machining. Thanks to a hair-thin, low-pressure water jet guiding the laser beam, an unsurpassed cutting quality is achieved, without heat damage and deposition.
The advantages, according to Synova, are low consumable costs, low thermal loading of the parts, no chipping and cracking, no heat-affected zone, fast cutting rates on brittle and hard materials and cleaner finished surfaces than seen with other laser processes.

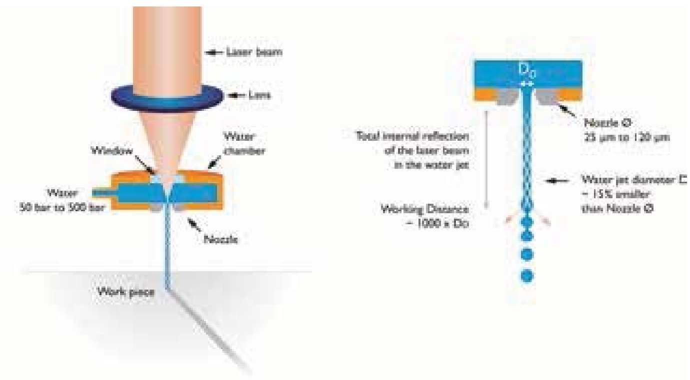

■ *Principle of operation of the Laser MicroJet.*

Synova laser cutting machines feature absolute precision from approx. 3 to 5 µm and large processing areas that range between 150 x 150 and 800 x 1200 mm. The high-precision, high-speed XY-table, based on the principle of separate axes on a granite base, allows unmatched accuracy and dynamics. The axes are driven by linear motors at a speed of up to 1,000 mm/s. Pulsed Nd:YAG lasers (infrared, green or UV) are typically used and the water jet diameter ranges from 25 to 70 µm.

All machines are equipped with vision cameras and powerful image processing software, allowing automatic alignment and quality inspection. Options include a fully automated handling system, chiller, alternative laser sources, water treatment system, reference scales and transformers.

WWW.TERHOEKVONKEROSIE.NL

Demcon keeps growing

In the next two years, Demcon, counting over 200 people now, expects to grow to a staff complement of over 300. The University of Twente spin-off has evolved into a medium-sized company: a high-end technology supplier of mechatronic products and systems, covering the focus areas of high-tech systems and medical devices. The new head office in Enschede, the Netherlands, can accommodate further growth and is now in the process of extension with new production facilities, including a cleanroom. Satellite offices are located in Eindhoven, Amsterdam, Oldenzaal and Münster (Germany).

According to CEO Dennis Schipper, the continuing growth can be attributed to a number of strategic decisions concerning the office in Eindhoven (established in 2011, near major clients in the Brainport Eindhoven region), the focus on medical devices (a stable growth market compared to the highly cyclical semicon market), take-overs and participations (medical device companies and technology experts), production (including in-house series production), and the newly established office in Germany (the neighbouring industrial giant).

The most recent take-over, early this year, involves BuNova Development, which was based in Zwolle, the Netherlands. BuNova specialises in the analysis of heat transfer, flow, structural integrity and mechanical behaviour of process technology equipment, using simulation modelling techniques such as CFD (Computational Fluid Dynamics) and FEA (Finite Element Analysis). The focus is on the interaction between fluid and gas flows and surrounding systems, concerning structural stresses and deformations, heat generation, temperature distributions and other aspects of material behaviour.

Demcon and BuNova have a history of collaboration, for example on the design of the Fluido, a device for the controlled warming of blood and infusion fluids. In view of the continuity of BuNova (five people) and the complementarity in competencies, Demcon decided to take over the high-tech consultancy firm. Demcon BuNova is now housed in the Enschede HQ.

WWW.DEMCON.NL

Integrated XY Ball-Screw Stage

Aerotech's PlanarSL mechanical bearing, ball-screw-driven XY stages offer exceptional performance in a cost-sensitive, low-profile package, according to an Aerotech press release. Combining two axes of motion in a compact package, the PlanarSL is a solution for applications ranging from surface metrology to general high-precision automation.

The PlanarSL comes standard with a precision-ground and preloaded ball screw. Unlike competitive designs where the ball screw is positioned on the side or off-centre, the PlanarSL ball screw is engineered to drive directly through the centres of friction and stiffness, resulting in superior geometric performance and accuracy. High-precision linear motion guide bearings provide excellent straightness and flatness with optimal support of the moving carriage over the entire XY travel. The PlanarSL structural elements have been optimised for the highest possible planar performance.

The PlanarSL is available with low-thermal expansion (3.3 ppm/°C) precision glass scales on both axes for high-accuracy and repeatable positioning over long periods of time. The linear encoder, available with amplified sine (1 V_{pp}) or 0.1 µm TTL digital outputs, is mounted near the centres of action, providing a stage design for high-accuracy positioning.

The PlanarSL comes with a 24 V_{DC} bipolar stepper motor. Aerotech can also provide brushless and brush DC motors with high-resolution rotary encoders.

WWW.AEROTECH.COM

CPE Certification for Summer School Manufacturability

The DSPE Certification Programme Committee has certified the 5-day Summer School Manufacturability organised by LiS Academy (part of the LiS – Leiden Instrument Makers School) and its partners. Participants in this LiS Academy course will earn five CPE points when successfully completing the course.

The 5-day course, which is held in Dutch, is for young professional engineers with a limited knowledge of and experiences with manufacturing technologies and associated manufacturability aspects. Milling, turning, grinding, casting, sheet metal work and electrical discharge machining (EDM) are some of the technologies presented and discussed.

The summer school is an initiative of DSPE and the LiS. A range of other partners are also very involved in what this attractive programme has to offer. These partners include the Hittech Group, Suplacon, Ter Hoek Vonkerosie, TNO, Settels Savenije van Amelsvoort and ECN. FME, DPT and Brainport Industries are ardent supporters of the programme too. The 2014 course will be held from 25-29 August. For more information and online registration, please go to the LiS Academy website.

More good news from the LiS: the Dutch Minister for Education Jet Bussemaker, the UTOPA Foundation, the LiS Foundation, the mayor of Leiden Henri Lenferink, Leiden University and industry representatives recently signed the covenant 'Growth of the LiS', which will provide €8 million for the expansion of the LiS. More on this in a forthcoming issue of Mikroniek.

WWW.LISACADEMY.NL

UPCOMING **EVENTS**

7-8 May 2014, Den Bosch (NL)

High-Tech Systems 2014

The second edition of this event focuses on the high-tech systems industry in all European areas with significant high-tech roadmaps. It entails advanced system engineering and architecture, precision engineering, mechatronics, high-tech components system design as well as advanced original equipment manufacturing (OEM). See page 46.

WWW.HIGHTECHSYSTEMS.EU

21 May 2014, Den Bosch (NL)

VCCN Cleanroom Symposium and 17th Contamination Control

Symposium and trade fair organised by the Dutch Contamination Control Association (VCCN).

WWW.VCCN.NL

22-23 May 2014, Aachen (DE)

28th Aachen Machine Tool Colloquium

The general topic of AWK 2014 (Aachen Machine Tool Colloquium, Aachener Werkzeugmaschinen-Kolloquium) is 'Industry 4.0 – The Aachen Approach', focusing on the potential as well as risks of implementing a cross-linked, intelligent production and demonstrating the technical realisation by means of case studies.

WWW.AWK-AACHEN.DE

2-6 June 2014, Dubrovnik (Croatia)

Euspen's 14th International Conference & Exhibition 2014

Topics:

- Renewable Energy Technologies
- Precision Engineering for Medical Products
- Additive Manufacturing for Precision Engineering
- Nano & Micro Metrology
- Ultra Precision Machines
- Ultra Precision Manufacturing & Assembly Processes
- Important/Novel Advances in Precision Engineering & Nano Technologies
- Motion Control in Precision Systems, Nano & Micro Manufacturing

WWW.EUSPEN.EU

11-12 June 2014, Veldhoven (NL)

Vision, Robotics & Mechatronics 2014 / Photonics Event 2014

Colocation of two Mikrocentrum events. Vision, Robotics & Mechatronics features innovations and solutions for vision systems, robotics, motion control, sensors and equipment automation. The Photonics Event focuses on knowledge, design, engineering, manufacturing and application of a key enabling technology for the high-tech industry.

WWW.VISION-ROBOTICS.NL
WWW.FOTONICA-EVENEMENT.NL

16-20 June 2014, Eindhoven (NL)

International Summer school Opto-Mechatronics 2014

Five days of intensive training, organised by DSPE, The High Tech Institute and Mechatronics Academy. See page 35.

WWW.SUMMER-SCHOOL.NL

25-29 August 2014, Leiden (NL)

Summer School Manufacturability

Summer school, organised by LiS Academy, dedicated to the manufacturabilty of precision components and targeted at young professional engineers with a limited knowledge of and experiences with manufacturing technologies and associated manufacturability aspects.

WWW.LISACADEMY.NL

2-3 September 2014, Sint-Michielsgestel (NL)

DSPE Conference on Precision Mechatronics

Second edition of conference on precision mechatronics, organised by DSPE and Brainport Industries. The target group includes technologists, designers and architects in precision mechatronics, who (through their respective organisations) are connected to DSPE, Brainport Industries, the mechatronics contact groups MCG/MSKE or selected companies or educational institutes. This year's theme is 'Revolution vs. Evolution', because progress is always a mix of evolution (optimisation) and revolution (disruptive technologies). See page 52.

WWW.DSPE-CONFERENCE.NL

12-13 November 2014, Veldhoven (NL)

Precision Fair 2014

Fourteenth edition of the Benelux premier trade fair and conference on precision engineering, organised by Mikrocentrum.

WWW.PRECISIEBEURS.NL

CPE COURSE CALENDAR

COURSE (content partner)	CPE points	Provider	Starting date (location, if not Eindhoven)
BASIC			
Mechatronic System Design - part 1 (MA)	5	HTI	29 September 2014
Mechatronic System Design - part 2 (MA)	5	HTI	25 Augustus 2014
Construction Principles	3	MC	6 May 2014 28 October 2014 (Utrecht)
System Architecting (Sioux)	5	HTI	16 June 2014
Design Principles Basic (SSvA)	5	HTI	12 May 2014
Motion Control Tuning (MA)	6	HTI	19 November 2014
DEEPENING			
Metrology and Calibration of Mechatronic Systems (MA)	3	HTI	1 December 2014
Actuation and Power Electronics (MA)	3	HTI	22 September 2014
Thermal Effects in Mechatronic Systems (MA)	3	HTI	5 November 2014
Summer school Opto-Mechatronics (DSPE/MA)	5	HTI	16 June 2014
Dynamics and Modelling (MA)	3	HTI	28 October 2014
Summer School Manufacturability	5	LiS	25 August 2014
SPECIFIC			
Applied Optics (T2Prof)	6.5	HTI	28 October 2014
Applied Optics	6.5	MC	11 September 2014
Machine Vision for Mechatronic Systems (MA)	2	HTI	25 September 2014
Electronics for Non-Electronic Engineers (T2Prof)	10	HTI	to be planned
Modern Optics for Optical Designers (T2Prof)	10	HTI	12 September 2014
Tribology	4	MC	14 May 2014 29 October 2014 (Utrecht)
Introduction in Ultra High and Ultra Clean Vacuum (SSvA)	4	HTI	to be planned
Experimental Techniques in Mechatronics (MA)	3	HTI	23 June 2014
Design for Ultra High and Ultra Clean Vacuum (SSvA)	3	HTI	22 May 2014
Advanced Motion Control (MA)	5	HTI	6 October 2014
Iterative Learning Control (MA)	2	HTI	3 November 2014
Advanced Mechatronic System Design (MA)	6	HTI	27 June 2014
Finite Element Method	5	ENG	to be planned

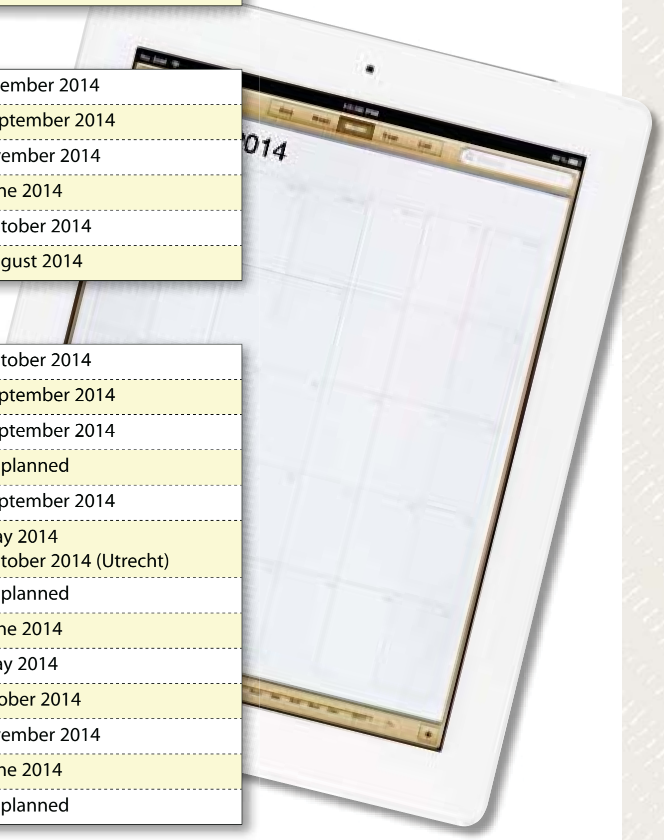

DSPE Certification Program

Precision engineers with a Bachelor's or Master's degree and with 2-10 years of work experience can earn certification points by following selected courses. Once participants have earned a total of 45 points (one point per course day) within a period of five years, they will be certified. The CPE certificate (Certified Precision Engineer) is an industrial standard for professional recognition and acknowledgement of precision engineering-related knowledge and skills. The certificate holder's details will be entered into the international Register of Certified Precision Engineers.

WWW.DSPEREGISTRATION.NL/LIST-OF-CERTIFIED-COURSES

Course providers

- Engenia (ENG)
  WWW.ENGENIA.NL
- The High Tech Institute (HTI)
  WWW.HIGHTECHINSTITUTE.NL
- Mikrocentrum (MC)
  WWW.MIKROCENTRUM.NL
- LiS Academy (LiS)
  WWW.LISACADEMY.NL

Content Partners

- Dutch Society for Precision Engineering (DSPE)
  WWW.DSPE.NL
- Mechatronics Academy (MA)
  WWW.MECHATRONICS-ACADEMY.NL
- Settels Savenije van Amelsvoort (SSvA)
  WWW.STTLS.NL
- Sioux
  WWW.SIOUX.EU
- Technical Training for Professionals (T2Prof)
  WWW.T2PROF.NL

Bearing and Linear Technology

Schaeffler Nederland B.V.
Gildeweg 31
3771 NB Barneveld
T +31 (0)342 - 40 30 00
F +31 (0)342 - 40 32 80
E info.nl@schaeffler.com
W www.schaeffler.nl

Schaeffler Group - LuK, INA and FAG - is a world wide leading company in developing, manufacturing and supplying of rolling bearings, linear systems, direct drives and maintenance products. Applications: automotive, industrial and aerospace.

Development

TNO
T + 31 (0)88-866 50 00
W www.tno.nl

TNO is an independent innovation organisation that connects people and knowledge in order to create the innovations that sustainably boost the competitiveness of industry and wellbeing of society.

member DSPE

Development and Engineering

ACE ingenieurs- & adviesbureau
werktuigbouwkunde en elektrotechniek BV
Dr. Holtroplaan 46
Postbus 7030, 5605 JA Eindhoven
5652 XR Eindhoven
T +31 (0)40 - 2578300
F +31 (0)40 - 2578397
E info@ace.eu
W www.ace.eu

ACE has developed into a leading engineering and consultancy firm with a strong focus on mechanics and mechatronics. Services include conceptualization, development, engineering and prototyping.

member DSPE

Lencon Engineering
Hondsdijk 3,
2396 HG Koudekerk aan den Rijn
Postbus 28
2396 ZG Koudekerk aan den Rijn
T: +31 (0)71 341 65 55
F: +31 (0)71 341 65 58
E: sales@lencon.nl
W: www.lencon.nl

Lencon provides maximum flexibility in high-end mechanical engineering and product development. Turn-key projects and detachment of experienced productengineers and precisionengineers.

member DSPE

Education

Leiden school for Instrumentmakers (LiS)
Einsteinweg 61
2333 CC Leiden
The Netherlands
T +31 (0)71-5581168
F +31 (0)71-5681160
E info@lis-mbo.nl
W www.lis-mbo.nl

The LiS is founded in 1901 by the famous scientist prof. Kamerlingh Onnes. Nowadays the LiS is a modern school for vocational training on level 4 MBO-BOL. The school encourages establishing projects in close cooperation with contractors and scientific institutes, allowing for high level “real life” work.

member DSPE

PAO Techniek
Stevinweg 1, 2628 CN Delft
Postbus 5048, 2600 GA Delft
T +31 (0)15 27 88 350
F +31 (0)15 27 84 619
E info@paotechniek.nl
W www.pao.tudelft.nl

Lasers, light and nano - motion

Laser 2000 Benelux C.V.
Voorbancken 13a
3645 GV Vinkeveen
Postbus 20, 3645 ZJ Vinkeveen
T +31(0)297 266 191
F +31(0)297 266 134
E info@laser2000.nl
W www.laser2000.nl

Laser 2000 Benelux considers it her mission to offer customers the latest photonics technologies available.
Their areas of expertise are:

- Lasers and laser systems for industry and research
- Light metrology instruments for LED and luminaire industry
- Piezo- and stepper motion products for nano- and micro-positioning
- LED illumination and high speed inspection in machine vision applications

Laser Systems

Applied Laser Technology
De Dintel 2
5684 PS Best
T +31 (0)499 375375
F +31 (0)499 375373
E techsupport@alt.nl
W www.alt.nl

member DSPE

3D Measurement Services

Mitutoyo Nederland B.V.
Storkstraat 40
3905 KX Veenendaal
T +31 (0)318-534911
F +31 (0)318-534811
E info@mitutoyo.nl
W www.mitutoyo.nl

Mechatronics Development

centre for concepts in mechatronics

CCM Centre for Concepts in Mechatronics
De Pinckart 24
5674 CC Nuenen
T +31 (0)40 2635000
F +31 (0)40 2635555
E info@ccm.nl
W www.ccm.nl

CCM translates technology into technique.
Commitment, motivation, education and skills of our employees are the solid basis for our business approach.

member DSPE

Janssen Precision Engineering
Azielaan 12
6199AG Maastricht-Airport
T +31 43 3585777
F +31 43 3580036
E huub.janssen@jpe.nl
W www.jpe.nl

Precision engineering and mechatronic solutions in ambient, vacuum and cryogenic environment

member DSPE

Mechatronics Development

CREATING MACHINES TOGETHER

Manufacturing Technical Assemblies (MTA) b.v.
Waterbeemd 8
5705 DN Helmond
T: +31 (0)492 474992
F: +31 (0)492 474510
E: info@m-t-a.nl
W: www.m-t-a.nl

MTA is an high-tech system supplier specialized in the development and manufacturing of mechatronic machines and systems.
Our clients are OEM s in the Packaging, Food, Graphics and High-tech industries.

Metal Precision Parts

METAL PRECISION PARTS

Etchform BV
Arendstraat 51
1223 RE Hilversum
T +31 (0)35 685 51 94
F info@etchform.com
W www.etchform.com

Etchform is a production and service company for etched and electroformed metal precision parts.

member DSPE

Metal Precision Parts

precision metal

A Member of the SPGPrints Group
Karel van Gelreweg 22
6961 LB Eerbeek
T +31 (0)313 672 911
E info.veco@spgprints.com
W www.vecoprecision.com

Having our own R&D and Engineering Center including clean room manufacturing and full automated inspection facilities Veco is an excellent co-maker for your extreme precision metal components.

member DSPE

Micro Drive Systems

driven by precision

Maxon Motor Benelux

The Netherlands

Head Office
maxon motor benelux bv
Josink Kolkweg 38
7545 PR Enschede

South
High Tech Campus 9
5656 AE Eindhoven
T: +31(053) 744 0 744
E: info@maxonmotor.nl
W: www.maxonmotor.nl

Belgium / Luxembourg

maxon motor benelux bv
Schaliënhoevedreef 20C
2800 Mechelen - Belgium
T: +32 (15) 20 00 10
F: +32 (15) 27 47 71
E: info@maxonmotor.be
W: www.maxonmotor.be

maxon motor is the worldwide leading supplier of high precision drives and systems. When it really matters! Try us.

Micro Drive Systems

MINIMOTOR Benelux
Miniature Drive Systems
FAULHABER

Minimotor Benelux

Belgium
Dikberd 14/6c
B-2200 Herentals
T +32 (0)14-21 13 20
F +32 (0)14-21 64 95
E info@minimotor.be

The Netherlands
Postbus 49
NL-1540 Koog a/d Zaan
T +31 (0)75-614 86 35
F +31 (0)75-614 86 36
E info@minimotor.nl
W www.faulhaber.com

Faulhaber is a leading manufacturer of miniature drive systems based on ironless micromotors with the highest power-to-volume ratio.

member DSPE

Micromachining

Reith Laser bv
Bijsterhuizen 24-29
6604 LK Wijchen
The Netherlands
T +31 (0)24 3787564
F +31 (0)24 3787586
E info@reithlaser.nl
W www.reithlaser.nl

For more than 22 years Reith Laser bv is the leading supplier of laser-processed products in Europe.
We can offer you a great diversity of lasermaterialprocessing activities:

- Laser- (micro-) cutting
- Laser drilling
- Laser welding
- Laser micromachining

Reith Laser is active in precision industry, medical industry, aerospace, semiconductor- and automotive industry.

ADVERTISERS INDEX